

ASYMMETRIC ORGANOCATALYTIC SULFA-MICHAEL REACTIONS OF  
THIOGLYCOLATE WITH ISATIN DERIVED NITROALKENES

A THESIS SUBMITTED TO  
THE GRADUATE SCHOOL OF NATURAL AND APPLIED SCIENCES  
OF  
MIDDLE EAST TECHNICAL UNIVERSITY

BY

SELİN SAĞESEN

IN PARTIAL FULFILLMENT OF THE REQUIREMENTS  
FOR  
THE DEGREE OF MASTER OF SCIENCE  
IN  
CHEMISTRY

SEPTEMBER 2018



Approval of the thesis:

**ASYMMETRIC ORGANOCATALYTIC SULFA-MICHAEL REACTIONS  
OF THIOGLYCOLATE WITH ISATIN DERIVED NITROALKENES**

submitted by **Selin Sağesen** in partial fulfillment of the requirements for the degree of **Master of Science in Chemistry Department, Middle East Technical University** by,

Prof. Dr. Halil Kalıpçılar  
Dean, Graduate School of **Natural and Applied Sciences** \_\_\_\_\_

Prof. Dr. Cihangir Tanyeli  
Head of Department, **Chemistry** \_\_\_\_\_

Prof. Dr. Cihangir Tanyeli  
Supervisor, **Dept. of Chemistry, METU** \_\_\_\_\_

**Examining Committee Members:**

Prof. Dr. Adnan Bulut  
Dept. of Chemistry, Kırıkkale University \_\_\_\_\_

Prof. Dr. Cihangir Tanyeli  
Dept. of Chemistry, METU \_\_\_\_\_

Assoc. Prof. Dr Akın Akdağ  
Chemistry Dept. of Chemistry, METU \_\_\_\_\_

Assist. Prof. Dr. Salih Özçubukçu  
Dept. of Chemistry, METU \_\_\_\_\_

Assist. Prof. Dr. Serhan Türkyılmaz  
Dept. of Chemistry, METU \_\_\_\_\_

**Date:** \_\_\_\_\_



**I hereby declare that all information in this document has been obtained and presented in accordance with academic rules and ethical conduct. I also declare that, as required by these rules and conduct, I have fully cited and referenced all material and results that are not original to this work.**

Name, Last name : Selin Sağesen

Signature :

## ABSTRACT

### ASYMMETRIC ORGANOCATALYTIC SULFA-MICHAEL REACTIONS OF THIOGLYCOLATE WITH ISATIN DERIVED NITROALKENES

Sağesen, Selin  
MSc, Department of Chemistry  
Supervisor : Prof. Dr. Cihangir Tanyeli

September 2018, 119 pages

Organosulfur compounds are present in many natural products and drugs. Sulfa-Michael reaction is the prominent method to synthesize these molecules. The novel bifunctional organocatalysts developed in our research group enable sulfa-Michael reaction to occur asymmetrically. In this thesis, biologically active isatin derived nitroalkenes were chosen as Sulfa-Michael acceptors. Addition of methyl thioglycolate to isatin derived nitroalkenes in the presence of the bifunctional organocatalysts was studied under different conditions. Solvent, temperature, catalyst loading and concentration screenings were done. Isatin derived nitroalkenes substituted from different positions were also tested in sulfa-Michael reactions under optimized conditions. Sulfa-Michael product was synthesized with 75% yield and 70% ee when 10 mol % 1-adamantyl squaramide/quinine catalyst was used. The nitro group in the structure was reduced catalytically in order to reveal the product to be utilized in further reactions.

Keywords: Sulfa-Michael, Isatin derived Nitroalkenes, Asymmetric Synthesis, Organocatalysis, Bifunctional Organocatalyst

## ÖZ

### TİYOGLİKOLATLARIN İSATİN TÜREVİ NİTROALKENLERLE ASİMETRİK ORGANKATALİTİK SULFA-MICHAEL TEPKİMELERİ

Sağesen, Selin  
Yüksek Lisans, Kimya Bölümü  
Tez Yöneticisi : Prof. Dr. Cihangir Tanyeli

Eylül 2018, 119 sayfa

Organosülfür bileşikleri birçok doğal bileşiğin ve ilacın yapısında bulunmaktadır. Bu bileşikler sentezleme yöntemlerinin başında sulfa-Michael tepkimeleri gelir. Araştırma grubumuzda geliştirilen özgün bifonksiyonel organokatalizörler, sulfa-Michael reaksiyonlarının asimetrik olarak gerçekleşmesini mümkün kılmaktadır. Bu tez çalışmasında, Sulfa-Michael akseptörü olarak biyolojik olarak aktif isatin türevi nitroalkenler seçilmiştir. Metil tiyoglikolatın, isatin türevi nitroalkenlere bifonksiyonel organokatalizörler eşliğinde ve farklı koşullarda asimetrik olarak katılması çalışılmıştır. Solvent, sıcaklık, katalizör miktarı ve derişim gibi taramaları yapılmıştır. En iyi hale getirilmiş koşullarda, isatin türevi nitroalkenlerin farklı pozisyonlarından türevlendirilmiş bileşikler de sulfa-Michael reaksiyonlarında test edilmiştir. % 10 mol 1-Adamantil skuramit/kinin organokatalizör ilavesinde %75 verim ve %70 enantioseçicilik ile sulfa-Michael ürünü sentezlenmiştir. Tepkime ürününün ileri tepkimelerde kullanılabileceği, yapıda bulunan nitro grubunun katalitik indirgenmesiyle gösterilmiştir.

Anahtar Kelimeler: Sülfä-Michael, İsatın türevi Nitroalkene, Asimetrik Sentez, Organokataliz, Bifonksiyonel Organokatalizör

To My *honnête et généreux* Grandfather Ahmet Ziya Sağesen...





## ACKNOWLEDGMENTS

I wish to express my sincere appreciation and special thanks to my supervisor Prof. Dr. Cihangir Tanyeli for giving me the opportunity to work in his research group, and also for his precious guidance, valuable advices, infinite patience, encouragement and teaching me not to give up.

I would like to express my sincere thanks to Seda Okumuş Karahan for teaching me laboratory techniques and many things. Words fail while talking about her, indeed. During three years of my master study, she always gave an eye on me, never hesitated to share anything with me, and showed me how a scientist should be.

I would like to thank Prof. Dr. Devrim Özdemirhan for her support and giving me opportunity to work in her project.

I would like to thank Betül Eymur for the NMR experiments.

I would like to give my special thanks to my labmates Esra Dündar and Merve Bozdemir. You were the perfect match for me and I cannot imagine our laboratory with somebody instead of you two. I will remember our chocolate, clean-up and horon sessions with a smile. Esra, I want to apologize for being stingy about acetone and force you to keep all the empty boxes. Merve, I could not imagine that I would love you that much. The truthfulness that made us friends, will keep us friends.

I would also thank other Tanyeli research group members, Ezgi Bayer, Dilşad Susam, Deniz Hasılcıoğulları, Faik Tümer and Arzu Bilgin for their friendship and guiding me about department. Especially, thanks to Ezgi Bayer for sharing the high spots of these there years with me.

I would like to thank academic staff of METU Chemistry Department, especially Assist. Prof. Dr. Salih Özçubukcu and Assoc. Prof. Dr. Görkem Günbaş for widening the horizons of my mind.

I sincerely thank examining committee members, Prof. Dr. Adnan Bulut, Prof. Dr. Cihangir Tanyeli, Assoc. Prof. Dr. Akın Akdağ, Assist. Prof. Dr. Salih Özçubukçu and Assist. Prof. Dr. Serhan Türkyılmaz for their contributions to my master thesis.

I would like thank Prof. Dr. Sebla Dinçer for her guidance about my entire life. It was my chance to get to know you, taking your courses and trying to gain the perspective you own.

My very special thanks go to Kardelen Göksu. Lucky me, I see eye to eye with you. Lucky me, we feel the same thing at the same time and sense this special case. Lucky me, you are there for me, away from the chaos, and I am also there for you at the end of the day. Lucky us, we have always trusted to each other and never regretted. I want to thank to Şevki Can Cevher for the discussions about Organic Chemistry, trying to understand me and pushing me to think from a different point of view.

I wish to give my special thanks to my best friend Can Şenoymak. There has never been a person understands me better than you. Your wisdom has always led me to the right way for 18 years and will keep on leading, for sure. I would also like to thank Deniz Yahyabeyoğlu, Mine Özkal, Burcu Nayman, Poyraz Sağtekin, Mehmet Taştan and Gökhan Akın for their precious friendship. You are always there for me.

I would also thank TÜBİTAK and METU-BAP for the financial support.

Lastly, I would like to thank all my family. My mother, Şengül Sağesen, you have always achieved to be perfect and toast my mood up. You taught not to bow to or discriminate anybody. My father Haluk Sağesen, thanks for forcing me to be responsible, calm and reasonable. My grandfather Ziya Sağesen, I cannot imagine how a human can be that much noble, tactful, polite, smart, lively and perseverant and fair at the same time. I am the biggest fan of you. Finally, I want to thank my sweet niece Lina Nayman for giving me hope about the future.

## TABLE OF CONTENTS

ABSTRACT.....	v
ÖZ.....	vi
ACKNOWLEDGMENTS .....	ix
CHAPTERS .....	1
INTRODUCTION .....	1
1.1 Importance of Asymmetric Synthesis .....	1
1.2 The Methods Applied in Asymmetric Synthesis .....	2
1.2.1 Chiral Pool .....	2
1.2.2 Chiral Auxiliary .....	2
1.2.3 Catalytic Asymmetric Synthesis .....	3
1.2 Asymmetric Sulfa-Michael Reactions .....	17
1.4 Isatin.....	25
1.5 Aim of the work.....	27
RESULTS AND DISCUSSION.....	31
2.1 Synthesis of 1-Adamantyl Squaramide/Quinine Type Organocatalyst (I).....	31
2.2 Synthesis of <i>N</i> -Methyl Isatin Derived Nitroalkene 117a .....	32
2.3 Organocatalytic Sulfa-Michael Reaction.....	33
2.3.1 Effect of <i>N</i> -Substitution on Isatin Derived Nitroalkene.....	39
2.3.2 Derivatization Studies .....	43
2.3.3 Utilization of Sulfa-Michael Adduct.....	45
EXPERIMENTAL.....	48
3.1 Materials and Methods.....	48
3.2 Synthesis of 9-Amino(9-deoxy)quinine (126) .....	49
3.3 Synthesis of 1-Adamantyl Mono-Squaramide 129.....	49
3.4 Synthesis of 1-Adamantyl Squaramide/ Quinine catalyst I .....	50
3.5 Synthesis of <i>N</i> -Methyl substituted Isatin derived Nitroalkene 117a.....	50
3.6 General Procedure for the synthesis of Isatin derived nitroalkenes 117b-n.....	51
3.7 Asymmetric Sulfa-Michael Reaction: Addition of Methyl Thioglycolate 120 to <i>N</i> -Methyl Substituted Isatin derived Nitroalkene 117a.....	52
3.8 General Procedure for the Addition of Methyl Thioglycolate 120 to Isatin derived Nitroalkene 116 and <i>N</i> -Alkyl Substituted Isatin derived Nitroalkene 117b-n.....	53
3.8.1 Addition of Methyl Thioglycolate 120 to Isatin derived Nitroalkene 116.....	53
3.8.2 Addition of Methyl Thioglycolate (120) to <i>N</i> -Ethyl Isatin derived Nitroalkene 117b.....	54

3.8.3 Addition of Methyl Thioglycolate (120) to <i>N</i> -Allyl Isatin derived Nitroalkene 117c.....	55
3.8.4 Addition of Methyl Thioglycolate (120) to <i>N</i> -Benzyl Isatin derived Nitroalkene 117d.....	55
3.8.5 Addition of Methyl Thioglycolate (120) to <i>N</i> -Benzyl 5-Fluoro Isatin derived Nitroalkene 117e.....	56
3.8.6 Addition of Methyl Thioglycolate (120) to <i>N</i> -Benzyl 5-Bromo Isatin derived Nitroalkene 117f.....	57
3.8.7 Addition of Methyl Thioglycolate (120) to <i>N</i> -Benzyl 5-Methyl Isatin derived Nitroalkene 117g.....	57
3.8.8 Addition of Methyl Thioglycolate (120) to <i>N</i> -Benzyl 5-Methoxy Isatin derived Nitroalkene 117h.....	58
3.8.9 Addition of Methyl Thioglycolate (120) to <i>N</i> -Benzyl 5-Nitro Isatin derived Nitroalkene 117i.....	59
3.8.10 Addition of Methyl Thioglycolate (120) to <i>N</i> -Benzyl 5,7- <i>di</i> Methyl Isatin derived Nitroalkene 117j.....	59
3.8.11 Addition of Methyl Thioglycolate (120) to <i>N</i> -Benzyl 5,7- <i>di</i> Chloro Isatin derived Nitroalkene 117k.....	60
3.8.12 Addition of Methyl Thioglycolate (120) to <i>N</i> -Benzyl 7-Floro Isatin derived Nitroalkene 117l.....	61
3.8.13 Addition of Methyl Thioglycolate (120) to <i>N</i> -Benzyl 7-Bromo Isatin derived Nitroalkene 117m.....	61
3.8.14 Addition of Methyl Thioglycolate (120) to <i>N</i> -Benzyl 7-Chloro Isatin derived Nitroalkene 117n.....	62
3.8.15 Reduction of Nitro Group of Sulfa-Michael Adduct 121d.....	63
CONCLUSION .....	64
REFERENCES.....	66
NMR DATA.....	70
APPENDIX B .....	106
HPLC DATA .....	106

## LIST OF TABLES

<b>Table 1.</b> Catalyst Screening .....	34
<b>Table 2.</b> Solvent screening .....	35
<b>Table 3.</b> Solvent screening with 2-adamantyl and thiourea squaramide/quinine ( <b>II-VIII</b> ) .....	36
<b>Table 4.</b> Temperature screening .....	37
<b>Table 5.</b> Catalyst loading screening .....	38
<b>Table 6.</b> Concentration screening .....	39
<b>Table 7.</b> Effect of N-substitution on isatin derived nitroalkene <b>129a-d</b> .....	41
<b>Table 8.</b> Further optimization studies for N-benzyl substituted isatin derived nitroalkene <b>128d</b> .....	42
<b>Table 9.</b> Derivatization Studies .....	44

## LIST OF FIGURES

<b>Figure 1.</b> Different effects of two enantiomers of the chiral drugs .....	1
<b>Figure 2.</b> The most common organocatalysts.....	7
<b>Figure 3.</b> Electrophilic activation modes.....	8
<b>Figure 4.</b> Dual activation of squaramides.....	10
<b>Figure 5.</b> The delocalization of electron density upon (thio)ureas and squaramides .....	10
<b>Figure 6.</b> The distances between two acidic hydrogens at thiourea and squaramide .....	11
<b>Figure 7.</b> Cinchona alkaloids.....	11
<b>Figure 8.</b> The activation modes of quinuclidine ring of cinchona alkaloids .....	13
<b>Figure 9.</b> Activation of bifunctional organocatalyst.....	15
<b>Figure 10.</b> Bifunctionality of L-proline ( <b>57</b> ) .....	15
<b>Figure 11.</b> Organosulfur compounds in living organisms .....	18
<b>Figure 12.</b> Wynberg's and Houk's transition state models .....	19
<b>Figure 13.</b> Bifunctional activation modes .....	20
<b>Figure 14.</b> Transition state of sulfa-Michael addition to nitroolefins.....	22
<b>Figure 15.</b> The natural products bearing isatin skeleton.....	25
<b>Figure 16.</b> Selected reactions of isatin.....	26
<b>Figure 17.</b> The isatin derived nitroalkene part in natural products.....	27
<b>Figure 18.</b> Transformation of nitro group into some functional groups .....	28
<b>Figure 19.</b> Natural product and drugs bearing thiomorpholine-3-one.....	30
<b>Figure A. 1</b> <sup>1</sup> H NMR spectrum of <b>I</b> .....	70
<b>Figure A. 2</b> <sup>13</sup> C NMR spectrum of <b>I</b> .....	71
<b>Figure A. 3</b> <sup>1</sup> H NMR spectrum of <b>116</b> .....	72
<b>Figure A. 4</b> <sup>13</sup> C NMR spectrum of <b>116</b> .....	72
<b>Figure A. 5</b> <sup>1</sup> H NMR spectrum of <b>117a</b> .....	73
<b>Figure A. 6</b> <sup>13</sup> C NMR spectrum of <b>117a</b> .....	73
<b>Figure A. 7</b> <sup>1</sup> H NMR spectrum of <b>117b</b> .....	75
<b>Figure A. 8</b> <sup>13</sup> C NMR spectrum of <b>117b</b> .....	75
<b>Figure A. 9</b> <sup>1</sup> H NMR spectrum of <b>117c</b> .....	76
<b>Figure A. 10</b> <sup>13</sup> C NMR spectrum of <b>117c</b> .....	76
<b>Figure A. 11</b> <sup>1</sup> H NMR spectrum of <b>117d</b> .....	77
<b>Figure A. 12</b> <sup>13</sup> C NMR spectrum of <b>117d</b> .....	77

<b>Figure A. 13</b> $^1\text{H}$ NMR spectrum of <b>117e</b> .....	78
<b>Figure A. 14</b> $^{13}\text{C}$ NMR spectrum of <b>117e</b> .....	78
<b>Figure A. 15</b> $^1\text{H}$ NMR spectrum of <b>117f</b> .....	79
<b>Figure A. 16</b> $^{13}\text{C}$ NMR spectrum of <b>117f</b> .....	79
<b>Figure A. 17</b> $^1\text{H}$ NMR spectrum of <b>117g</b> .....	80
<b>Figure A. 18</b> $^{13}\text{C}$ NMR spectrum of <b>117g</b> .....	80
<b>Figure A. 19</b> $^1\text{H}$ NMR spectrum of <b>117h</b> .....	81
<b>Figure A. 20</b> $^{13}\text{C}$ NMR spectrum of <b>117h</b> .....	81
<b>Figure A. 21</b> $^1\text{H}$ NMR spectrum of <b>117i</b> .....	82
<b>Figure A. 22</b> $^{13}\text{C}$ NMR spectrum of <b>117i</b> .....	82
<b>Figure A. 23</b> $^1\text{H}$ NMR spectrum of <b>117j</b> .....	83
<b>Figure A. 24</b> $^{13}\text{C}$ NMR spectrum of <b>117j</b> .....	83
<b>Figure A. 25</b> $^1\text{H}$ NMR spectrum of <b>117k</b> .....	84
<b>Figure A. 26</b> $^{13}\text{C}$ NMR spectrum of <b>117k</b> .....	84
<b>Figure A. 27</b> $^1\text{H}$ NMR spectrum of <b>117l</b> .....	85
<b>Figure A. 28</b> $^{13}\text{C}$ NMR spectrum of <b>117l</b> .....	85
<b>Figure A. 29</b> $^1\text{H}$ NMR spectrum of <b>117m</b> .....	86
<b>Figure A. 30</b> $^{13}\text{C}$ NMR spectrum of <b>117m</b> .....	86
<b>Figure A. 31</b> $^1\text{H}$ NMR spectrum of <b>117n</b> .....	87
<b>Figure A. 32</b> $^{13}\text{C}$ NMR spectrum of <b>117n</b> .....	87
<b>Figure A. 33</b> $^1\text{H}$ NMR spectrum of <b>121a</b> .....	88
<b>Figure A. 34</b> $^{13}\text{C}$ NMR spectrum of <b>121a</b> .....	88
<b>Figure A. 35</b> $^1\text{H}$ NMR spectrum of <b>121b</b> .....	89
<b>Figure A. 36</b> $^{13}\text{C}$ NMR spectrum of <b>121b</b> .....	89
<b>Figure A. 37</b> $^1\text{H}$ NMR spectrum of <b>121c</b> .....	90
<b>Figure A. 38</b> $^{13}\text{C}$ NMR spectrum of <b>121c</b> .....	90
<b>Figure A. 39</b> $^1\text{H}$ NMR spectrum of <b>121d</b> .....	91
<b>Figure A. 40</b> $^{13}\text{C}$ NMR spectrum of <b>121d</b> .....	91
<b>Figure A. 41</b> $^1\text{H}$ NMR spectrum of <b>121e</b> .....	92
<b>Figure A. 42</b> $^{13}\text{C}$ NMR spectrum of <b>121e</b> .....	92
<b>Figure A. 43</b> $^1\text{H}$ NMR spectrum of <b>121f</b> .....	93
<b>Figure A. 44</b> $^{13}\text{C}$ NMR spectrum of <b>121f</b> .....	93
<b>Figure A. 45</b> $^1\text{H}$ NMR spectrum of <b>121g</b> .....	94
<b>Figure A. 46</b> $^{13}\text{C}$ NMR spectrum of <b>121g</b> .....	94
<b>Figure A. 47</b> $^1\text{H}$ NMR spectrum of <b>121h</b> .....	95



<b>Figure A. 48</b>	$^{13}\text{C}$ NMR spectrum of <b>121h</b> .....	95
<b>Figure A. 49</b>	$^1\text{H}$ NMR spectrum of <b>121i</b> .....	96
<b>Figure A. 50</b>	$^{13}\text{C}$ NMR spectrum of <b>121i</b> .....	96
<b>Figure A. 51</b>	$^1\text{H}$ NMR spectrum of <b>121j</b> .....	97
<b>Figure A. 52</b>	$^{13}\text{C}$ NMR spectrum of <b>121j</b> .....	97
<b>Figure A. 53</b>	$^1\text{H}$ NMR spectrum of <b>121k</b> .....	98
<b>Figure A. 54</b>	$^{13}\text{C}$ NMR spectrum of <b>121k</b> .....	98
<b>Figure A. 55</b>	$^1\text{H}$ NMR spectrum of <b>121l</b> .....	99
<b>Figure A. 56</b>	$^{13}\text{C}$ NMR spectrum of <b>121l</b> .....	99
<b>Figure A. 57</b>	$^1\text{H}$ NMR spectrum of <b>121m</b> .....	100
<b>Figure A. 58</b>	$^{13}\text{C}$ NMR spectrum of <b>121m</b> .....	100
<b>Figure A. 59</b>	$^1\text{H}$ NMR spectrum of <b>121n</b> .....	101
<b>Figure A. 60</b>	$^{13}\text{C}$ NMR spectrum of <b>121n</b> .....	101
<b>Figure A. 61</b>	$^1\text{H}$ NMR spectrum of <b>122d</b> .....	102
<b>Figure A. 62</b>	$^{13}\text{C}$ NMR spectrum of <b>122d</b> .....	102
<b>Figure A. 63</b>	$^1\text{H}$ NMR spectrum of <b>132a</b> .....	103
<b>Figure A. 64</b>	$^{13}\text{C}$ NMR spectrum of <b>132a</b> .....	103
<b>Figure A. 65</b>	$^1\text{H}$ NMR spectrum of <b>133</b> .....	104
<b>Figure A. 66</b>	$^{13}\text{C}$ NMR spectrum of <b>133</b> .....	104
<b>Figure B. 1</b>	HPLC chromatogram of rac- <b>121a</b> .....	106
<b>Figure B. 2</b>	HPLC chromatogram of enantiomerically enriched <b>121a</b> .....	106
<b>Figure B. 3</b>	HPLC chromatogram of rac- <b>121b</b> .....	107
<b>Figure B. 4</b>	HPLC chromatogram of enantiomerically enriched <b>121b</b> .....	107
<b>Figure B. 5</b>	HPLC chromatogram of rac- <b>121c</b> .....	108
<b>Figure B. 6</b>	HPLC chromatogram of enantiomerically enriched <b>121c</b> .....	108
<b>Figure B. 7</b>	HPLC chromatogram of rac- <b>121d</b> .....	109
<b>Figure B. 8</b>	HPLC chromatogram of enantiomerically enriched <b>121d</b> .....	109
<b>Figure B. 9</b>	HPLC chromatogram of rac- <b>121e</b> .....	110
<b>Figure B. 10</b>	HPLC chromatogram of enantiomerically enriched <b>121e</b> .....	110
<b>Figure B. 11</b>	HPLC chromatogram of rac- <b>121f</b> .....	111
<b>Figure B. 12</b>	HPLC chromatogram of enantiomerically enriched <b>121f</b> .....	111
<b>Figure B. 13</b>	HPLC chromatogram of rac- <b>121g</b> .....	112
<b>Figure B. 14</b>	HPLC chromatogram of enantiomerically enriched <b>121g</b> .....	112

<b>Figure B. 15</b> HPLC chromatogram of rac- <b>121h</b> .....	113
<b>Figure B. 16</b> HPLC chromatogram of enantiomerically enriched <b>121h</b> .....	113
<b>Figure B. 17</b> HPLC chromatogram of rac- <b>121i</b> .....	114
<b>Figure B. 18</b> HPLC chromatogram of enantiomerically enriched <b>121i</b> .....	114
<b>Figure B. 19</b> HPLC chromatogram of rac- <b>121j</b> .....	115
<b>Figure B. 20</b> HPLC chromatogram of enantiomerically enriched <b>121j</b> .....	115
<b>Figure B. 21</b> HPLC chromatogram of rac- <b>121k</b> .....	116
<b>Figure B. 22</b> HPLC chromatogram of enantiomerically enriched <b>121k</b> .....	116
<b>Figure B. 23</b> HPLC chromatogram of rac- <b>121l</b> .....	117
<b>Figure B. 24</b> HPLC chromatogram of enantiomerically enriched <b>121l</b> .....	117
<b>Figure B. 25</b> HPLC chromatogram of rac- <b>121m</b> .....	118
<b>Figure B. 26</b> HPLC chromatogram of enantiomerically enriched <b>121m</b> .....	118
<b>Figure B. 27</b> HPLC chromatogram of rac- <b>121n</b> .....	119
<b>Figure B. 28</b> HPLC chromatogram of enantiomerically enriched <b>121n</b> .....	119
<b>Figure B. 29</b> HPLC chromatogram of rac- <b>133</b> .....	120
<b>Figure B. 30</b> HPLC chromatogram of enantiomerically enriched <b>133</b> .....	120

## LIST OF SCHEMES

<b>Scheme 1.</b> Synthesis of (S)-(-)-4-Isopropyl-2-oxazolidinone ( <b>3</b> ) by chiral pool method ...	2
<b>Scheme 2.</b> Evan's aldol reaction with oxazolidinone derivative used as chiral auxiliary.....	3
<b>Scheme 3.</b> The selective reduction biocatalyzed by Baker's yeast.....	4
<b>Scheme 4.</b> Kinetic resolution done with Novozyme 435.....	4
<b>Scheme 5.</b> Knowles's asymmetric hydrogenation of carbon-carbon double bond.....	5
<b>Scheme 6.</b> Sharpless epoxidation of allylic alcohol.....	5
<b>Scheme 7.</b> BINAP-Ruthenium complex catalyzed hydrogenation.....	6
<b>Scheme 8.</b> The first use of urea derivatives as organocatalyst.....	8
<b>Scheme 9.</b> (Thio)urea organocatalyzed Strecker reaction .....	9
<b>Scheme 10.</b> Application of acid functionalities as organocatalysts .....	9
<b>Scheme 11.</b> Rawal's squaramide type organocatalyst at Michael addition .....	10
<b>Scheme 12.</b> The first asymmetric sulfa-Michael addition .....	12
<b>Scheme 13.</b> DMAP catalyzed nucleophilic addition .....	13
<b>Scheme 14.</b> DMAP as an alternative to enzymes in kinetic resolutions.....	14
<b>Scheme 15.</b> Application of Fu's planar chiral DMAP derivative catalyst.....	14
<b>Scheme 16.</b> L-proline ( <b>57</b> ) catalyzed aldol reaction .....	15
<b>Scheme 17.</b> Takemoto's organocatalysts used in aldol reactions .....	16
<b>Scheme 18.</b> The application of 2-AminoDMAP/squaramide type organocatalysts .....	17
<b>Scheme 19.</b> The application of quinine/squaramide type organocatalysts .....	17
<b>Scheme 20.</b> The metabolism of acrylamide.....	18
<b>Scheme 21.</b> Sulfa-Michael addition in the defense mechanism of unicellular caulerpa taxifolia.....	18
<b>Scheme 22.</b> The first catalytic sulfa-Michael reaction.....	19
<b>Scheme 23.</b> Squaramide type quinine catalyzed sulfa-Michael addition.....	20
<b>Scheme 24.</b> Organocatalytic sulfa-Michael addition to nitrostyrene .....	21
<b>Scheme 25.</b> Michael addition to nitroolefins .....	21
<b>Scheme 26.</b> Desymmetrization of $\beta$ -lactam derivative .....	22
<b>Scheme 27.</b> Phosphoric acid catalyzed sulfa-Michael addition to isatin derived ketimines .....	23
<b>Scheme 28.</b> Quinine derived sulfonamide catalyzed sulfa-Michael addition to isatin derived ketimines .....	23

<b>Scheme 29.</b> A sulfa-Michael/Michael cascade reaction .....	24
<b>Scheme 30.</b> A domino sulfa-Michael/Michael reaction .....	24
<b>Scheme 31.</b> A sulfa-Michael/aldol cascade reaction .....	25
<b>Scheme 32.</b> An instance for the synthesis of spirooxindoles.....	27
<b>Scheme 33.</b> Sulfa-Michael addition of methyl thioglycolate ( <b>120</b> ) to isatin derived nitroalkenes <b>117</b> .....	29
<b>Scheme 34.</b> The second part of the synthetic plan.....	29
<b>Scheme 35.</b> Synthetic route applied for 1-adamantyl squaramide/quinine ( <b>I</b> ) .....	31
<b>Scheme 36.</b> Synthetic route applied for N-methyl substituted isatin derived nitroalkene <b>117a</b> .....	32
<b>Scheme 37.</b> The background sulfa-Michael reaction .....	33
<b>Scheme 38.</b> Synthetic route for N-substituted isatin derived nitroalkene <b>128b-d</b> .....	40
<b>Scheme 39.</b> Synthetic route for isatin derived nitroalkene <b>128a</b> .....	40
<b>Scheme 40.</b> Various N-benzyl substituted isatin derived nitroalkenes <b>117e-n</b> and their isolated yields.....	43
<b>Scheme 41.</b> Reduction of nitro group.....	46
<b>Scheme 42.</b> Trials for the cyclization reaction .....	46

## LIST OF ABBREVIATIONS

<b>BINAP</b>	2,2'-bis(Diphenylphosphino)-1,1'-binaphthyl
<b>DABCO</b>	1,4-diazabicyclo[2.2.2]octane
<b>DBU</b>	1,8-Diazabicyclo[5.4.0]undec-7-ene
<b>DIAD</b>	<i>di</i> Isopropyl azodicarboxylate
<b>DMAP</b>	4- <i>di</i> Methylamino pyridine
<b>DOPA</b>	3,4-dihydroxyphenylalanine
<b>DPPA</b>	<i>di</i> Phenylphosphoryl azide
<b>HOMO</b>	Highest occupied molecular orbital
<b>LUMO</b>	Lowest unoccupied molecular orbital
<b><i>t</i>-Boc</b>	<i>tert</i> -Butoxycarbonyl

# CHAPTER 1

## INTRODUCTION

### 1.1 Importance of Asymmetric Synthesis

The majority of the compounds related to living organisms are chiral. The chiral molecules are asymmetric in other words, they do not possess mirror plane symmetry. The asymmetric molecule has at least one carbon that substituted four different groups. In the case of having one chiral carbon, the molecule has two nonsuperimposable enantiomers.<sup>1</sup> Although, enantiomers have the same physical properties, they are different on physiologic aspects. The chiral molecules in living systems, for instance enzymes are binding to substrates with a specific orientation, otherwise noxious formations may show up. It is also valid for pharmaceuticals. Each enantiomer of many chiral drugs, has different activity on human body. Penicillamine,<sup>2</sup> propranolol,<sup>3</sup> and thalidomide<sup>4</sup> are known instances (Figure 1).

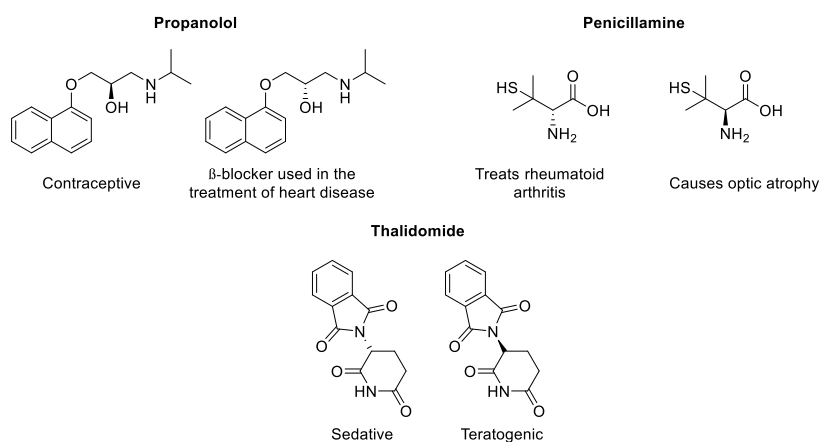


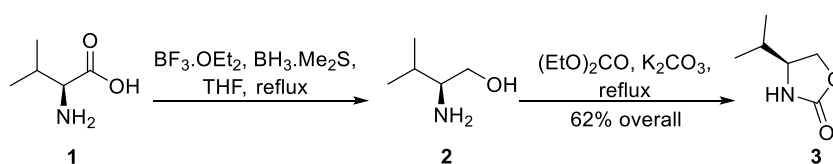
**Figure 1.** Different effects of two enantiomers of the chiral drugs

Since the asymmetry of the molecules are that much vital for human life, scientists work on asymmetric synthesis for a long time. Synthesis of one enantiomer selectively is reasonable in many respect. Biologically active compounds are almost enantiopure. When the racemate of the target molecule is synthesized, half of the material will be the waste after the isolation of desired enantiomer. This method also doubles the work required in the process, hence it is time and energy consuming.

## 1.2 The Methods Applied in Asymmetric Synthesis

### 1.2.1 Chiral Pool

Chiral pool method aims to convert enantiopure natural products to chiral target molecules. The method is efficient but the number of enantiopure natural products is finite. Therefore, the applicability of the method is restricted.<sup>5</sup> As a representative example, the transformation of *L*-valine (**1**) is used as a chiral pool in the synthesis of (*S*)-(-)-4-Isopropyl-2-oxazolidinone (**3**) (Scheme 1).<sup>6</sup>

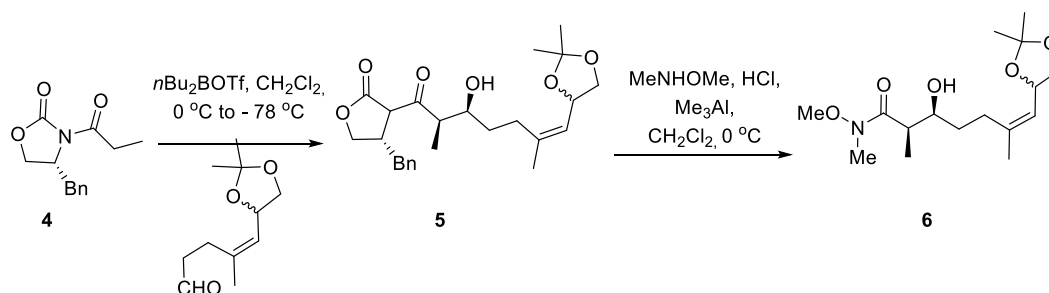


**Scheme 1.** Synthesis of (*S*)-(-)-4-Isopropyl-2-oxazolidinone (**3**) by chiral pool method

### 1.2.2 Chiral Auxiliary

Chiral auxiliaries are enantiopure molecules and have well-determined configurations. They are generally derived from natural products such as carbohydrates and amino acids. Chiral auxiliary is bonded to substrate to introduce chiral information to the product. Generally, chiral auxiliary is removed

easily in the final step under mild conditions. Oxazolidinone derivatives **4** are popular chiral auxiliaries which are highly studied by Evans and coworkers. In the synthesis of quassine and bruceatine, the degraded triptene lactones, the key step is Evans aldol reaction of an aldehyde with oxazolidinone derivative (Scheme 2).<sup>7</sup>



**Scheme 2.** Evan's aldol reaction with oxazolidinone derivative used as chiral auxiliary

### 1.2.3 Catalytic Asymmetric Synthesis

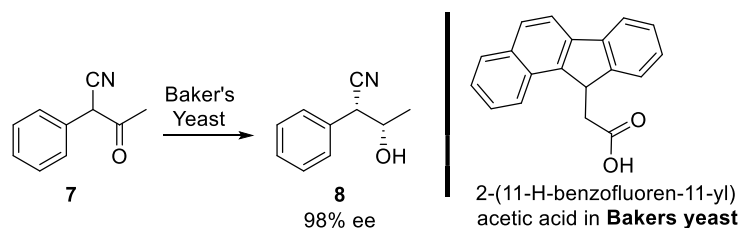
Asymmetric synthesis is performed in the presence of the chiral reagents in either stoichiometric or catalytic amount. The stoichiometric process converts one mol of starting material into one mol of product by using one mole of chiral reagent. As there is no catalytic turnover, the reaction becomes costly by means of atom economy. It is obvious that transformation of larger amounts of substrates with catalytic amount of chiral reagent is much more valuable synthetically.<sup>8</sup> The asymmetric catalysts are divided into three groups namely, biocatalysts, transition metal catalysts and organocatalysts.

#### 1.2.3.1 Biocatalysts

Enzymes or peptides catalyze the reactions in living organisms. They perform in biological transformations besides, biocatalysts also have synthetic applications. These catalysts can form the enantiopure compounds via either kinetic resolution or direct introduction of chiral information. They lower the activation barrier of the reaction and provide high stereoselectivity. Biocatalysts are biodegradable and

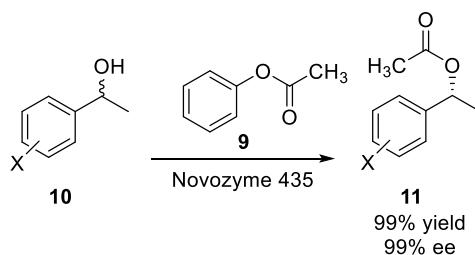


nontoxic. 2-(11H-benzofluoren-11-yl)acetic acid in Baker's yeast, the leavening agent of baking bread is used as biocatalysts in the selective reduction of butanenitrile derivative **7** (Scheme 3).<sup>9</sup>



**Scheme 3.** The selective reduction biocatalyzed by Baker's yeast

Novozyme 435, a commercially available biocatalyst is utilized as biocatalyst in the kinetic resolution of *rac*-1-phenyl ethanol (**10**) to phenylacetate (**11**) at high yield and ee (Scheme 4).<sup>10</sup>

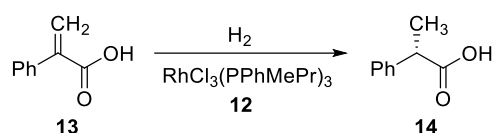


**Scheme 4.** Kinetic resolution done with Novozyme 435

### 1.2.3.2 Transition Metal Catalyst

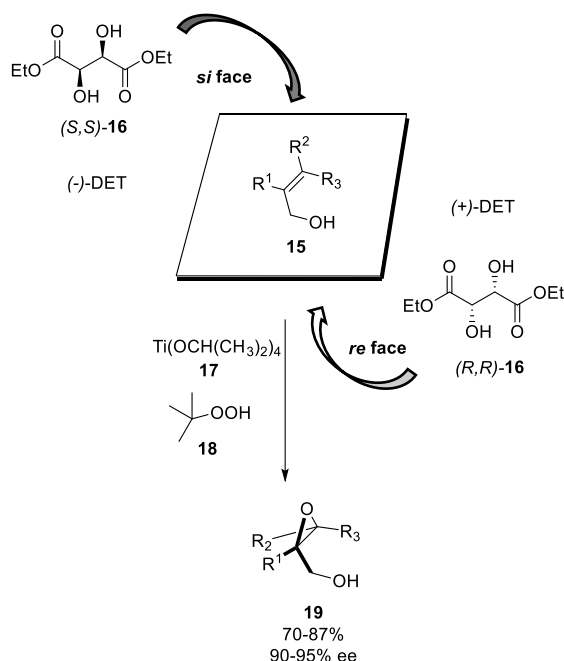
Metals, generally transition metals, and chiral ligands coordinated to the metal, constitutes transition metal catalyst. Highly enantioselective adducts can be synthesized with transition metal catalysts however, heavy metal pollution continues to be a critical concern. The pioneering works in this area were done by Knowless, Noyori and Sharpless who were awarded the Nobel Prize in Chemistry in 2001.

In 1968, Knowles discovered Rhodium metal with chiral ligand, can catalyze the hydrogenation of carbon-carbon double bond in the reduction of  $\alpha$ -phenylacrylic acid (**13**) to (+)-hydratopic acid (**14**) (Scheme 5).<sup>11</sup> Afterwards, he applied this method in the synthesis of L-DOPA, a biologically active amino acid.



**Scheme 5.** Knowles's asymmetric hydrogenation of carbon-carbon double bond

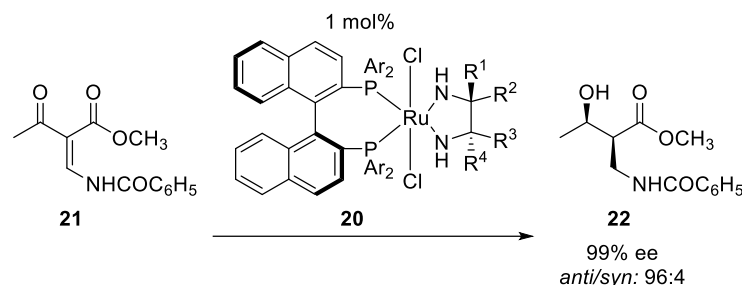
Sharpless developed a number of catalysts which catalyze oxidation, especially epoxidation reactions. But his seminal work was the asymmetric epoxidation of allylic alcohols **15** with titanium tetrakisopropoxide catalyst **17** which led to high enantioselectivities (up to 95% ee) (Scheme 6).<sup>12</sup>



**Scheme 6.** Sharpless epoxidation of allylic alcohol

Noyori designed BINAP-Ruthenium complex **20** as a catalyst to be used in the hydrogenation of olefins **21**. BINAP-Ruthenium complex catalyst promotes the

synthesis of (*R*)-1,2-propanediol (**22**) which is included some antibiotic (Scheme 7).<sup>13</sup>



**Scheme 7.** BINAP-Ruthenium complex catalyzed hydrogenation

### 1.2.3.3 Organocatalyst

Organocatalysts accelerate the transformations by directing the reaction to a different pathway with lower activation barrier. They promote the reactions via binding substrates. They can act as acids and bases while activating electrophile and/or nucleophile.

Organocatalysts have superior properties over metal and biocatalysts. In the nature, the reactions are mostly metal-free because of the ingenious balance between metal-free and metal-mediated transformations. Metal sources product contamination undoubtedly, besides they are high priced. Organocatalysts can be used under oxygen atmosphere with wet solvents. They are more stable than enzymes and can be anchored to solid support in consideration of reusability.

Organocatalysts drew attention about 20 years ago by spearheading studies of List, Barbas, MacMillan, Jørgensen and Jacobsen. Figure 2 demonstrates some of the organocatalysts developed in these studies.<sup>14a-d</sup>

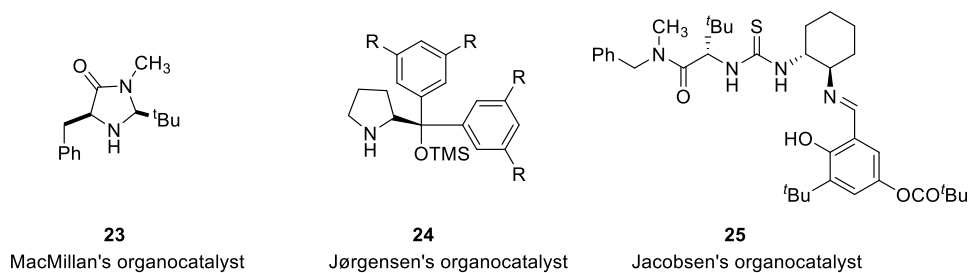


**Figure 2.** The most common organocatalysts

### Classification of Organocatalysts:

**Covalent:** covalent intermediate between substrate and catalyst. Enamine and iminium catalysis can be classified in this group. In enamine catalysis, the nucleophile, in the case of being enolate anion, can be transformed into enamine with chiral secondary amine, reversibly.<sup>15</sup> The most common example of enamine catalysts is the natural, cheap, and very successful *L*-proline (**57**).<sup>16</sup> Another instance is iminium catalysis where a chiral secondary amine activates the acceptor, reversibly.

**Noncovalent:** bases on noncovalent interactions such as hydrogen bonding or formation of ion pairs. Typical hydrogen bond donors, namely (thio)ureas, act as pseudo Lewis acids.

Catalytic functions of hydrogen bonds:

1. Arrangement the reactants. Hydrogen bond donor attached to a chiral pool, determines the selectivity.
2. Activation of the reactants by changing the electron density.
3. Stabilization of the developing negative charge of transition state or intermediate. Due to being noncovalent interaction, hydrogen bond is flexible and the length of the bond can expand or shorten.<sup>17</sup>

Organocatalytic aldol reactions proceed basically through three activation modes.

The first one is acid catalyzed activation mode. The Lewis or Brønsted acid catalysts activates the electrophile toward nucleophilic attack, mimicking enzymes.<sup>18</sup>

Metal-mediated Lewis acid, iminium ion formation and hydrogen bonding are utilized for electrophilic activation (Figure 3).<sup>19</sup>

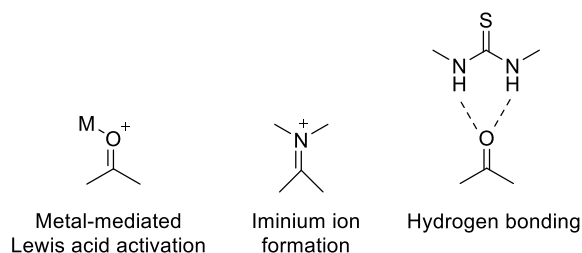
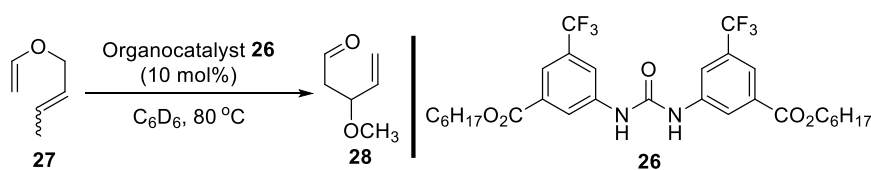


**Figure 3.** Electrophilic activation modes

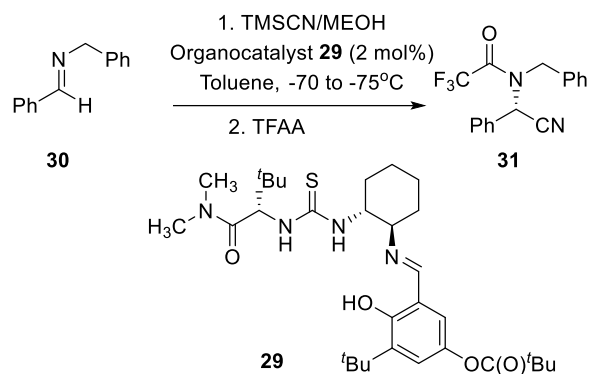
The hydrogen bonding catalysts such as (thio)ureas which were designed as the potential ligands to Lewis acidic metals, decreases the electron density around the acceptor.

In 1994, Curran and coworkers first used urea derivative **21** as catalyst in Claisen rearrangement of allyl vinyl ether **22** (Scheme 8).<sup>20</sup>



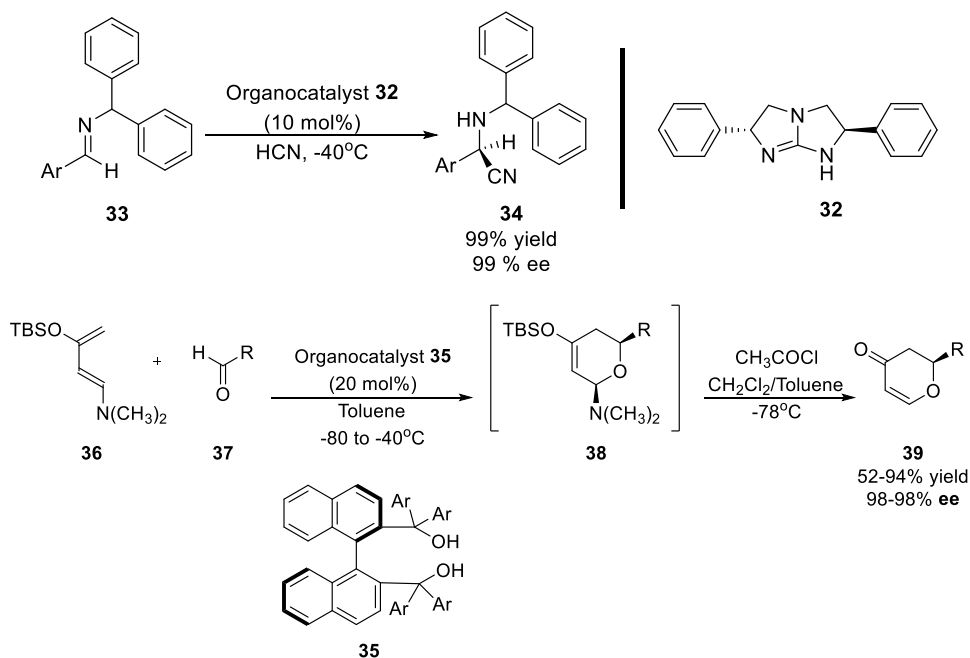
**Scheme 8.** The first use of urea derivatives as organocatalyst

Afterwards, Jacobsen and coworkers discovered that urea and thiourea derivatives **24** catalyzed the Strecker reaction and enhanced enantioselectivity (Scheme 9).<sup>21</sup>



**Scheme 9.** (Thio)urea organocatalyzed Strecker reaction

Chiral acidic organocatalysts with different hydrogen bond donor functionalities such as guanidines **32** or BINAP derivatives **35** were developed after that breakthrough study of Jacobsen (Scheme 10).<sup>22</sup>



**Scheme 10.** Application of acid functionalities as organocatalysts

In 2008, Rawal and coworkers introduced squaramide acidic moiety which resembles (thio)urea derivatives but has superior features compared to them. They tested the squaramide moiety attached to cinchona alkaloid **40** in Michael addition



The distance between two N-H groups in squaramide is greater than that in (thio)ureas, which give rise to a higher spacer. The square geometry of the squaramide makes the formed hydrogen bond more linear and supplies different binding properties in transition states (Figure 6).<sup>26</sup>

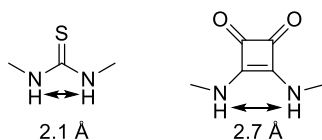


**Figure 6.** The distances between two acidic hydrogens at thiourea and squaramide

The base catalyzed mode is the second activation mode of catalytic asymmetric aldol reactions.

Brønsted base catalysts are widely used, longstanding catalysts. They activate the nucleophile via abstracting its hydrogen and let it attack. The first emerged Brønsted base catalysts are cinchona alkaloids which are natural products and isolated from the bark cinchona trees. Cinchona alkaloids are versatile molecules, they possess many functional groups such as alcohol and vinyl units, quinuclidine ring and quoniline moiety with many stereogenic centers which enable to catalyze the reactions asymmetrically. Cinchona alkaloid family consists of quinine, quinidine, cinchonidine and cinchonine which are pseudoenantiomers of each other (Figure 7).<sup>27</sup>

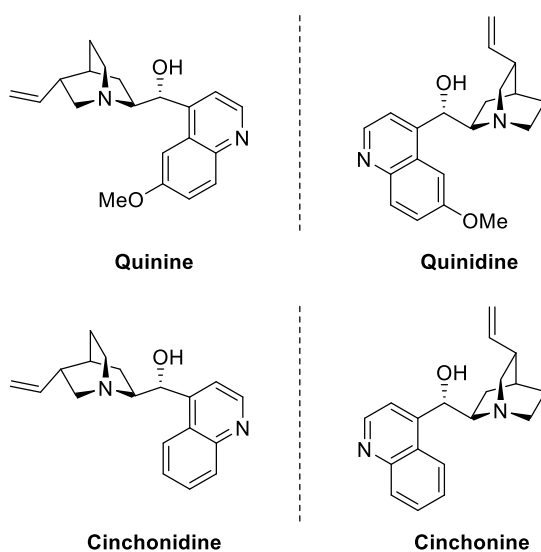
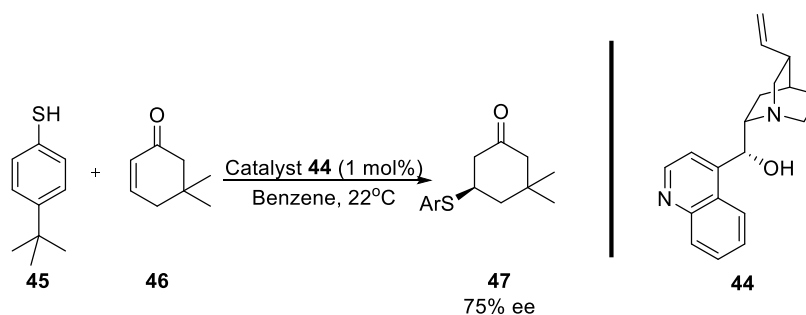


**Figure 7.** Cinchona alkaloids



Wynberg states that, the natural organocatalysts, enzymes can produce only one enantiomer of the chiral compounds, though, each enantiomers of chiral compounds may compose versatile end product. Thus, it is clear that scientists need to synthesize enzyme alternatives.<sup>28</sup>

In 1977, Wynberg utilized Brønsted base catalyst Cinchonine (**44**) in conjugate addition of 4-(*tert*-butyl)benzene thiol (**45**) to 5,5-dimethylcyclohex-2-en-1-one (**46**) (Scheme 12). The study was a milestone in asymmetric organocatalysis, since the cinchona alkaloids are still utilized to catalyze numerous carbon-carbon and carbon-heteroatom bond forming reaction.<sup>29</sup>



**Scheme 12.** The first asymmetric sulfa-Michael addition

Cinchona alkaloid organocatalyst have three roles in terms of activation. Quinuclidine part can act as Brønsted base and deprotonate the pronucleophile. In another case, quinuclidine ring can behave as nucleophile activator and react with pronucleophile. The third mission is the formation of quaternary ammonium salt of the N-substituted quinuclidine ring which acts as phase-transfer catalyst and stabilizes nucleophile (Figure 8).<sup>30</sup>

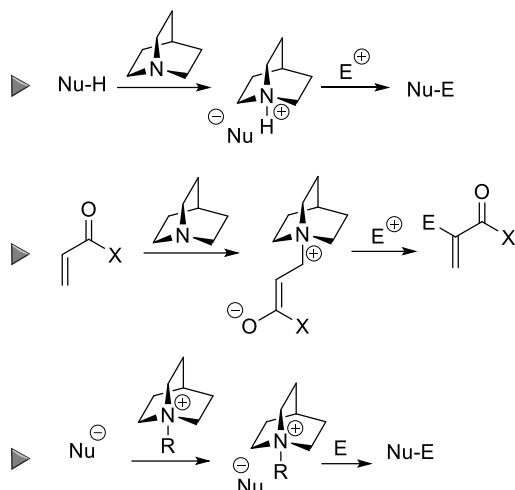
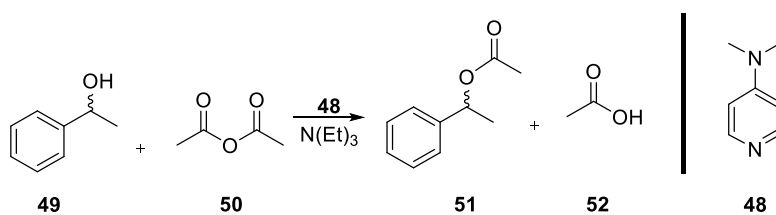


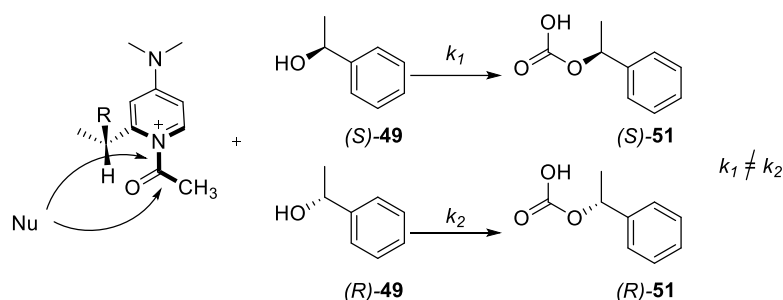
**Figure 8.** The activation modes of quinuclidine ring of cinchona alkaloids

Dialkylaminopyridines are widely used Lewis base catalysts. They act as nucleophilic catalysts in acetylation, alkylation reactions and several rearrangements (Scheme 13).<sup>31</sup> The mechanistic studies show that the reaction starts with the nucleophilic attack of DMAP (**48**), resulted in the formation of ion pair by the elimination of acetyl group. The interaction between the nucleophile **49** and electrophile **50**, DMAP (**48**) is eliminated, and catalytic cycle is completed.<sup>32</sup>



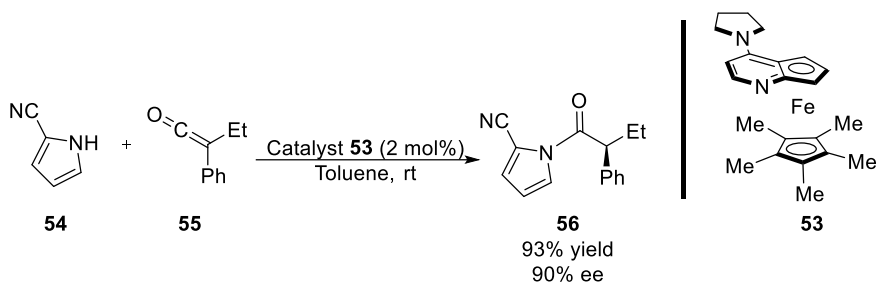
**Scheme 13.** DMAP catalyzed nucleophilic addition

DMAP (**48**) is an alternative to enzymes in kinetic resolutions. The different reaction rates of two enantiomers provides kinetic resolution while reacting to intermediates, comprise of chiral DMAP (**48**) and the substrate (Scheme 14).<sup>33</sup>



**Scheme 14.** DMAP as an alternative to enzymes in kinetic resolutions

Fu and coworkers developed planar chiral DMAP derivatives which acts as Brønsted base catalyst. In their study, 2-cyanopyrrole (**54**) was added to prochiral ketene **55** enantioselectively with 4-(pyrrolidino)pyridine derivative **53**. Their study was seminal with regard to utilizing DMAP for many purposes (Scheme 15).<sup>34</sup>



**Scheme 15.** Application of Fu's planar chiral DMAP derivative catalyst

The last but most precious activation mode for asymmetric reactions is bifunctional activation. The bifunctional organocatalysts involves both acidic and basic moiety. These moieties cause dual activation of nucleophile and electrophile simultaneously. The basic part is responsible for raising the HOMO of the nucleophile, while the acidic part decreases the LUMO of the electrophile, thereby the activation energy of the reaction is reduced (Figure 9).

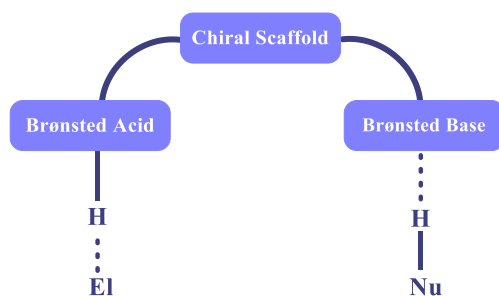
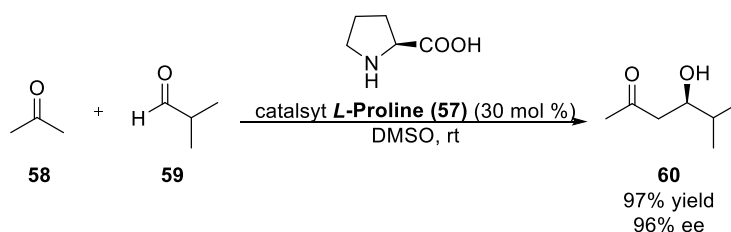


**Figure 9.** Activation of bifunctional organocatalyst

The organocatalysts are defined as artificial enzymes.<sup>35</sup> Enzymes are proteins that catalyze the reactions in living organisms. But a much smaller of its substitute, amino acids also have bifunctional character. The most common, simple, successful, cheap and readily available amino acid is *L*-proline (**57**).<sup>16</sup> In 2000, List and Barbas investigated asymmetric aldol reaction of acetone (**58**) with isobutyraldehyde **59** by the catalysis of *L*-proline (**57**) with excellent enantioselectivity and yield (Scheme 16).



**Scheme 16.** *L*-proline (**57**) catalyzed aldol reaction

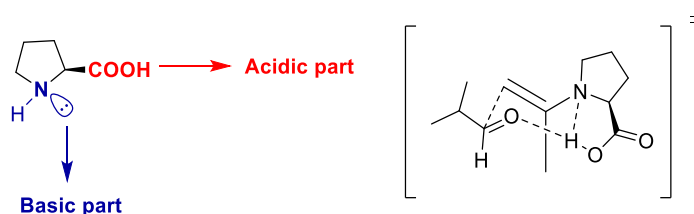
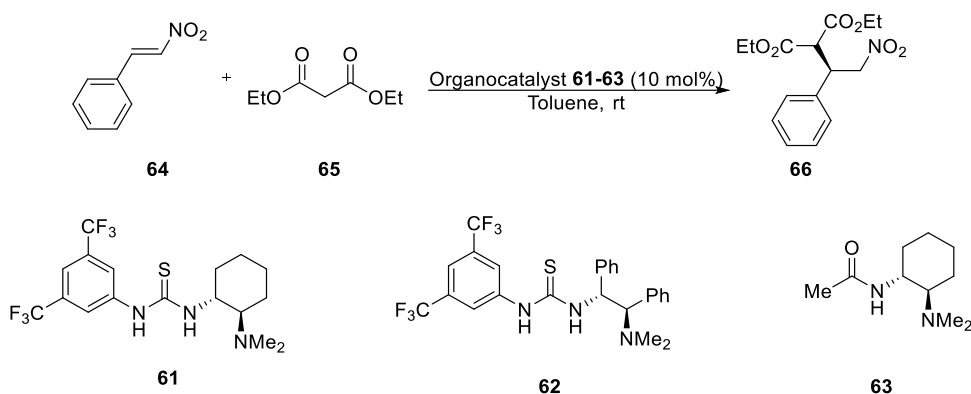


**Figure 10.** Bifunctionality of *L*-proline (**57**)

The transition state of the aldol reaction points out the bifunctionality of (*L*)-proline (**57**). A six-membered cyclic structure is formed at the transition state.

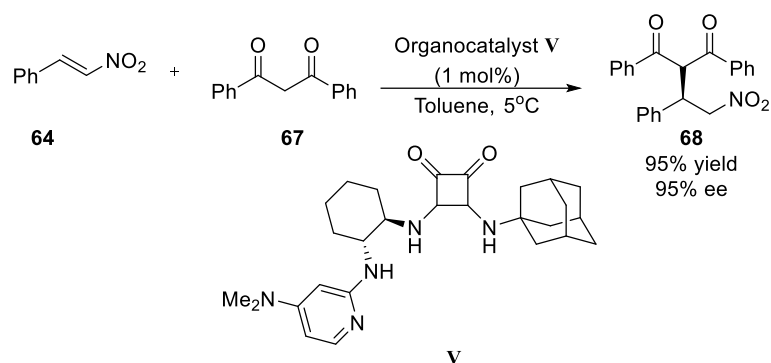
While acid hydrogen activates isobutyraldehyde (**59**) through hydrogen bonding, nitrogen of secondary amine forms enamine with acetone (**58**), thereby restricted substrates react with a defined orientation (Figure 10).

A ground-breaking study came out in 2003 by Takemoto and coworkers. Their organocatalysts bearing thiourea and amino groups were inspired by Schreiner's thioureacatalyst. The catalytic activity of the organocatalysts **61-63** was investigated in the conjugate addition of diethyl malonate (**65**) to *trans*-( $\beta$ )-nitrostyrene (**64**), and accomplished encouraging results (35-93% ee) (Scheme 17).<sup>36</sup>



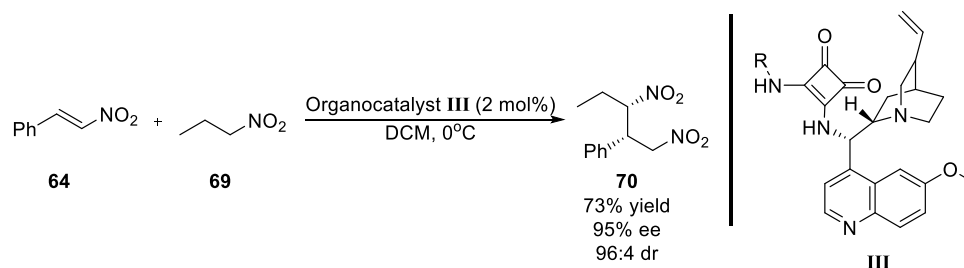
**Scheme 17.** Takemoto's organocatalysts used in aldol reactions

In 2014, Tanyeli and coworkers reported unique 2-aminoDMAP/Squaramides which are efficient as bifunctional organocatalysts. They investigated the catalytic activity of 2-aminoDMAP/Squaramides **V** in conjugate addition of dibenzoylmethane (**67**) to *trans*-( $\beta$ )-nitrostyrene derivatives **64**. The addition occurred with very high enantioselectivity at 1 mol% catalyst loading (Scheme 18).<sup>37</sup>



**Scheme 18.** The application of 2-AminoDMAP/squaramide type organocatalysts

Two years later, they published an article about quinine- based squaramides, merging two well-known catalyst parts. In their study, Michael additions of nitroethane (**69**) to various *trans*-( $\beta$ )-nitrostyrenes (**64**) were carried out in the presence of a number of quinine-based *t*-butyl squaramide **V** with advanced diastereomeric ratios and enantiomeric excesses (Scheme 19).<sup>38</sup>



**Scheme 19.** The application of quinine/squaramide type organocatalysts

## 1.2 Asymmetric Sulfa-Michael Reactions

Sulfa-Michael reaction is the conjugate addition of thiol to an unsaturated compound. Asymmetric sulfa-Michael reactions enable enantiomerically enriched thioethers that can be used as chiral building blocks. Organosulfur compounds, such as amino acids (cysteine, methionine), peptides have vital functions in metabolism of living things (Figure 11).<sup>39</sup>

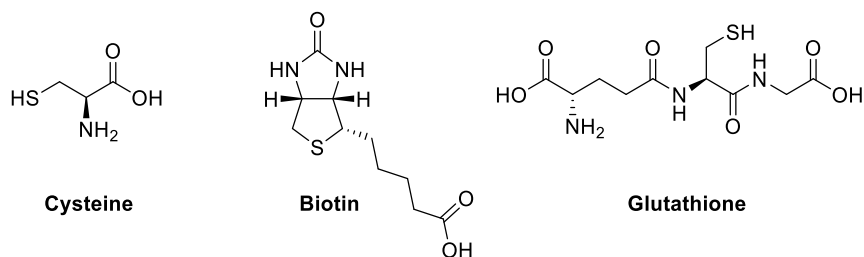
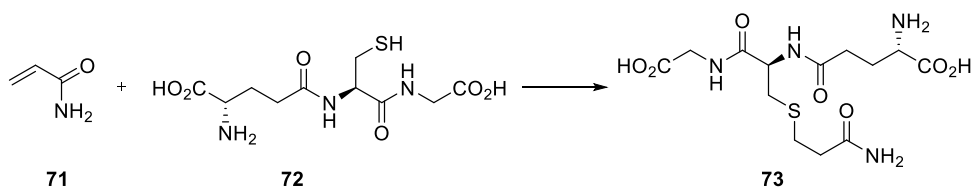


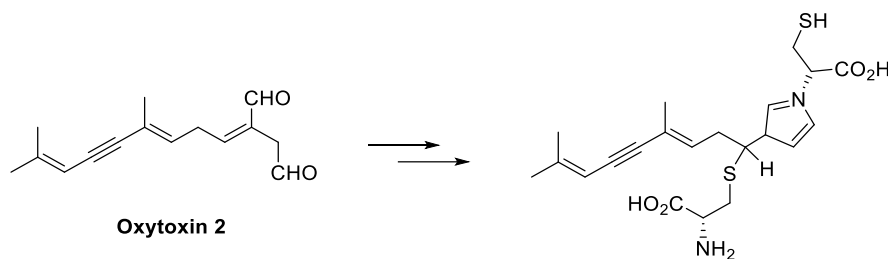
**Figure 11.** Organosulfur compounds in living organisms

The metabolism of acrylamide (**71**) that is a toxic constituent of heated food, is led off by sulfa-Michael addition of glutathione **72** to the double bond of acrylamide (**71**) (Scheme 20).



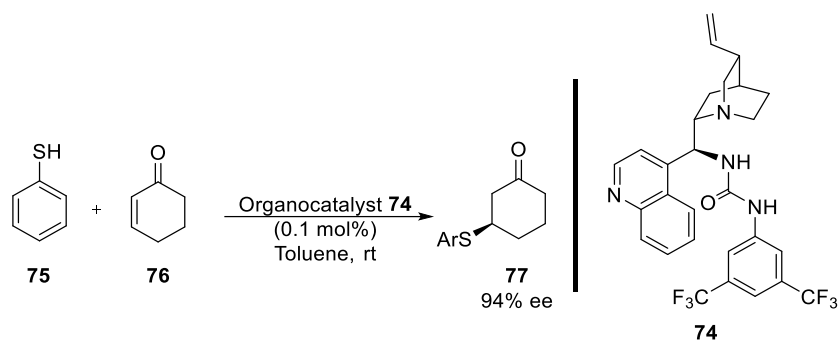
**Scheme 20.** The metabolism of acrylamide

The sulfa-Michael addition of cysteine to oxytoxin 2 takes part in the defense mechanism of unicellular caulerpa taxifolia against mechanic injury via wound closure in the presence of lysine (Scheme 21).



**Scheme 21.** Sulfa-Michael addition in the defense mechanism of unicellular caulerpa taxifolia

In 2016, Houk and coworkers studied the mechanism of catalytic sulfa-Michael reaction, as the addition of thiophenol (**75**) to cyclohexenone (**76**) using cinchonidine/urea organocatalyst **74** (Scheme 22).<sup>40</sup>



**Scheme 22.** The first catalytic sulfa-Michael reaction

The cinchonidine/urea catalyst **74** produced greater ee than cinchonidine (**44**) produced. Hence, Houk and coworkers proposed that changing catalyst may alter the mechanism. Dual activation of cinchonidine/urea catalyst **74** may stabilize transition state, further. Wynberg's model represents thiolate-quinuclidinium tight ion pair and quinine hydroxy group-cyclohexanone oxygen hydrogen bond. Houk's computational investigation confutes Wynberg's model, herein, thiolate is bonded to hydroxy group of cinchonidine (**44**) and cyclohexanone (**76**) is activated by ammonium ion of quinuclidinium ring. The Houk's model is preferred because of the stabilization of developing alkoxide by proton transfer from quinuclidinium ring (Figure 12).

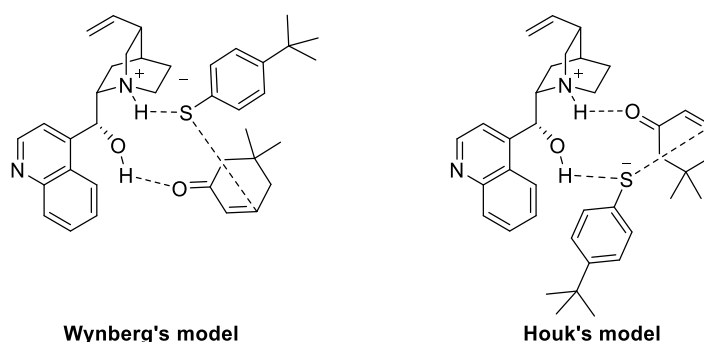


**Figure 12.** Wynberg's and Houk's transition state models

Their study also reveals that the urea acidic part prevents self-aggregation of the catalyst via the interaction with methoxy group of quinoline ring due to the increasing steric demands. The increasing steric demands can conduce to catalyst concentration independent enantioselectivity.



After one year, Wong and coworkers postulated the modes of bifunctional activation of carbon-sulfur bond forming step. Mode A resembles Wynberg's model whereas Mode B represents Houk's model. Two alternative modes, C and D were suggested, but they were not found to be energetically favored. Moreover, the steric repulsion between chalcone and catalyst disabled the interaction. The investigations indicate that mode B is more favored in terms of further stabilization of the developing alkoxide (Figure 13).

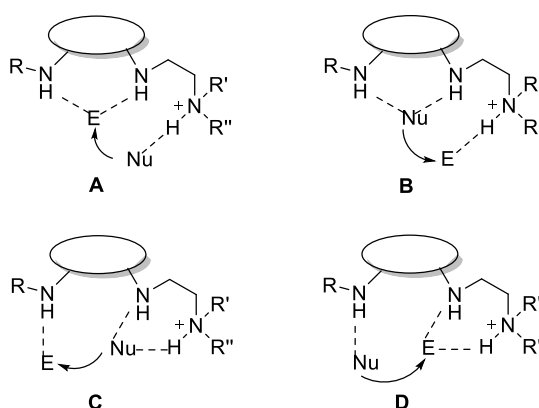
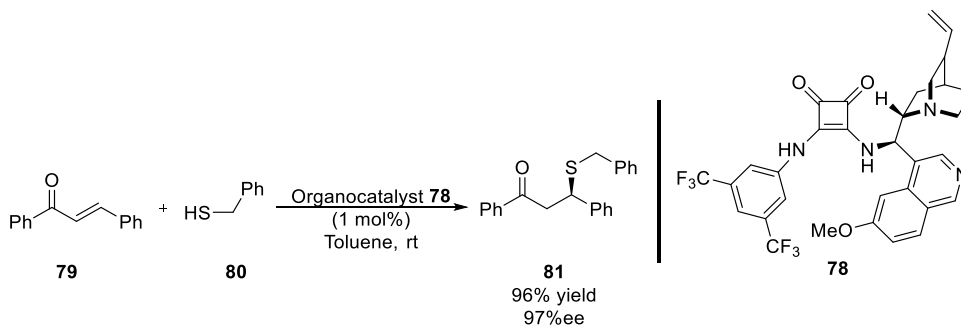


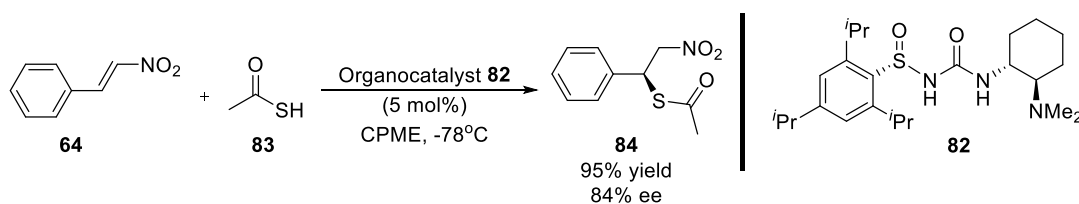
**Figure 13.** Bifunctional activation modes

Wong and coworkers tested the possible modes of activation in the sulfa-Michael addition of phenylmethanethiol (**80**) to chalcone (**79**), using squaramide type quinine catalyst **78**. Mode B is favored also for squaramide type catalyst **78**. More acidic squaramide stabilized thiolate ion better and trifluoromethyl groups also increased acidity and stabilize the transition state more. Consequently, excellent yield and ee were obtained (Scheme 23).<sup>41</sup>



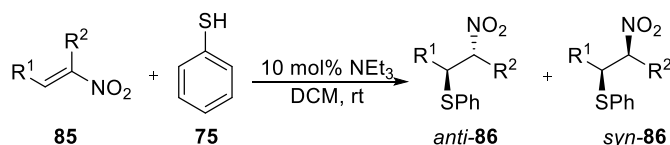
**Scheme 23.** Squaramide type quinine catalyzed sulfa-Michael addition

In 2009, Ellmann and coworkers performed sulfa-Michael addition of thioacetic acid (**83**) to the most common Michael acceptor, *trans*-( $\beta$ )-nitrostyrenes (**64**) by the catalysis of *tert*-amine/sulfinyl urea **82** with excellent yield and ee. The formed aminothiols **84** involves in compounds of pharmaceutical interest (Scheme 24).



**Scheme 24.** Organocatalytic sulfa-Michael addition to nitrostyrene

The investigation of the diastereoselectivity in sulfa-Michael reactions are limited, compared to the ones about enantioselectivity. One of these studies, belongs to Wang and coworkers, examines kinetic and thermodynamic control in sulfa-Michael addition of thiols to nitroalkenes (Scheme 25).<sup>42</sup>



**Scheme 25.** Michael addition to nitroolefins

The reaction yields both *anti*- and *syn*- products. Full conversion occurs after 1 hour. But, after addition of triethylamine and stirring only for 10 seconds, 70% yield is obtained and *anti*/*syn* selectivity is 93:7. Interestingly, after 1 hour, *anti*/*syn* selectivity drops to 40:60. The decrease in selectivity is attributed to the kinetic and thermodynamic control of the reaction. Sulfa-Michael addition is kinetically controlled at first, but thermodynamically controlled at the end. Hence, the reaction time is key factor for diastereoselectivity. Epimerization occurs in the

presence of triethylamine. The steric bulkiness on vicinal carbon to nitro group causes a depression in diastereoselectivity. On the other hand, increased steric hindrance on germinal carbon declines the epimerization and improves the diastereoselectivity (Figure 14).

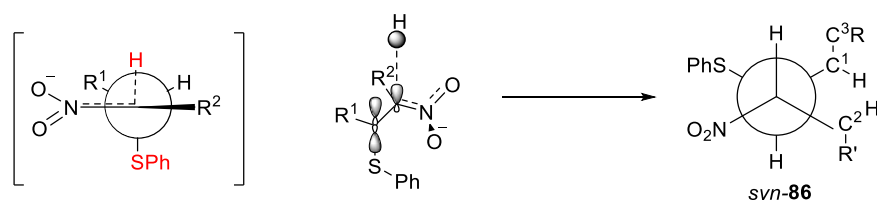
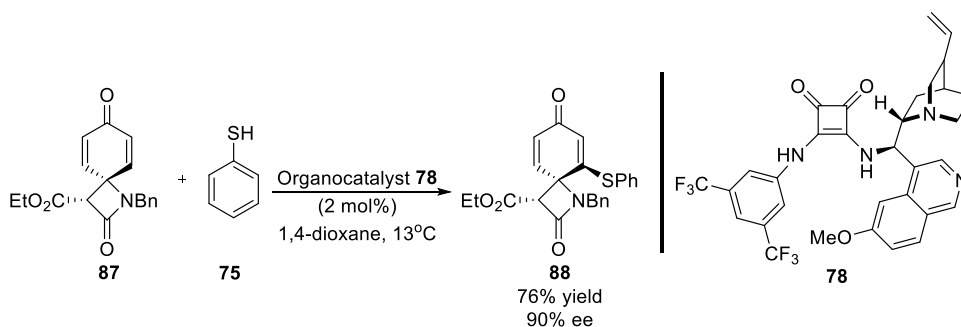


**Figure 14.** Transition state of sulfa-Michael addition to nitroolefins

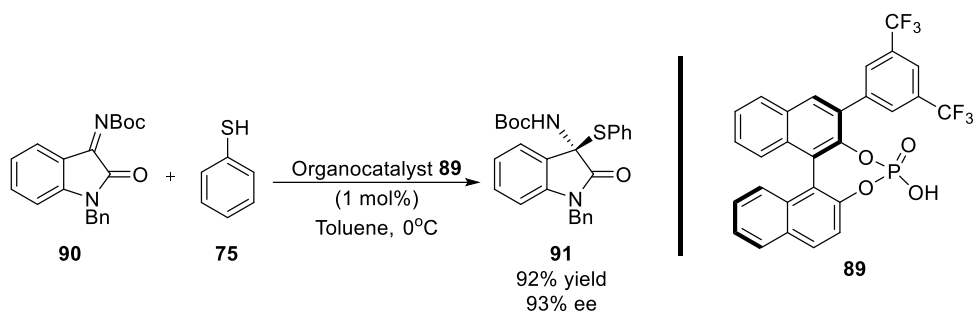
The  $\beta$ -lactam systems are well-known because of their antibiotic properties and various biological activities. Although the intramolecular addition of  $\beta$ -lactams is highly studied, there are not much articles about intermolecular addition of  $\beta$ -lactams for desymmetrization. Chauhan and coworkers planned an asymmetric sulfa-Michael addition/ protocol for 2,5-cyclohexadienone  $\beta$ -lactam (**87**) which led to dynamic kinetic resolution. A quinine based squaramide type organocatalyst **78** was employed in the addition of thiophenol (**75**) to 2,5-cyclohexadienone  $\beta$ -lactam (**87**) to form spirocyclohexene  $\beta$ -lactam **88** with excellent ee and good yield (Scheme 26).<sup>43</sup>



**Scheme 26.** Desymmetrization of  $\beta$ -lactam derivative

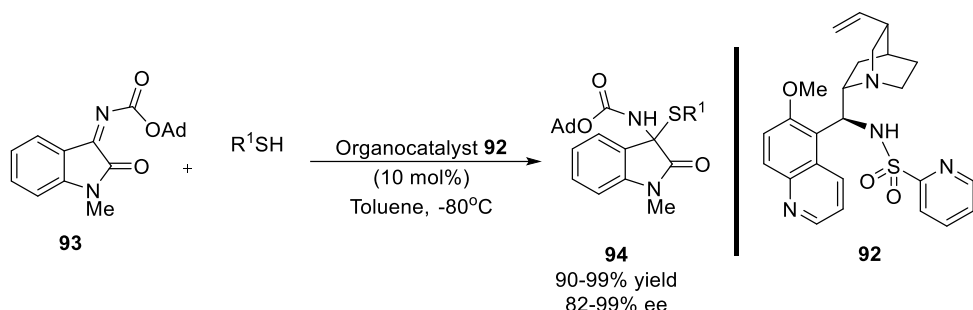
Biologically active and synthetically useful isatin derived ketimines are used in many transformations. One of them is the addition of thiophenol (**75**) to *N*-Boc protected isatin derived ketimine **90** in the presence of chiral phosphoric acid organocatalyst **89**. 1,2-Addition of thiols is not a common protocol, besides this

work is the first example of asymmetric 1,2-addition of thiols to isatin derived ketimines. The highly selective adduct, oxindole based (*S, N*)-acetal **91** may be precursor for bioactive compounds (Scheme 27).<sup>44</sup>



**Scheme 27.** Phosphoric acid catalyzed sulfa-Michael addition to isatin derived ketimines

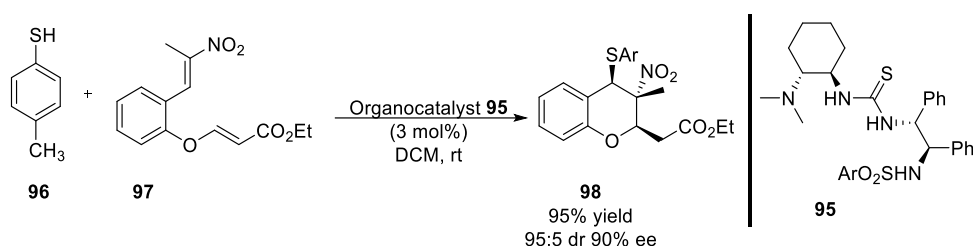
In the same year, Nakamura and coworkers also developed a protocol for 1,2-addition of thiols to isatin derived ketimines **93**. The addition reaction was performed in the presence of quinine derived sulfonamide catalyst **92** with various thiols. They also obtained oxindole based (*S, N*)-acetal **94** with excellent ee (Scheme 28).<sup>39</sup>



**Scheme 28.** Quinine derived sulfonamide catalyzed sulfa-Michael addition to isatin derived ketimines

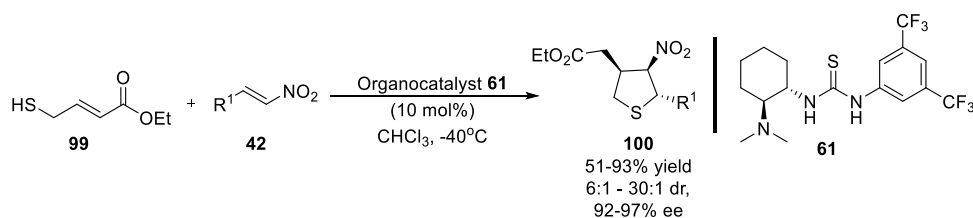
The cascade Michael/Michael reactions lead to many bicyclic and spiro compounds. Moreover, starting from simple and readily available starting materials transforms into complex molecules in reduced steps, with reduced waste. One of the pronounced method is the synthesis of chromans. Chroman skeleton is present in many biologically active compounds such as (-)-siccanin, exhibiting anti-fungal activity, and Gamma secretase inhibitor, a potent in the

treatment of Alzheimer's disease. In 2010, Chen and coworkers investigated the sulfa-Michael/Michael cascade reaction of *p*-thiocresol (**96**) and nitroolefin enoate **97** by the catalysis of *tert*-amine attached thiourea **95**. At low catalyst loading, the diastereo- and enantioselectivity of the chroman **98** reached to 90% (Scheme 29).<sup>45</sup>



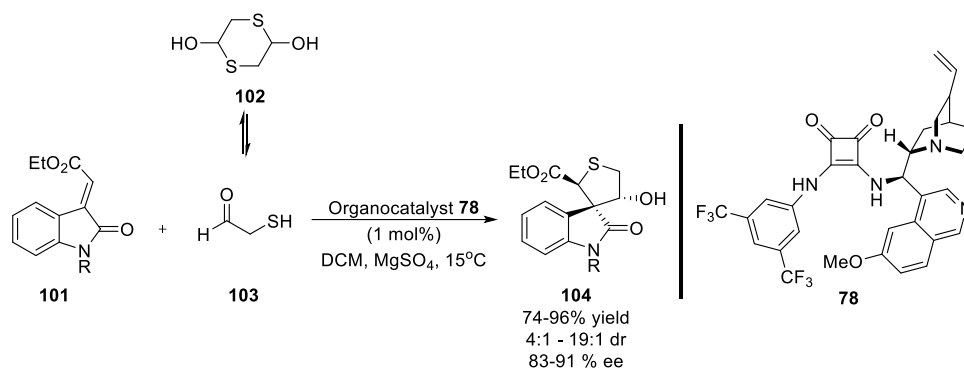
**Scheme 29.** A sulfa-Michael/Michael cascade reaction

A withstanding instance of Domino sulfa-Michael/Michael reactions is the synthesis of trisubstituted tetrahydrothiophenes **100** from mercapto-2-butenolate **99** and nitrostyrenes **42** with *tert*-amine/thiourea catalyst **61** with good selectivity. The authors stated that dynamic kinetic resolution occurs in addition to stereocontrol through hydrogen bonding (Scheme 30).<sup>46</sup>



**Scheme 30.** A domino sulfa-Michael/Michael reaction

In 2012, Xiao and coworkers published an inspiring study about organocatalytic sulfa-Michael/aldol cascade reaction of 3-ylidexindoles **101** and 1,4-dithiane-2,5-diol (**102**). The quinine derived squaramide **78** mediated reaction proceeded through formal [3+2] annulation to yield spirocyclic oxindole **104**. Excellent enantioselectivities were obtained in mild conditions (Scheme 31).<sup>47</sup>



**Scheme 31.** A sulfa-Michael/aldol cascade reaction

## 1.4 Isatin

Isatin was independently discovered by Erdmann and Laurent in 1841, as an oxidation product of indigo. Hofmann and Baeyer conducted several experiments in order to find out the structure of isatin. But its current structure was suggested by Kekulé. As Baeyer found out isatic acid salt with the treatment of isatin (**105**) with a base, Kekulé discovered that isatin (**105**) is the lactam of the isatic acid salt.<sup>48</sup>

Isatin is found in plants of *genus* *Isatis* and a metabolic derivative of adrenaline in human body.<sup>49</sup> Furthermore, it is found in many natural and synthetic pharmaceuticals. (*R*)-(+)-Dioxibrassinin (**106**) is located in the cytoplasm of cell and also in brassicas and cauliflower, which makes it a potential biomarker. 1,4-benzothiazine linked isatin derivatives **107** have antifungal activity.<sup>50</sup> Phthalimidoxo substituted spiro-thiazolidinone **108** has good antibacterial activity (Figure 15).<sup>51</sup>

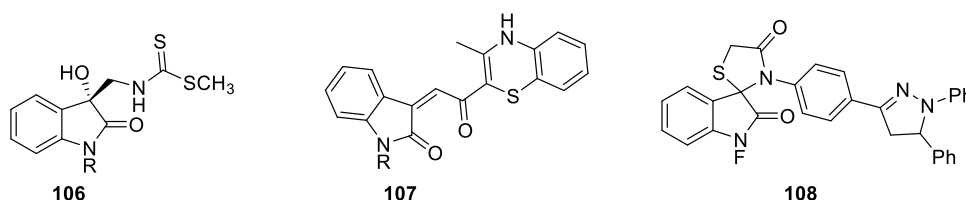


**Figure 15.** The natural products bearing isatin skeleton

Its precious structure permits isatin (**105**) to take part into many transformations. The carbonyl carbon at third position has highly electrophilic character whereas, nitrogen of the amino group acts as nucleophile. As demonstrated in Figure 16, the reaction of C3 of isatin (**105**) with hydrazinecarbothioamide forms thiosemicarbazone (**109**). In the presence of a nitroalkane and a base, the C3 gives Henry adduct **110**. Indolylolation of isatin (**105**) in acidic media yields **111**. *N*-alkyl substituted isatins **112** are synthesized from isatin (**105**) with an alkyl halide in the presence of potassium carbonate. *N*-halosacchrains are monohalogenation reagents for mono-halogenation of isatin (**105**). Schiff base of isatin **113** can be easily produced by using a primary amine and acetic acid. A secondary amine addition to the Schiff base **113** in formaldehyde transforms it into Mannich base **115** (Figure 16).<sup>50</sup>

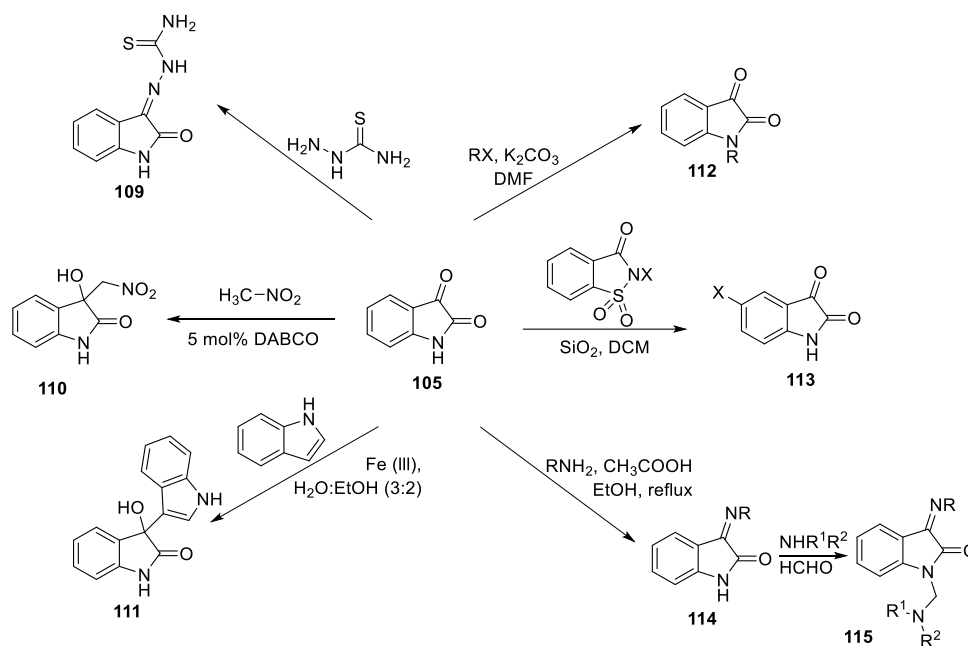


**Figure 16.** Selected reactions of isatin

The Henry adduct **110** can undergo the elimination reaction of the hydroxyl group. The product, isatin derived nitroalkene **116** is found in the structure of the natural products such as Wasalexin A (**117**) which is antimicrobial and antioxidative substance, and found in Japanese horseradish.<sup>52</sup> *N*-alkyl substituted isatin derived nitroalkenes **118** also shows cytotoxic activity against lung cancer cells (Figure 17).<sup>53</sup>

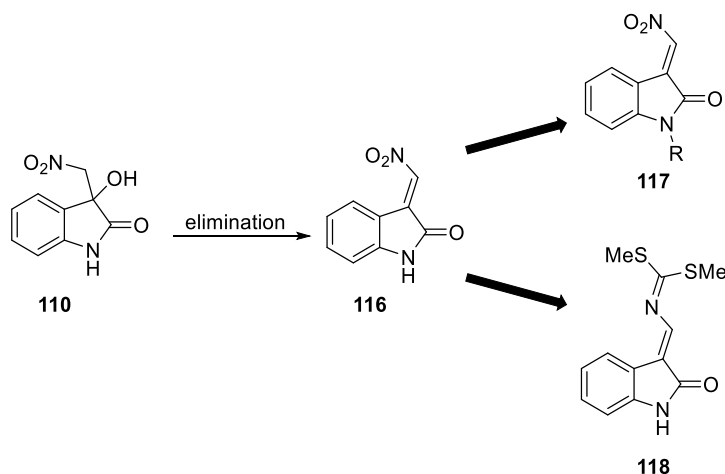
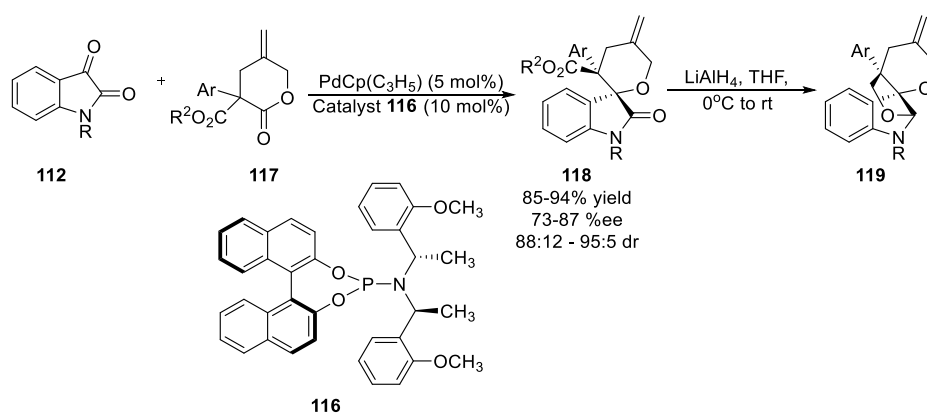


**Figure 17.** The isatin derived nitroalkene part in natural products

The diversified reactivity of isatin enables to form spirooxindoles that are potent drug molecules. For instance, decarboxylative cyclization of *N*-substituted isatin **112** with carboxylate **117** gives spirooxindole **118** in the presence of Pd metal and BINAP catalysts **116** selectively. Further transformations are possible after cyclization such as reduction of amine carbonyl of the product **118** (Scheme 32).

50



**Scheme 32.** An instance for the synthesis of spirooxindoles

### 1.5 Aim of The Work

The nitroolefines are the most common Michael acceptors due to their high reactivity. The electronwithdrawing effect of the nitro group eases any



nucleophilic attack through nitroolefin.<sup>54</sup> Moreover, the nitro group is a multifunctional group, it can transform into several functional groups such as oxime, nitrile oxide, amine, azide, and even carbonyl compounds by Nef reaction (Figure 18).<sup>55</sup>

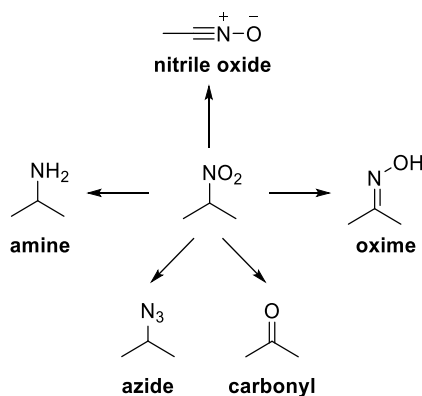
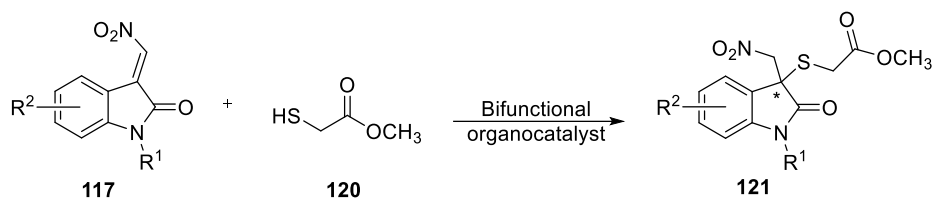


**Figure 18.** Transformation of nitro group into some functional groups

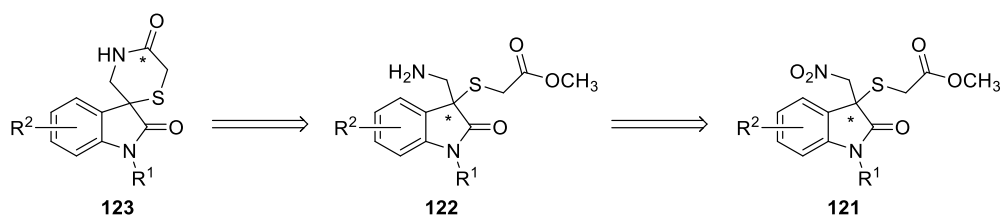
On the other hand, the pharmaceutical properties of isatin (**105**) such as antifungal, anxiogenic and antibacterial activities, aforementioned above, make isatin an attractive precursor for many transformations. The highly reactive C-3 carbonyl group of isatin (**105**) is a prochiral center as well.<sup>49</sup>

In the light of this information, isatin derived nitroalkene **117** can be a beneficial acceptor for Michael additions. The asymmetric sulfa-Michael addition, the valuable one among other Michael additions, gives rise to enantio enriched organosulfur compounds that can be utilized for pharmaceutical purposes or further transformations.<sup>56</sup> Thioglycolates are less toxic and relatively inexpensive sulfa-Michael donor. What is more, the study of Northrop and coworkers reveals that  $\alpha,\beta$ -unsaturated ketones reacts selectively methyl thioglycolate (**120**) in the presence of thiophenol (**75**).<sup>57</sup> Considering all of these, enantioselective sulfa-Michael addition of methyl thioglycolate (**120**) to isatin derived nitroalkenes **117** would be a convenient work (Scheme 33).



**Scheme 33.** Sulfa-Michael addition of methyl thioglycolate (**120**) to isatin derived nitroalkenes **117**

The asymmetric sulfa-Michael reaction was planned to achieve by the catalysis of our bifunctional organocatalysts. Solvent, temperature, catalyst loading and concentration screenings and derivatization studies were done in order to enhance enantioselectivity. The second part of our synthetic plan was the reduction of nitro group of **121** in order to cyclize the resultant molecule. (Scheme 34)



**Scheme 34.** The second part of the synthetic plan

The cyclization product involves thiomorpholine-3-one moiety which is present in natural products and drugs. For instance, thiazine derivatives have potassium channel opening activity.<sup>58</sup> One of the natural products, Conicaquione A is used in the treatment of brain tumor.<sup>59</sup> Thienothiazine based compounds are vasopressin receptors and have antagonistic activity (Figure 19).<sup>60</sup>

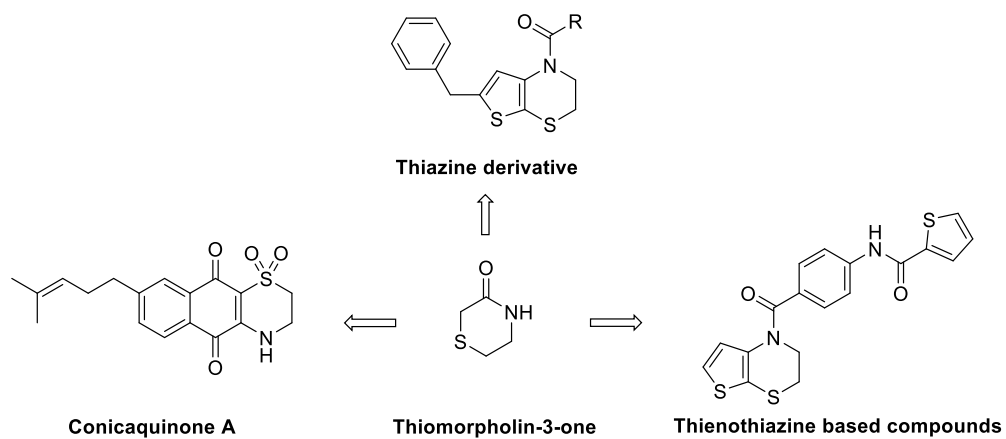


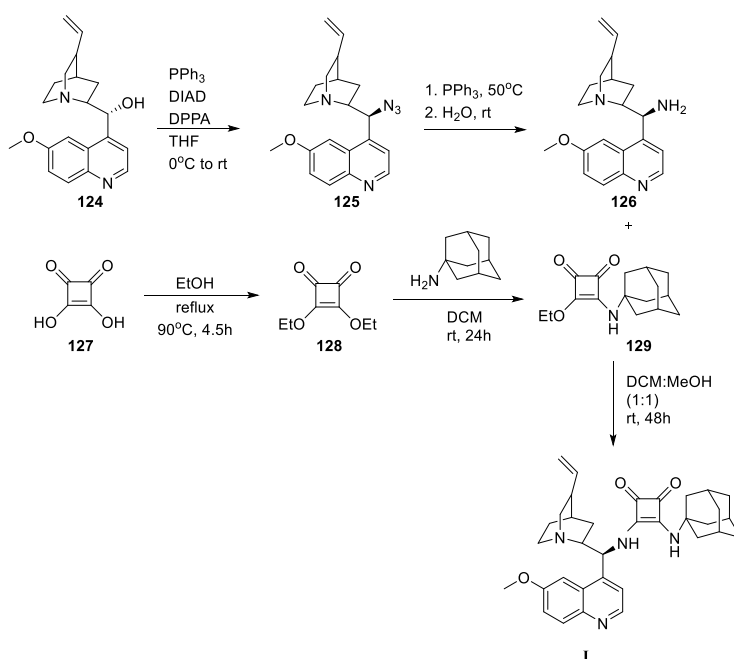
**Figure 19.** Natural product and drugs bearing thiomorpholine-3-one

## CHAPTER 2

### RESULTS AND DISCUSSION

#### 2.1 Synthesis of 1-Adamantyl Squaramide/Quinine Type Organocatalyst (I)

All the studies done in this thesis aimed to get enantiomerically enriched methyl thioglycolate attached isatin derived nitroalkene derivatives. Chiral induction has been tried by asymmetric bifunctional acid/base type organocatalysts developed in our research group which are quinine and 2-aminoDMAP based bifunctional organocatalysts. Their acidic parts consist of 1-adamantyl squaramide, 2-adamantyl squaramide, *tert*-butyl squaramide, urea and thiourea units.<sup>61</sup> As a representative example, herein, the synthesis of 1-adamantyl squaramide quinine **I** is given (Scheme 35).<sup>38</sup>

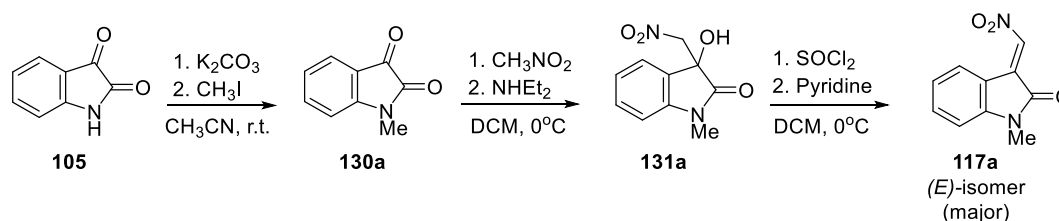


**Scheme 35.** Synthetic route applied for 1-adamantyl squaramide/quinine (**I**)

The basic part of organocatalyst was prepared by applying Mitsunobu reaction, followed by Staudinger reduction.<sup>62</sup> The acidic part synthesis of target organocatalysts begins with squaric acid (**127**) which was refluxed in ethanol for 4.5 h to afford diethyl squarate (**128**) with quantitative yield.<sup>23</sup> Subsequent addition of 1-adamantyl amine to diethyl squarate (**128**) in DCM resulted in monosquaramide **129** at room temperature for 24 h. The already prepared acidic and basic parts combined by stirring in 1:1 ratio of DCM:MeOH solvent system to yield desired organocatalyst **I**.<sup>63</sup>

## 2.2 Synthesis of *N*-Methyl Isatin Derived Nitroalkene **117a**

As the first step, *N*-alkylation reaction was carried out. Methyl group was chosen as model alkyl group due to its simplicity. The procedure in the literature was applied.<sup>55</sup> Potassium carbonate and iodomethane were added to the solution of isatin (**105**) in acetonitrile. After acidic workup, the product **130a** was purified by recrystallization with ethyl acetate. In the second step, Henry reaction was performed via the addition of diethyl amine and nitromethane to the *N*-methyl substituted isatin **131a** in DCM. The resultant hydroxyl unit was transformed into a good leaving group by thionyl chloride and subsequent elimination triggered by pyridine afforded the target isatin derived nitroalkene **117a** as (*E*)- and (*Z*)- isomers ((*E*):(*Z*) ratio 3:1) with moderate yield (74%) (Scheme 36).<sup>58</sup>

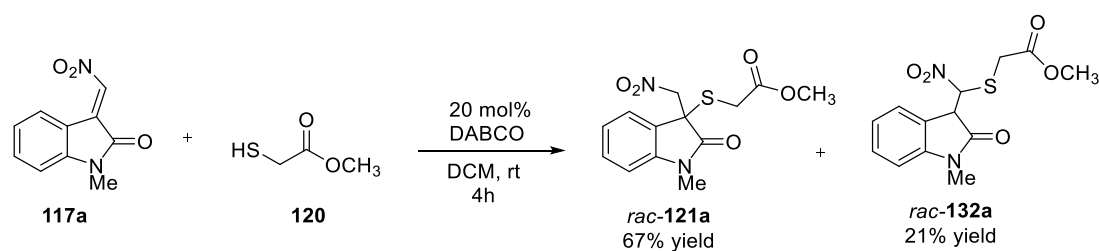


**Scheme 36.** Synthetic route applied for *N*-methyl substituted isatin derived nitroalkene **117a**

The structure of diastereomers was identified by means of  $^1\text{H}$  NMR. The nitroalkene hydrogen of (*E*)-**117a** resonated at 7.91 ppm because of the effect of the deshielding zone of the amide carbonyl group whereas (*Z*)-**117a** olefinic hydrogen was observed at relatively higher field as 7.50 ppm.  $^1\text{H}$  NMR spectra of (*E*)- and (*Z*)- isomers are given in Figure A.2.

### 2.3 Organocatalytic Sulfa-Michael Reaction

The background sulfa-Michael reaction of methyl thioglycolate (**120**) with *N*-methyl substituted *N*-methyl substituted isatin derived nitroalkene **117a** was carried out at room temperature with DABCO used as base catalyst in DCM. The major isomer **121a** as a result of sulfa-Michael reaction with respect to nitro unit was formed in 67% yield, whereas minor isomer **132a** as a result of sulfa-Michael addition with respect to amide carbonyl moiety was also isolated in 21% yield (Scheme 35).

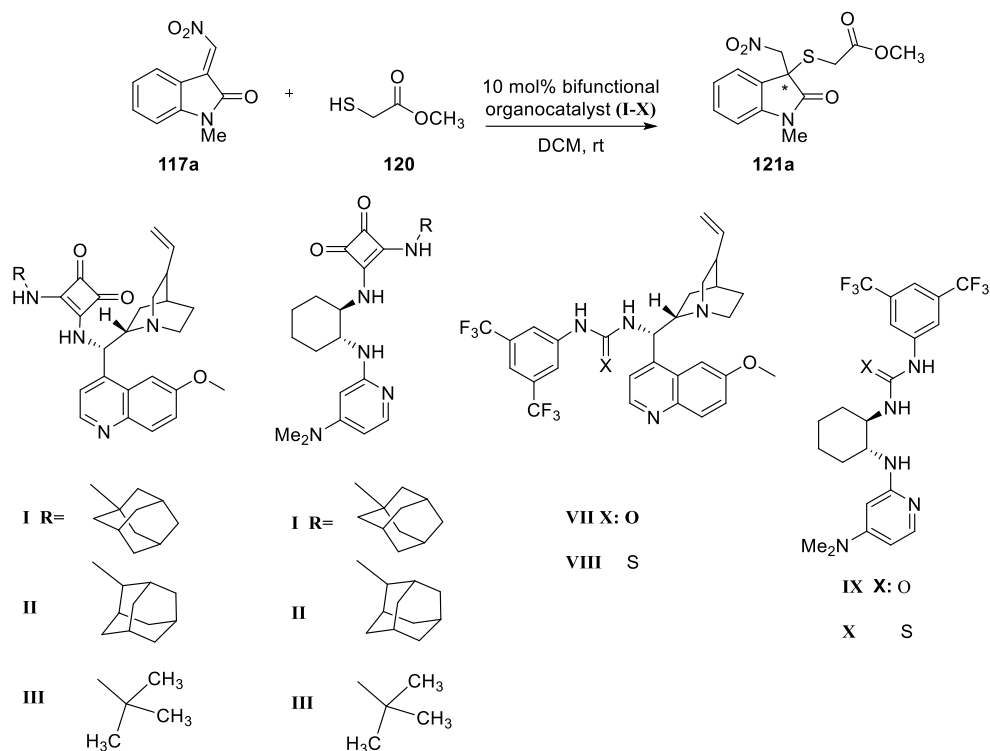


**Scheme 37.** The background sulfa-Michael reaction

The structure elucidation of *rac*-**121a** has been done by  $^1\text{H}$  and  $^{13}\text{C}$  NMR. In  $^1\text{H}$  NMR, diastereotopic methylene protons aligned between sulfur and carbonyl moiety resonated at 3.60 ppm as doublet of doublet ( $J = 16.4$  Hz) whereas the other methylene diastereotopic protons resonated at 5.16 ppm as doublet of doublet ( $J = 14.3$  Hz). Thiol-ene reaction was also considered as the reaction that formed **121a**. Therefore, the reaction was carried out at dark atmosphere and TLC check has also be done at dark medium, yet the results do not change under these conditions.

Asymmetric version of sulfa-Michael reaction has been screened with a series of chiral bifunctional organocatalysts in DCM with 10 mol% catalyst loading at room temperature. The results are summarized in Table 1.

**Table 1.** Catalyst Screening



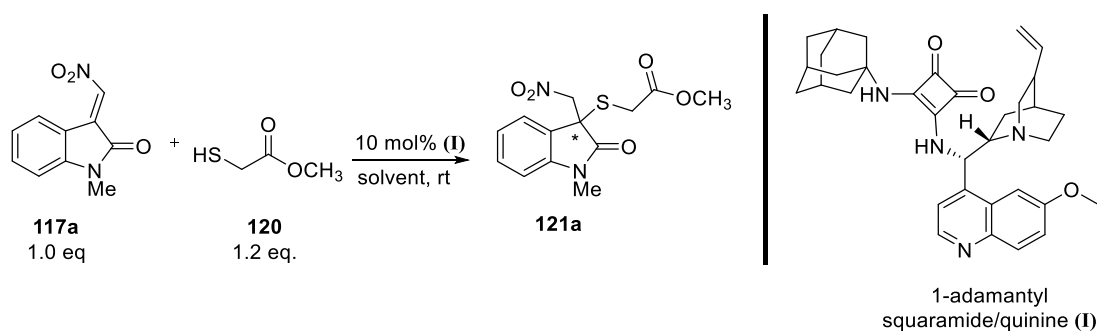
Entry	Organocatalyst	Time	Yield % <sup>a</sup>	ee % <sup>b</sup>
1	I	48 h	62	43
2	II	48 h	26	39
3	III	48 h	13	9
4	IV	48 h	18	7
5	V	1 h	67	28
6	VI	4 h	22	3
7	VII	8 h	59	1
8	VIII	48 h	27	41
9	XI	24 h	17	10
10	X	10 h	10	31

All of the experiments are conducted with 0.2 M. *a*: isolated yield *b*: Determined by HPLC using ASH chiral column with 80:20 *n*-hexane: *i*-propanol eluent at 1mL/min flow rate and 254 nm

The yields were low because of the side reactions. 1-Adamantyl squaramide quinine was detected as the best working catalyst. 2-Adamantyl squaramide/quinine (**II**) and thiourea/quinine (**VIII**) catalysts were the promising one among the others in terms of enantioselectivity.

After choosing the best working catalyst, solvent screening was done with 1-adamantyl squaramide/quinine (**I**) with 10 mol % percent catalyst loading. Again, temperature was kept constant and the electrophile:nucleophile ratio was 1:1.2.

**Table 2.** Solvent screening



Entry	Solvent	Time	Yield % <sup>a</sup>	ee % <sup>b</sup>
1	Toluene	24 h	27	12
2	THF	10 min	53	59
3	Chloroform	48 h	20	11
4	Xylene	4 h	21	57
5	1,4-dioxane	30 min	19	45
6	Diethyl ether	2 h	31	31
7	<i>n</i> -Hexane		no rxn	
8	Acetonitrile	48 h	45	46
9	1,2-Dichloroethane	72 h	8	46

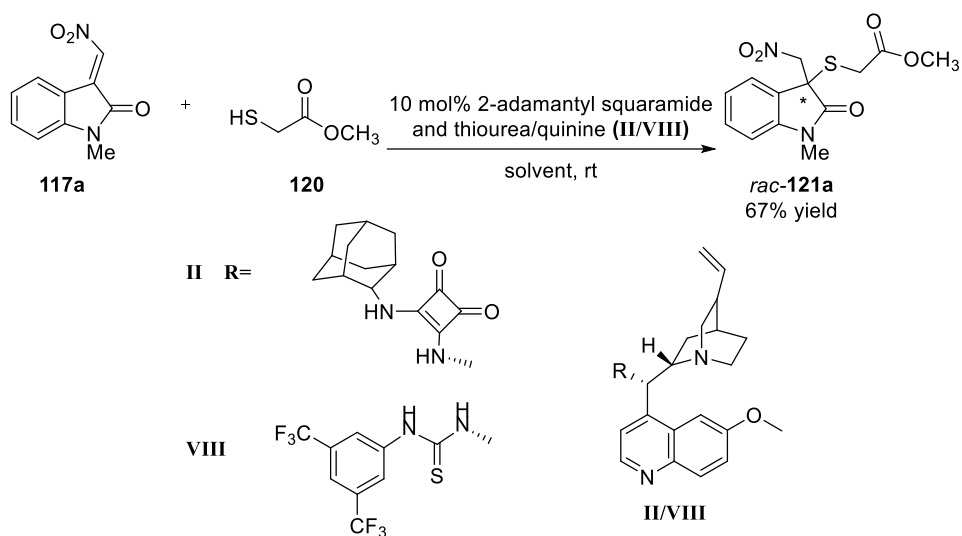
All of the experiments are conducted with 0.2 M. *a*: isolated yield *b*: Determined by HPLC using ASH chiral column with 80:20 *n*-hexane: *i*-propanol eluent at 1mL/min flow rate and 254 nm



The model reaction was tried by using nine solvents. Using THF increased enantioselectivity considerably and the reaction duration decreased drastically to 10 min. The other solvents did not have a good impact upon enantioselectivity.

The promising 2-adamantyl squaramide/quinine (**II**) and thiourea/quinine (**VIII**) catalysts were also tried with various solvents. The chosen solvents were the ones gave relatively better results. But we did not observe a cut above result (Table 3).

**Table 3.** Solvent screening with 2-adamantyl and thiourea squaramide/quinine (**II-VIII**)

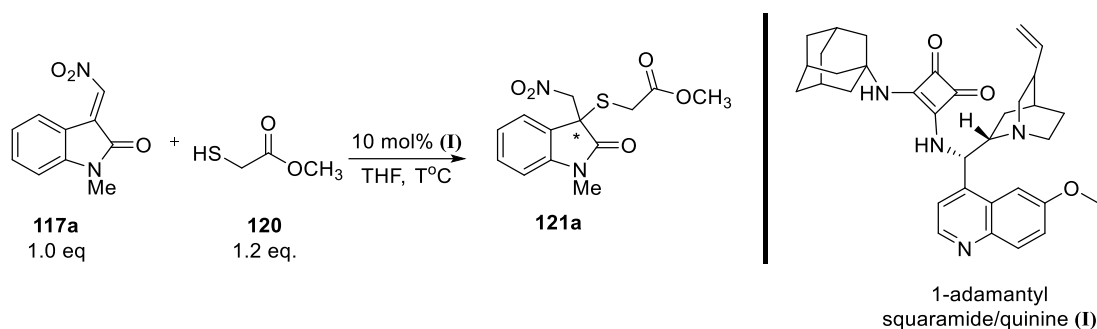


Entry	Organocatalyst	Solvent	Time	Yield % <sup>a</sup>	ee % <sup>b</sup>
1	II	Toluene	48 h	22	46
2	II	THF	4 h	23	4
3	II	Chloroform	40 h	32	13
4	II	Xylene	16 h	26	40
5	II	1,4-dioxane	30 h	9	42
6	III	Toluene	48 h	10	20
7	III	THF	6 h	40	32

All of the experiments are conducted with 0.2 M. <sup>a</sup>: isolated yield <sup>b</sup>: Determined by HPLC using ASH chiral column with 80:20 *n*-hexane: *i*-propanol eluent at 1 mL/min flow rate and 254 nm

The next optimization step was changing temperature. Lowering the temperature was known to increase enantioselectivity. The catalyst, its loading, solvent and electrophile:nucleophile ratio kept constant. However, both yield and ee decreased drastically. The result was attributed to low solubility of 1-adamantyl squaramide/quinine at low temperatures (Table 4).

**Table 4.** Temperature screening



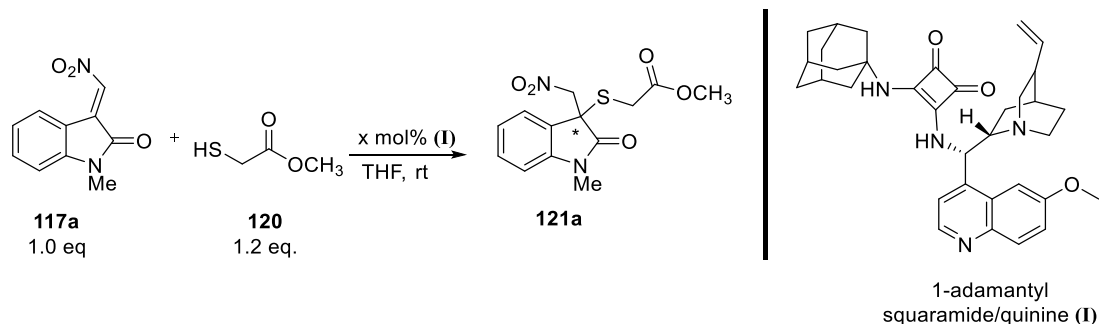
Entry	Temperature	Time	Yield % <sup>a</sup>	ee % <sup>b</sup>
<b>1</b>	<b>0</b>	30 min	41	57
<b>2</b>	<b>-20</b>	1 h	21	3
<b>3</b>	<b>-40</b>	6 h	22	3

All of the experiments are conducted with 0.2 M. *a*: isolated yield *b*: Determined by HPLC using ASH chiral column with 80:20 *n*-hexane: *i*-propanol eluent at 1mL/min flow rate and 254 nm

10 mol % catalyst loading could cause the self-aggregation of 1-adamantyl squaramide (**I**). It has tendency to make H-bonding itself consequently, the coordination ability of the organocatalyst with isatin derived nitroalkene **123** might have been decreased which affects the enantioselectivity adversely. Thus, 2 and 5 mol % catalyst loadings were screened at formerly optimized conditions. Catalyst loading was not scaled up further than 10 mol % because low catalyst loading is prized in concern with atom-economy. The screening study indicated that self-aggregation is not the reason for the moderate selectivity. Decreasing the

catalyst loading to 5 mol % declined enantioselectivity. We did not even observe product at 2 mol % catalyst loading (Table 5).

**Table 5.** Catalyst loading screening



Entry	Catalyst loading %	Time	Yield % <sup>a</sup>	ee % <sup>b</sup>
<b>1</b>	<b>5</b>	48 h	54	30
<b>2</b>	<b>2</b>	not isolat		

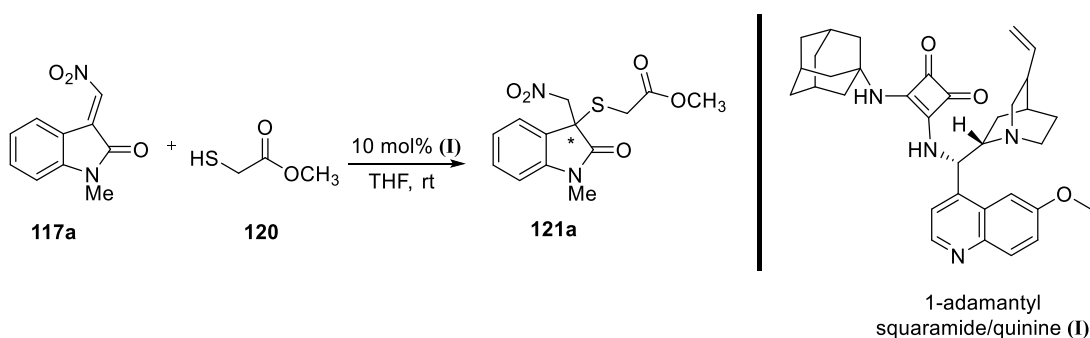
All of the experiments are conducted with 0.2 M. *a*: isolated yield *b*: Determined by HPLC using ASH chiral column with 80:20 *n*-hexane: *i*-propanol eluent at

Last parameter was the concentration of the reaction mixture. The reaction duration were not prolonged, nevertheless the side reactions overcame the sulfa-Michael reaction when concentration of isatin derived nitroalkene was raised due to the sensitive nature of isatin (**120**). We observed slight increase in terms of ee from 59% to 61% by increasing the nucleophile concentration twofold (Table 6, entry 4).

**Table 6.** Concentration screening

Entry	[E1]	[Nu]	Time	Yield % <sup>a</sup>	ee % <sup>b</sup>
1	0.24	0.2	10 min	22	28
2	0.2	0.2	10 min	54	33
3	0.2	0.3	20 min	54	51
4	0.2	0.4	14 min	56	61

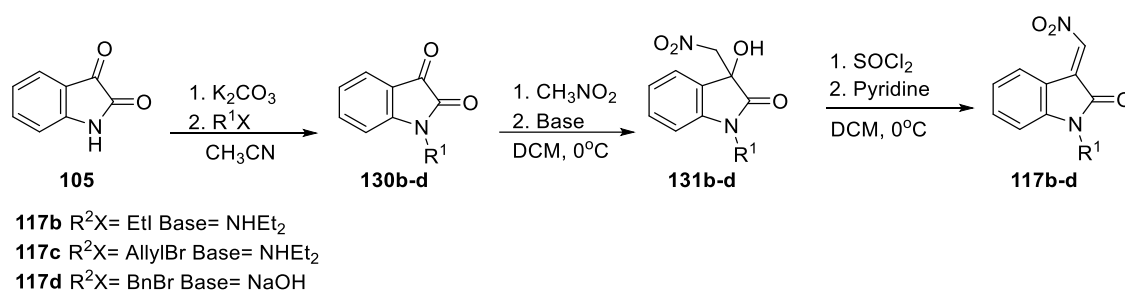
All of the experiments are conducted with 0.2 M. *a*: isolated yield *b*: Determined by HPLC using ASH chiral column with 80:20 *n*-hexane: *i*-propanol eluent at 1mL/min flow rate and 254 nm



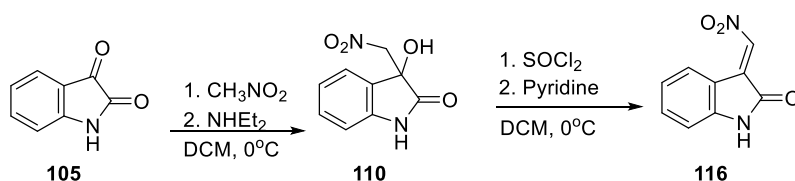
### 2.3.1 Effect of *N*-Substitution on Isatin Derived Nitroalkene

Any substitution on *N*-position of isatin (**120**) can change both the reactivity and spatial orientation of the molecule. Derivatization studies began with *N*-alkylation

reaction of isatin (**105**). Therefore, we have synthesized *N*-ethyl, allyl, and benzyl substituted derivatives by using corresponding alkyl, allyl and benzyl halides. *N*-ethyl substitution reaction was carried out by using ethyl iodide under reflux. In *N*-allylation and benzylation reactions, allyl bromide and benzyl bromide were used as alkyl halides and potassium iodide was added for Finkelstein reaction. Afterward, Henry reaction procedure was applied to *N*-ethyl and allyl substituted isatins **130b-c**. *N*-benzyl substituted isatin **130d** did not afford Henry adduct with the same procedure. More harsh conditions was required in the synthesis of it. (Scheme 38). Unsubstituted isatin (**105**) was also tried (Scheme 39). At the end, isatin (**105**) and three types of *N*-alkyl substituted isatins **130b-d** yielded isatin derived nitroalkenes **116** and **117b-d** via addition-elimination mechanism.



**Scheme 38.** Synthetic route for *N*-substituted isatin derived nitroalkene **117b-d**

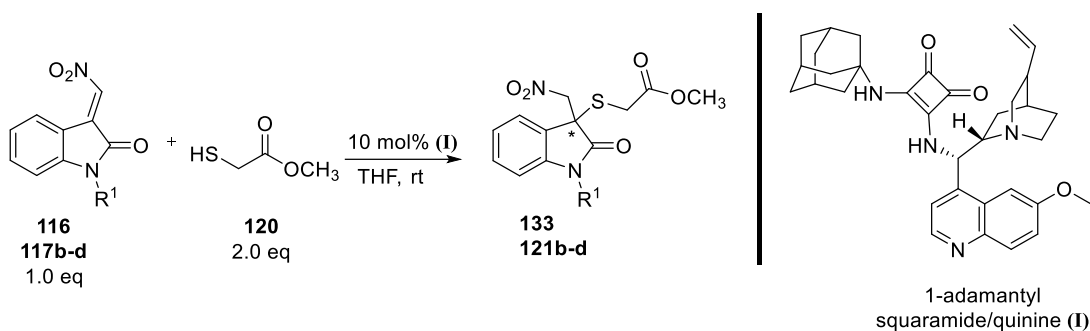


**Scheme 39.** Synthetic route for isatin derived nitroalkene **116**

Optimized conditions were applied with derivatized substrates **117b-d**. Interestingly, yields of all derivatives were greater than that of *N*-methyl substituted adduct **121a**. Unsubstituted substrate **116** also gave good yield. The

side reactions were diminished by the aid of *N*-substitution derivatization. Although a considerable increase was not detected with other derivatives, *N*-benzyl substitution led to a significant increase in enantioselectivity (upto 70% ee) (Table 7).

**Table 7.** Effect of *N*-substitution on isatin derived nitroalkene **129a-d**

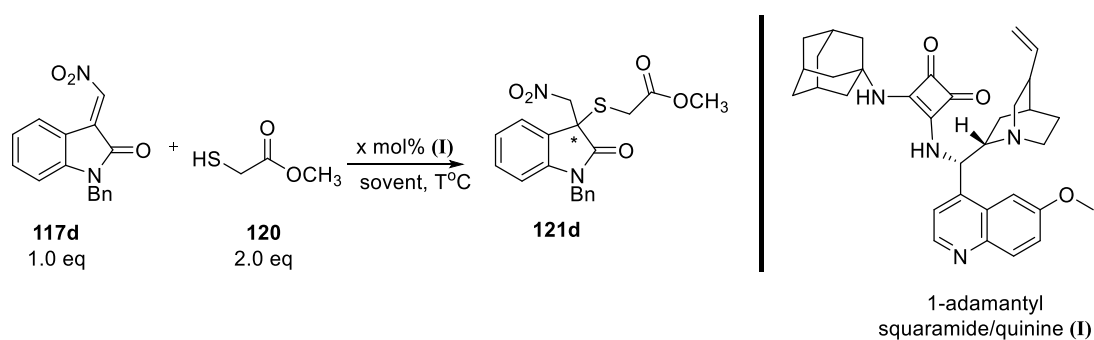


Entry	R <sup>1</sup>	Time	Yield % <sup>a</sup>	ee % <sup>b</sup>
<b>1</b>	<b>H</b>	10 h	80	25
<b>2</b>	<b>Ethyl</b>	24 h	80	57
<b>3</b>	<b>Allyl</b>	1 h	84	59
<b>4</b>	<b>Benzyl</b>	<b>2 h</b>	<b>75</b>	<b>70</b>

All of the experiments are conducted with 0.2 M. *a*: isolated yield *b*: Determined by HPLC using ASH chiral column with 80:20 *n*-hexane: *i*-propanol eluent at 1 mL/min flow rate and 254 nm

As we observed the significant increase in enantioselectivity with *N*-benzyl substitution, we decided to do further optimization studies. DCM and toluene were tried as solvent, methyl thioglycolate (**120**) concentration was increased, catalyst loading and temperature were decreased. Though, we could not improve the enantioselectivity (Table 8).

**Table 8.** Further optimization studies for *N*-benzyl substituted isatin derived nitroalkene **128d**

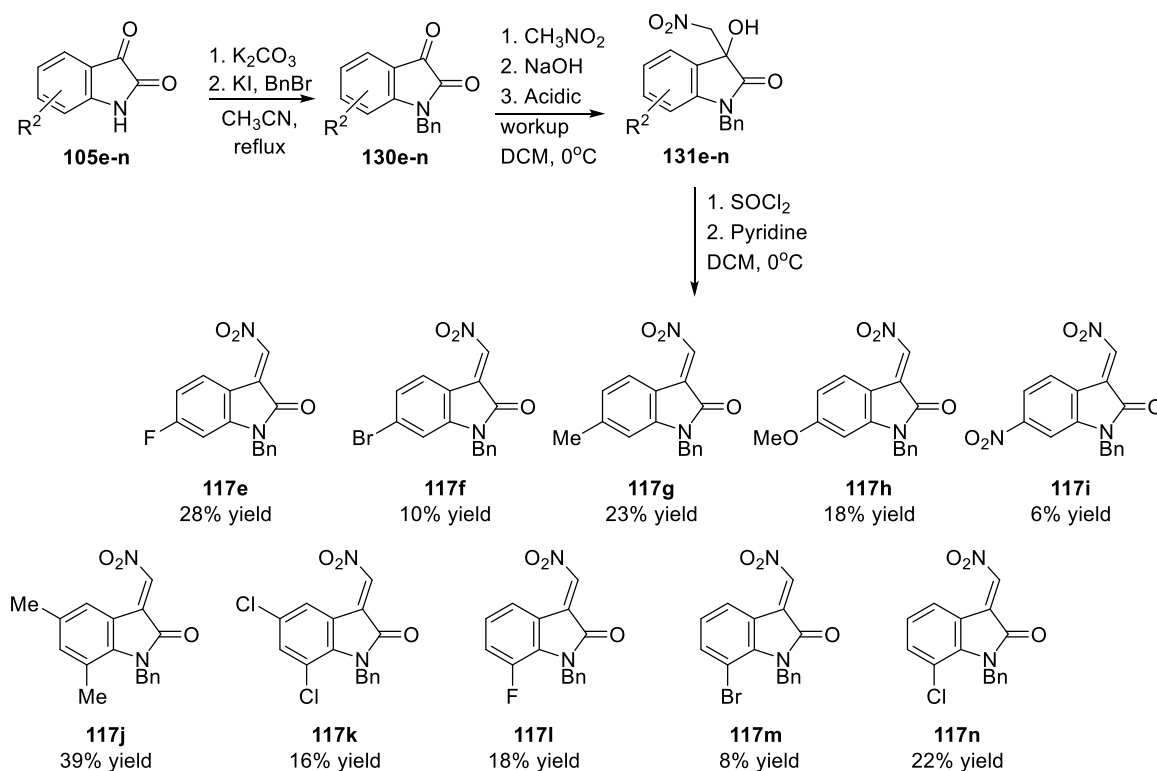


Entry	[Nu]	Cat. (mol %)	Solvent	T (°C)	Time	Yield % <sup>a</sup>	ee % <sup>b</sup>
1	0.4	10	DCM	rt	20 h	63	51
2	0.4	10	Toluene	rt	24 h	39	47
3	0.6	10	DCM	rt	4 h	41	35
4	0.6	10	THF	rt	8 h	69	13

<b>5</b>	0.4	<b>5</b>	DCM	rt	24 h	92	27
<b>6</b>	0.4	<b>2</b>	DCM	rt		-	
<b>7</b>	0.4	10	DCM	<b>0 °C</b>	48 h	70	37
<b>8</b>	0.4	10	DCM	<b>-20 °C</b>	40 h	43	41

### 2.3.2 Derivatization Studies

Various isatin derived nitroalkenes **117e-n** were synthesized starting from commercially available substituted isatins. The formation of both (*E*)- and (*Z*)-**117e-n** were also observed while synthesizing these derivatives. All the reactions were carried out by using 20 mol% DABCO as base in THF at room temperature. The yields are summarized in Scheme 40.

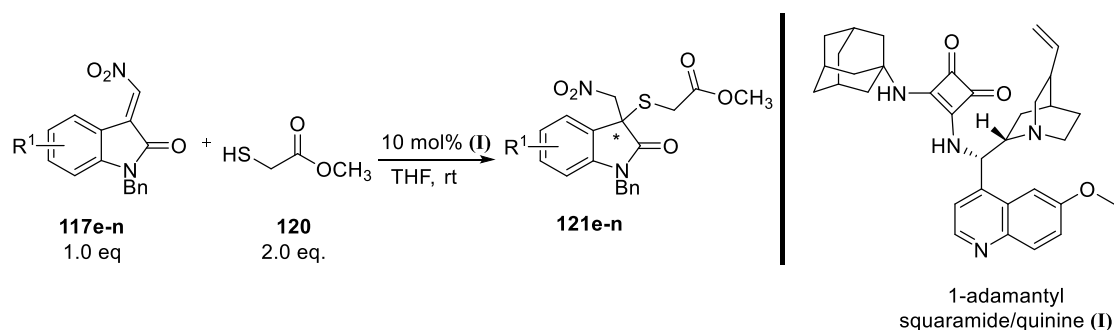


**Scheme 40.** Various N-benzyl substituted isatin derived nitroalkenes **117e-n** and their isolated yields

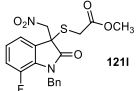
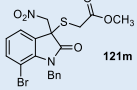
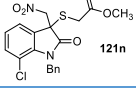


Subsequently, all further derivatives underwent to sulfa-Michael reactions under optimized conditions. While the yields are moderate, ee values could not reach that of *N*-benzyl substituted nitroalkene **121d**. Unexpectedly, the electron-withdrawing groups had a detractive effect on ee (Table 9, entry 1, 5, 7). While electron-donating groups affected enantioselectivity mildly (Table 9, entry 3-4).

**Table 9.** Derivatization Studies



Entry	121e-n	Time	Yield % <sup>a</sup>	ee % <sup>b</sup>
<b>1</b>		48 h	50	25
<b>2</b>		36 h	58	47
<b>3</b>		2 h	78	47
<b>4</b>		24 h	44	59
<b>5</b>		30 min	67	9
<b>6</b>		2 h	70	59
<b>7</b>		22 h	80	39

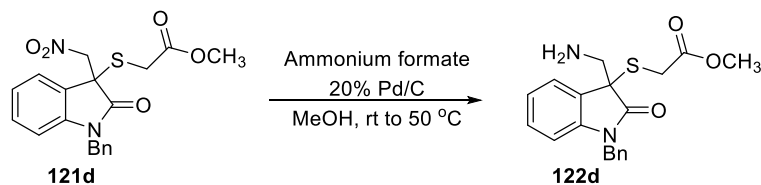
<b>8</b>		1 h	75	29
<b>9</b>		3 h	66	47
<b>10</b>		6 h	71	13

All of the experiments are conducted with 0.2 M. a: isolated yield  
 b: Determined by HPLC using ASH chiral column with 80:20 n-hexane: i-propanol eluent at 1mL/min flow rate and 254 nm.

### 2.3.3 Utilization of Sulfa-Michael Adduct

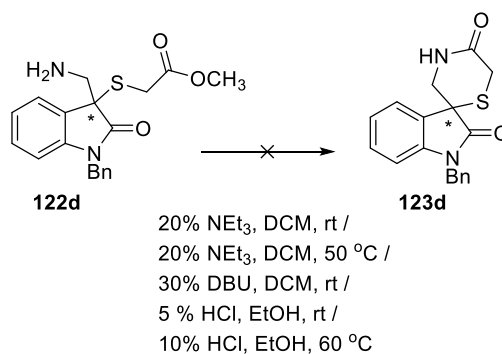
It is known that isatin (**105**) take part in lots of spiro annulation reactions which yield numerous biologically active compounds. In our research, we attend to synthesize spirooxindole thiomorpholin-3-one **123d** through the reduction of nitro group following nucleophilic attack of amine group to the glycolate carbonyl carbon. In the first step, the reduction was achieved by ammonium formate and Pd/C catalyst. The procedure in the literature was adapted. The reaction was set up at room temperature and heated to 50 °C, and stirred overnight. Having been

filtered through a bed of Celite, the product was purified by column chromatography and obtained with an acceptable yield (60%).<sup>56</sup>



**Scheme 41.** Reduction of nitro group

In the second step, the cyclization reaction was tried to achieve. The applied procedures were prepared by getting inspired from some works in the literature.<sup>64a-c</sup> The reaction was carried out under both acidic and basic conditions. The temperature was increased. But the attempts did not lead to success.



**Scheme 42.** Trials for the cyclization reaction



## CHAPTER 3

### EXPERIMENTAL

#### 3.1 Materials and Methods

The instruments used for the characterization of the compounds are listed below.

Nuclear magnetic ( $^1\text{H}$  NMR and  $^{13}\text{C}$  NMR) spectra were recorded on Bruker Spectrospin Avance DPX 400 spectrometer, using  $\text{CDCl}_3$  as solvent. Chemical shifts are reported in parts per million (ppm) from tetramethylsilane as internal reference. Spin multiplicities were specified as s (singlet), bs (broad singlet), d (doublet), dd (doublet of doublet), ddd (doublet of doublet of doublet), dq (doublet of quartet), t (triplet), q (quartet), m (multiplet), sep (septet). The coupling constants ( $J$ ) were reported in Hertz (Hz).  $^1\text{H}$  NMR and  $^{13}\text{C}$  NMR spectra of the materials are given in appendix A.

HPLC chromatograms were recorded on Thermo-Finnigan HPLC system. Daicel ASH and ODH chiral columns were used with *n*-hexane/2-propanol as eluent. HPLC chromatograms are given in appendix A. Optical rotations were measured with Rudolph Scientific Autopol III polarimeter and reported as follows  $[\alpha]_D^T$  (c in g per 100 mL solvent).

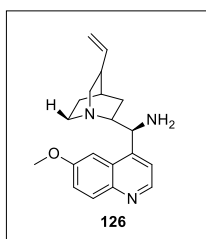
Infrared spectra were obtained on Bruker Alpha Platinum ATR and band positions were reported in  $\text{cm}^{-1}$  in spectra. HRMS data were detected on Agilent 6224 TOF LC/MS at UNAM, Bilkent University.

All the reactions were monitored by TLC using precoated silica gel plates (Merck Silica Gel 60 F<sub>254</sub>). Visualized by UV-light. Flash column chromatography was

performed on silica gel 60 with particle size of 0.063-0.200 mm by using thick-walled glass columns.

Compounds were named by using ChemBio Draw Ultra.

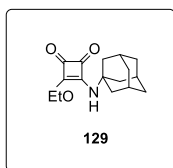
### 3.2 Synthesis of 9-Amino(9-deoxy)quinine (126)



The literature procedure was applied. Quinine (**124**) (3.24 g, 10.0 mmol) and 1.2 eq triphenyl phosphine (3.15 g, 12.0 mmol) were dissolved in 50 mL of dry THF. After the solution was cooled to 0°C, 1.2 eq diisopropyl azodicarboxylate (2.43 g, 12.0 mmol) was added to the solution. The solution of diphenyl phosphoryl azide (3.30 g, 12 mmol) in 20 mL of dry THF was cooled to 0°C and added dropwise to the initial solution. After the reaction mixture reached to room temperature, 1 mL of water was added. The reaction was stirred for 3 h. The solvent was evaporated *in vacuo*, The residue was dissolved in 1:1 ratio of 100 mL of 10% hydrochloric acid:DCM. The aqueous phase was washed with DCM for four times. The combined organic phases were dried over MgSO<sub>4</sub>, and filtered. The solvent was removed *in vacuo*. The residue was purified by column chromatography on silica gel (EtOAc/ MeOH/ NEt<sub>3</sub> = 50/ 50/ 1 as eluent). 9-amino(9-deoxy)quinine (**126**) was obtained as yellowish viscous oil with 70% yield.

Spectroscopic data were consistent with the literature.<sup>53</sup>

### 3.3 Synthesis of 1-Adamantyl Mono-Squaramide 129

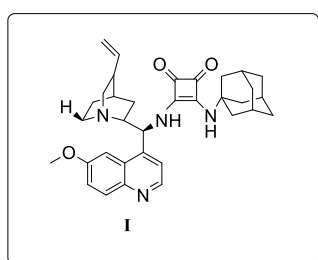


Squaric acid **127** (500 mg, 4.3 mmol) was refluxed for 3 h with 7 mL of dry ethanol under argon atmosphere. Having evaporated the solvent *in vacuo*, the method was repeated for three times for 30 minutes reflux. The removal of ethanol yields pale yellow oil diethyl squarate **128** with quantitative yield. After dissolving diethyl squarate **128**

in 4 mL DCM, 1 eq 1-adamantyl adamine (650 mg, 4.3 mmol) was added to the solution. The reaction was stirred for 24 h at room temperature and 1-adamantyl Mono-Squaramide **129** was purified with silica gel and 1:3 ratio of EtOAc:*n*-Hexane as eluent, and obtained as white solid with 90% yield.

Spectroscopic data were consistent with the literature.<sup>38</sup>

### 3.4 Synthesis of 1-Adamantyl Squaramide/ Quinine catalyst I

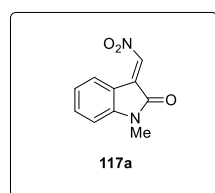


1-adamantyl Mono-Squaramide **129** (3.55 mmol, 1000mg) was added to a solution of 9-amino(9-deoxy)quinine (**126**) (3.55 mmol, 1146 mg) in the mixture of DCM:MeOH (1:1). The reaction was stirred for 48 h at room temperature and loaded into

silica gel column (EtOAc/ MeOH = 90/ 10). The organocatalyst **I** was obtained as white solid with 92% yield.

Spectroscopic data were consistent with the literature.<sup>38</sup>

### 3.5 Synthesis of *N*-Methyl substituted Isatin derived Nitroalkene 117a



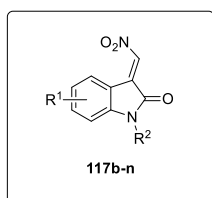
According to literature procedure, isatin (**105**) (400 mg, 2.72 mmol) was dissolved in 15 mL of dry acetonitrile. 1.2 eq  $K_2CO_3$  (450 mg, 3.26 mmol) and 3 eq iodomethane (1158 mg, 8.16 mmol) were added to the solution at once. After stirring

the reaction overnight, the solvent was removed *in vacuo* and the residue was diluted with EtOAc. After the aqueous phase was washed with EtOAc for four times, the combined organic layers were extracted with 5%  $Na_2CO_3$  solution and washed with water. The organic phase washed with water one more time and dried over  $MgSO_4$ . *N*-methyl substituted isatin **130a** was afforded by recrystallization with EtOAc with quantitative yield.<sup>55</sup> *N*-methyl substituted isatin **130a** (400 mg, 2.48 mmol) was dissolved in 6 mL of DCM and cooled to 0 °C. 4

eq NHEt<sub>2</sub> and CH<sub>3</sub>NO<sub>2</sub> was added to the solution respectively. After observing the consumption of *N*-methyl substituted isatin **130a**, 1.5 eq thionyl chloride (442 mg, 3.72 mmol) and 2 eq pyridine (446 mg, 5.64 mmol) were added dropwise to the reaction mixture at 0°C. *N*-methyl substituted isatin derived nitroalkene was obtained with 56 % yield.<sup>56</sup>

Spectroscopic data were consistent with the literature.<sup>56</sup>

### 3.6 General Procedure for the synthesis of Isatin derived nitroalkenes **117b-n**

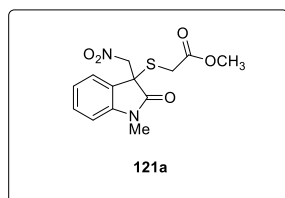


According to literature procedure, 5- or 7-substituted isatin (**117b-n**) (2.72 mmol) was dissolved in 15 mL of dry acetonitrile. 1.2 eq K<sub>2</sub>CO<sub>3</sub> (3.26 mmol), 0.1 eq KI (0.33 mmol) and 3 eq alkyl bromide (8.16 mmol) were added to the solution at once. After stirring the reaction overnight, the solvent was removed *in vacuo* and the residue was diluted with EtOAc. After the aqueous phase was washed with EtOAc for four times, the combined organic layers were extracted with 5% Na<sub>2</sub>CO<sub>3</sub> solution and washed with water. The organic phase washed with water one more time and dried over MgSO<sub>4</sub>. *N*-alkyl substituted isatin **130b-n** was afforded by recrystallization with EtOAc with quantitative yield.<sup>55</sup> *N*-alkyl substituted isatin (**105**) and **130b-c** were dissolved in 6 mL of DCM and cooled to 0°C. 4 eq NHEt<sub>2</sub> and CH<sub>3</sub>NO<sub>2</sub> were added to the solution respectively. After observing the consumption of isatin (**105**) and *N*-alkyl substituted isatin **130b-c**, 1.5 eq thionyl chloride (442 mg, 3.72 mmol) and 2 eq pyridine (446 mg, 5.64 mmol) were added dropwise to the reaction mixture at 0 °C. *N*-ethyl and alkyl substituted isatin derived nitroalkenes **117b-c** were obtained by column chromatography with EtOAc:*n*-hexane as eluent.<sup>56</sup> *N*-aryl substituted isatin **117d-n** was dissolved in EtOH and cooled to 0 °C. 1.1 eq NaOH and CH<sub>3</sub>NO<sub>2</sub> was added to the solution respectively. After the reaction finished, the reaction mixture was quenched into acidic crushed ice and extracted with EtOAc. After drying organic phase over MgSO<sub>4</sub>, The same procedure and purification method were applied for the synthesis of *N*-aryl substituted isatin derived nitroalkenes **117d-n**.



Spectroscopic data were consistent with the literature.<sup>56</sup>

### 3.7 Asymmetric Sulfa-Michael Reaction: Addition of Methyl Thioglycolate **120** to *N*-Methyl Substituted Isatin derived Nitroalkene **117a**



#### *Racemic Synthesis:*

1 eq *N*-methyl substituted isatin derived nitroalkene **125** (40 mg, 0.19 mmol) and 0.2 eq DABCO (4.48 mg, 0.04 mmol) were dissolved in 0.25 mL of THF. In another flask 2 eq methyl thioglycolate (**124**) (252.6 mg, 0.38 mmol) was dissolved in 0.25 mL of THF and added dropwise to the former solution.

#### *Asymmetric Synthesis:*

1 eq *N*-methyl substituted isatin derived nitroalkene **117a** (25 mg, 0.12 mmol) and 0.1 eq 1-adamantyl squaramide/quinine **I** (6.57 mg, 0.01 mmol) were dissolved in 0.25 mL of THF. In another flask 2 eq methyl thioglycolate (**120**) (252.6 mg, 0.24 mmol) was dissolved in 0.25 mL of THF and added dropwise to the former solution.

Optical rotation was detected as  $[\alpha]_{589}^{29} = +10.7^\circ$  ( $c = 0.01$  g/mL,  $\text{CH}_2\text{Cl}_2$ ).

**mp:** 112 °C

**<sup>1</sup>H NMR** (400 MHz,  $\text{CDCl}_3$ ):  $\delta$  7.34-7.30 (dt,  $J = 7.8, 1.2$  Hz, 1H), 7.23-7.21 (dd,  $J = 7.4, 0.6$  Hz, 1H), 7.05-7.01 (dt,  $J = 7.6, 0.9$  Hz, 1H), 6.87-6.85 (d,  $J = 7.9$  Hz, 1H), 5.23-5.19 (d,  $J = 14.6$ , 1H), 5.15-5.11 (d,  $J = 14.6$ , 1H), 3.95-3.91 (d,  $J = 16.4$ , 1H), 3.69 (s, 3H), 3.26 (s, 3H).

**<sup>13</sup>C NMR** (100 MHz,  $\text{CDCl}_3$ ):  $\delta$  211.6, 169.7, 142.5, 132.3, 127.7, 127.6, 126.7, 124.5, 74.3, 58.9, 56.6, 38.4.

**HPLC:** Daicel ASH column, 80:20 (*n*-hexane:*i*-PrOH), flow rate 1.0 mL/min, 254 nm, temp=25°C,  $t_{\text{major}}=17.0$  min  $t_{\text{minor}}=22.0$  min

**IR(neat):** 3309, 2924, 2650, 1750, 1699, 1611, 1556, 1458, 1374, 741  $\text{cm}^{-1}$

**HRMS:** Calculated for  $\text{C}_{13}\text{H}_{14}\text{N}_2\text{O}_5\text{S}$   $[\text{M} + \text{H}]^+$  310.0623, found 310.0707.

### 3.8 General Procedure for the Addition of Methyl Thioglycolate **120** to Isatin derived Nitroalkene **116** and *N*-Alkyl Substituted Isatin derived Nitroalkene **117b-n**

#### *Racemic Synthesis:*

1 eq isatin derived nitroalkene **116** or *N*-alkyl substituted isatin derived nitroalkene **117b-n** (0.20 mmol) and 0.2 eq DABCO (0.04 mmol) were dissolved in 0.25 mL of THF. In another flask 2 eq methyl thioglycolate (**120**) (0.40 mmol) was dissolved in 0.25 mL of THF and added dropwise to the former solution.

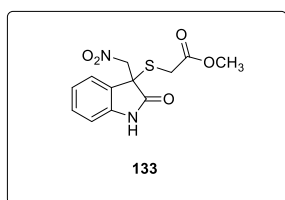
#### *Asymmetric Synthesis:*

1 eq isatin derived nitroalkene **116** or *N*-alkyl substituted isatin derived nitroalkene **117b-n** (0.20 mmol) and 0.1 eq 1-adamantyl squaramide/quinine **I** (0.02 mmol) were dissolved in 0.25 mL of THF. In another flask 2 eq methyl thioglycolate (**120**) (0.40 mmol) was dissolved in 0.25 mL of THF and added dropwise to the former solution.

#### 3.8.1 Addition of Methyl Thioglycolate **120** to Isatin derived Nitroalkene **116**

General procedure starting from isatin derived nitroalkene **116** and methyl thioglycolate (**120**) was applied. After 10 h, the desired product **133** was afforded with 80% yield and 25% ee.

Optical rotation was detected as  $[\alpha]_{589}^{29} = -3.7^\circ$  ( $c = 0.01 \text{ g/mL}$ ,  $\text{CH}_2\text{Cl}_2$ ).



**mp:** 108 °C

**<sup>1</sup>H NMR** (400 MHz, CDCl<sub>3</sub>):  $\delta$  8.29-8.27 (d,  $J = 7.8$  Hz, 1H), 7.68 (s, 1H), 7.42-7.38 (t,  $J = 7.8$  Hz, 1H), 7.19 (s, 1H), 7.05-7.01 (dt,  $J = 8.2, 7.4$  Hz, 1H), 6.79- 6.77 (d,  $J = 14.2$  Hz, 1H), 3.76-3.72 (d,  $J = 7.2$  Hz, 1H), 3.68-3.64 (d,  $J = 7.2$  Hz, 1H), 1.57 - 1.18 (m, 5H).

**<sup>13</sup>C NMR** (100 MHz, CDCl<sub>3</sub>): δ 211.6, 169.7, 142.5, 132.3, 127.7, 127.6, 126.7, 124.5, 74.3, 58.9, 56.6, 38.4.

**HPLC**: Daicel ASH column, 80:20 (*n*-hexane:*i*-PrOH), flow rate 1.0 mL/min, 254 nm, temp=25 °C, *t*<sub>major</sub>=19.9 min *t*<sub>minor</sub>=25.2 min

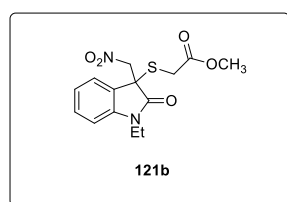
**IR(neat)**: 3300, 2600 1750, 1700, 1460 cm<sup>-1</sup>

**HRMS**: Calculated for C<sub>12</sub>H<sub>12</sub>N<sub>2</sub>O<sub>5</sub>S [M + H]<sup>+</sup> 296.0466, found 296.0543.

### 3.8.2 Addition of Methyl Thioglycolate (**120**) to *N*-Ethyl Isatin derived Nitroalkene **117b**

General procedure starting from *N*-ethyl isatin derived nitroalkene **117b** and methyl thioglycolate (**120**) was applied. After 1 h, the desired product **121b** was afforded with 84% yield and 57% ee.

Optical rotation was detected as  $[\alpha]_{589}^{29} = +22.0^{\circ}$  (*c* = 0.01g/mL, CH<sub>2</sub>Cl<sub>2</sub>).



**mp**: 112 °C

**<sup>1</sup>H NMR** (400 MHz, CDCl<sub>3</sub>): δ 7.35 – 7.26 (m, 2H), 7.12 – 6.92 (m, 2H), 5.35 – 5.24 (m, 3H), 5.22- 5.19 (d, *J* = 14.6 Hz, 1H), 5.17-5.13 (d, *J* = 14.6 Hz, 1H), 4.50 – 4.37 (m, 3H), 4.02 – 3.98 (t, *J* = 0.9 Hz, 3H), 3.80- 3.59 (m, 5H).

**<sup>13</sup>C NMR** (100 MHz, CDCl<sub>3</sub>): δ 172.2, 169.8, 169.2, 142.5, 129.5, 123.2, 122.0, 121.9, 108.0, 52.4, 51.7, 41.3, 28.9.

**HPLC**: Daicel ODH column, 90:10 (*n*-hexane:*i*-PrOH), flow rate 1.0 mL/min, 254 nm, temp=25 °C, *t*<sub>major</sub>=16.1 min *t*<sub>minor</sub>=21.0 min

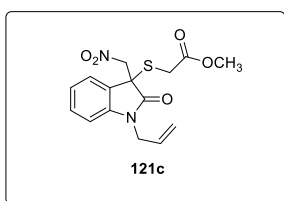
**IR(neat)**: 3310, 2925, 2650, 1750, 1700, 1610, 1566, 1457, 1374, 753 cm<sup>-1</sup>

**HRMS**: Calculated for C<sub>14</sub>H<sub>16</sub>N<sub>2</sub>O<sub>5</sub>S [M + H]<sup>+</sup> 324.0779, found 325.0867.

### 3.8.3 Addition of Methyl Thioglycolate (**120**) to *N*-Allyl Isatin derived Nitroalkene **117c**

General procedure starting from *N*-allyl isatin derived nitroalkene **117c** and methyl thioglycolate (**120**) was applied. After 24 h, the desired product **121c** was afforded with 80% yield and 59% ee.

Optical rotation was detected as  $[\alpha]_{589}^{29} = -4.0^{\circ}$  ( $c = 0.01 \text{ g/mL}$ ,  $\text{CH}_2\text{Cl}_2$ ).



**mp:** 122 °C

**<sup>1</sup>H NMR** (400 MHz,  $\text{CDCl}_3$ ):  $\delta$  7.65 – 7.63 (dd,  $J = 12.3$ , 4.4 Hz, 1H), 7.47 – 7.45 (m, 1H), 7.30 – 7.21 (m, 1H), 7.03 – 6.86 (dd,  $J = 7.7$  Hz, 1H), 5.24 – 5.20 (d,  $J = 14.8$ , 1H), 5.18–5.14 (d,  $J = 14.8$  Hz, 1H), 4.16 - 3.94 (m, 2H), 3.90 – 3.87 (m, 3H), 3.72 – 3.68 (m, 5H), 3.30 – 3.26 (d,  $J = 4.4$  Hz, 1H).

**<sup>13</sup>C NMR** (100 MHz,  $\text{CDCl}_3$ ):  $\delta$  172.2, 169.2, 142.4, 129.4, 123.2, 122.1, 122.0, 108.1, 51.7, 47.7, 28.9, 28.5, 25.7.

**HPLC:** Daicel ASH column, 80:20 (*n*-hexane:*i*-PrOH), flow rate 1.0 mL/min, 254 nm, temp=25 °C,  $t_{\text{major}}=17.0$  min  $t_{\text{minor}}=22.0$  min

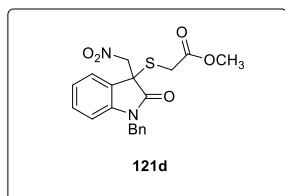
**IR(neat):** 2650, 1700, 1698, 1550, 1458, 1374, 885, 752, 669, 624  $\text{cm}^{-1}$

**HRMS:** Calculated for  $\text{C}_{15}\text{H}_{16}\text{N}_2\text{O}_5\text{S}$   $[\text{M} + \text{H}]^+$  336.0779, found 337.0838.

### 3.8.4 Addition of Methyl Thioglycolate (**120**) to *N*-Benzyl Isatin derived Nitroalkene **117d**

General procedure starting from *N*-benzyl isatin derived nitroalkene **117d** and methyl thioglycolate (**120**) was applied. After 2 h, the desired product **121d** was afforded with 75% yield and 70% ee.

Optical rotation was detected as  $[\alpha]_{589}^{29} = +90.0^{\circ}$  ( $c = 0.01 \text{ g/mL}$ ,  $\text{CH}_2\text{Cl}_2$ ).



**mp:** 137 °C

**<sup>1</sup>H NMR** (400 MHz, CDCl<sub>3</sub>): δ 7.84 (s, 1H), 7.53 – 7.52 (d, *J* = 6.0 Hz, 1H), 7.27 – 7.21 (m, 3H), 7.12 – 7.01 (m, 3H), 4.94 – 4.92 (d, *J* = 17.8 Hz, 1H), 3.92-3.74 (d, *J* = 17.8 Hz, 1H), 3.79 – 3.29 (m, 6H).

**<sup>13</sup>C NMR** (100 MHz, CDCl<sub>3</sub>): δ 166.9, 146.2, 138.3, 134.8, 134.7, 129.9, 129.0, 128.1, 127.3, 123.5, 117.3, 109.9, 44.1.

**HPLC:** Daicel ODH column, 90:10 (*n*-hexane:*i*-PrOH), flow rate 1.0 mL/min, 254 nm, temp=25 °C, *t*<sub>major</sub>=38.2 min *t*<sub>minor</sub>=45.8 min

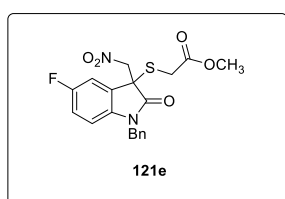
**IR(neat):** 2750, 1720, 1699, 1557, 1457, 1374, 1173, 906, 727, 696 cm<sup>-1</sup>

**HRMS:** Calculated for C<sub>19</sub>H<sub>18</sub>N<sub>2</sub>O<sub>5</sub>S [M + H]<sup>+</sup> 386.0936, found 386.2069.

### 3.8.5 Addition of Methyl Thioglycolate (120) to *N*-Benzyl 5-Fluoro Isatin derived Nitroalkene 117e

General procedure starting from *N*-benzyl 5-fluoro isatin derived nitroalkene **117e** and methyl thioglycolate (**120**) was applied. After 48 h, the desired product **121e** was afforded with 50% yield and 25% ee.

Optical rotation was detected as [α]<sub>589</sub><sup>29</sup> = +2.6° (*c* = 0.01 g/mL, CH<sub>2</sub>Cl<sub>2</sub>).



**mp:** 140 °C

**<sup>1</sup>H NMR** (400 MHz, CDCl<sub>3</sub>): δ 7.46- 7.39 (m, 3H), 7.37 – 7.26 (m, 2H), 7.24 - 7.20 (m, 1H), 7.18 – 7.15 (m, 1H), 7.07 – 7.01 (m, 1H), 5.62 – 5.58 (d, *J* = 15.3 Hz, 1H), 5.36-5.32 (d, *J* = 15.3 Hz, 1H), 4.77 – 4.59 (dd, *J* = 9.3, 0.6 Hz, 2H), 3.77 (s, 3H), 1.98 – 1.80 (d, *J* = 7.6 Hz, 2H).

**<sup>13</sup>C NMR** (100 MHz, CDCl<sub>3</sub>): δ 166.6, 164.3, 135.0, 129.8, 129.3, 128.9, 127.9, 127.5, 127.4, 126.8, 126.5, 120.2, 117.8, 115.9, 114.8, 110.3, 56.7, 43.8.

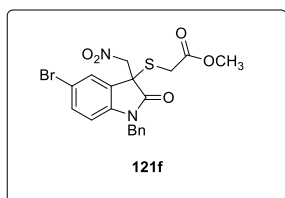
**HPLC:** Daicel ODH column, 90:10 (*n*-hexane:*i*-PrOH), flow rate 1.0 mL/min, 254 nm, temp=25 °C, *t*<sub>major</sub>=43.1 min *t*<sub>minor</sub>=62.6 min

**IR(neat):** 2760, 1720, 1698, 1557, 1457, 1362, 1178, 908, 796, 669 cm<sup>-1</sup>

### 3.8.6 Addition of Methyl Thioglycolate (**120**) to *N*-Benzyl 5-Bromo Isatin derived Nitroalkene **117f**

General procedure starting from *N*-benzyl 5-bromo isatin derived nitroalkene **117f** and methyl thioglycolate (**120**) was applied. After .. h, the desired product **121f** was afforded with 58% yield and 47% ee.

Optical rotation was detected as  $[\alpha]_{589}^{29} = +0.7^{\circ}$  ( $c = 0.01$  g/mL, CH<sub>2</sub>Cl<sub>2</sub>).



**mp:** 137 °C

**<sup>1</sup>H NMR** (400 MHz, CDCl<sub>3</sub>): δ 7.98 (s, 1H), 7.53 – 7.49 (m, 1H), 7.43– 7.28 (m, 2H), 7.25 – 7.21 (m, 2H), 7.19 – 7.15 (m, 1H), 6.98 – 6.92 (d,  $J = 6.5$  Hz, 1H), 5.74–5.66 (d,  $J = 18.2$  Hz, 1H), 5.56 – 5.48 (d,  $J = 18.2$ , 1H), 4.91 – 4.63 (m, 3H), 3.86 (s, 3H), 2.53 – 2.49 (d,  $J = 8.7$  Hz, 2H).

**<sup>13</sup>C NMR** (100 MHz, CDCl<sub>3</sub>): δ 167.6, 167.0, 140.5, 138.3, 134.9, 134.8, 129.1, 128.1, 127.4, 127.3, 123.5, 117.3, 112.8, 111.7, 110.0, 108.9, 53.6, 44.2, 29.7.

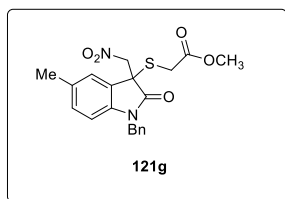
**HPLC:** Daicel ODH column, 80:20 (*n*-hexane:*i*-PrOH), flow rate 1.0 mL/min, 254 nm, temp=25 °C,  $t_{\text{major}}=15.0$  min  $t_{\text{minor}}=20.0$  min.

**IR(neat):** 2750, 1750, 1705, 1556, 1412, 1158, 900, 790 cm<sup>-1</sup>

### 3.8.7 Addition of Methyl Thioglycolate (**120**) to *N*-Benzyl 5-Methyl Isatin derived Nitroalkene **117g**

General procedure starting from *N*-benzyl 5-methyl isatin derived nitroalkene **117g** and methyl thioglycolate (**120**) was applied. After 2 h, the desired product **121g** was afforded with 78% yield and 47% ee.

Optical rotation was detected as  $[\alpha]_{589}^{29} = -4.46^{\circ}$  ( $c = 0.01$ g/mL, CH<sub>2</sub>Cl<sub>2</sub>).



**mp:** 135 °C

**<sup>1</sup>H NMR** (400 MHz, CDCl<sub>3</sub>): δ 8.76 – 8.62 (d, *J* = 36.6 Hz, 1H), 7.26 – 7.08 (m, 5H), 6.91– 6.79 (m, 1H), 6.50 – 6.44 (m, 1H), 4.84 – 4.80 (d, *J* = 4.5 Hz, 1H), 3.86 – 3.48 (m, 6H), 2.28 – 2.20 (m, 3H).

**<sup>13</sup>C NMR** (100 MHz, CDCl<sub>3</sub>): δ 168.8, 165.9, 136.2, 131.7, 128.9, 128.7, 127.5, 124.7, 122.0, 108.8, 108.6, 53.1, 43.7, 45.5, 37.0, 36.5, 21.2, 21.1.

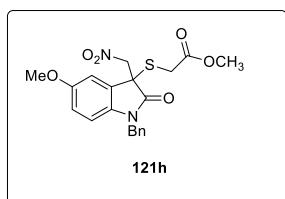
**HPLC:** Daicel ODH column, 90:10 (*n*-hexane:*i*-PrOH), flow rate 1.0 mL/min, 254 nm, temp=25 °C, *t*<sub>major</sub>=19 min *t*<sub>minor</sub>=25 min

**IR(neat):** 2765, 1750, 1699, 1553, 1456, 1362, 1178, 908, 796, 669 cm<sup>-1</sup>

### 3.8.8 Addition of Methyl Thioglycolate (120) to *N*-Benzyl 5-Methoxy Isatin derived Nitroalkene 117h

General procedure starting from *N*-benzyl 5-methoxy isatin derived nitroalkene **117h** and methyl thioglycolate (**120**) was applied. After 24 h, the desired product **121h** was afforded with 44% yield and 59% ee.

Optical rotation was detected as  $[\alpha]_{589}^{29} = +46.6^\circ$  (*c* = 0.01g/mL, CH<sub>2</sub>Cl<sub>2</sub>).



**mp:** 141 °C

**<sup>1</sup>H NMR** (400 MHz, CDCl<sub>3</sub>): δ 7.78 (s, 1H), 7.22 – 7.16 (m, 2H), 7.10 - 7.09 (m, 3H), 6.62 – 6.59 (m, 1H), 6.53 – 6.49 (m, 1H), 4.85 – 4.84 (d, *J* = 2.4 Hz, 1H), 3.73 – 3.53 (m, 8H), 1.27 – 1.13 (m, 2H).

**<sup>13</sup>C NMR** (100 MHz, CDCl<sub>3</sub>): δ 165.8, 155.6, 138.8, 136.2, 135.9, 135.8, 128.8, 128.7, 127.5, 127.4, 127.2, 113.2, 110.0, 109.2, 95.9, 93.4, 55.9, 43.7, 36.9.

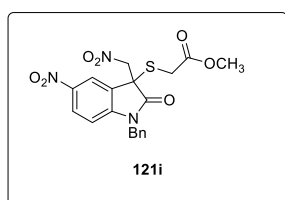
**HPLC:** Daicel ODH column, 90:10 (*n*-hexane:*i*-PrOH), flow rate 1.0 mL/min, 254 nm, temp=25 °C, *t*<sub>major</sub>=48.5 min *t*<sub>minor</sub>=89.5 min

**IR(neat):** 2755, 1745, 1699, 1552, 1497, 1375, 1288, 1035, 734 cm<sup>-1</sup>

### 3.8.9 Addition of Methyl Thioglycolate (**120**) to *N*-Benzyl 5-Nitro Isatin derived Nitroalkene **117i**

General procedure starting from *N*-benzyl 5-nitro isatin derived nitroalkene **117i** and methyl thioglycolate (**120**) was applied. After 30 min, the desired product **121i** was afforded with 67% yield and 9% ee.

Optical rotation was detected as  $[\alpha]_{589}^{29} = -0.2^\circ$  ( $c = 0.01$  g/mL, CH<sub>2</sub>Cl<sub>2</sub>).



**mp:** 138 °C

**<sup>1</sup>H NMR** (400 MHz, CDCl<sub>3</sub>): δ 8.42 - 8.38 (m, 1H), 8.12 - 8.08 (m, 1H), 7.62 - 7.48 (m, 1H), 7.31 - 7.27 (m, 4H), 6.73 - 6.67 (m, 1H), 5.02 - 4.98 (dd,  $J = 5.3, 0.9$  Hz, 2H), 4.02 - 3.98 (dd,  $J = 4.3$  Hz, 2H), 3.73 (s, 1H), 2.28 - 2.12 (m, 2H).

**<sup>13</sup>C NMR** (100 MHz, CDCl<sub>3</sub>): δ 173.5, 169.7, 148.5, 140.8, 137.0, 128.8, 128.8, 128.5, 128.5, 128.0, 118.6, 112.4, 62.3, 58.9, 47.4, 44.9.

**HPLC:** Daicel ODH column, 90:10 (*n*-hexane:*i*-PrOH), flow rate 1.0 mL/min, 254 nm, temp=25 °C,  $t_{\text{major}}=17.7$  min  $t_{\text{minor}}=23.4$  min

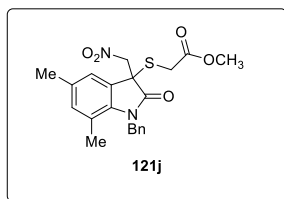
**IR(neat):** 3292, 2750, 1760, 1708, 1550, 1490, 1457, 1374, 1267, 1097, 813, 783, 676 cm<sup>-1</sup>

### 3.8.10 Addition of Methyl Thioglycolate (**120**) to *N*-Benzyl 5,7-*di*Methyl Isatin derived Nitroalkene **117j**

General procedure starting from *N*-benzyl 5,7-*di*methyl isatin derived nitroalkene **117j** and methyl thioglycolate (**120**) was applied. After 2 h, the desired product **121j** was afforded with 70% yield and 59% ee.

Optical rotation was detected as  $[\alpha]_{589}^{29} = +33.1^\circ$  ( $c = 0.01$  g/mL, CH<sub>2</sub>Cl<sub>2</sub>).





**mp:** 134 °C

**<sup>1</sup>H NMR** (400 MHz, CDCl<sub>3</sub>): δ 7.31 – 7.27 (m, 1H), 7.21 – 7.11 (m, 5H), 6.82 (s, 2H), 5.26 – 5.18 (dd, *J* = 5.3, 1.2 Hz, 2H), 5.13 – 4.99 (dd, *J* = 12.1, 2.6 Hz, 3H), 2.24 – 2.16 (dd, *J* = 9.6 Hz, 2H), 1.98 (s, 6H).

**<sup>13</sup>C NMR** (100 MHz, CDCl<sub>3</sub>): δ 189.7, 188.3, 137.1, 137.0, 136.7, 136.3, 133.6, 132.8, 128.7, 126.9, 125.4, 123.2, 123.2, 61.5, 58.9, 47.8, 45.3, 28.5, 18.4.

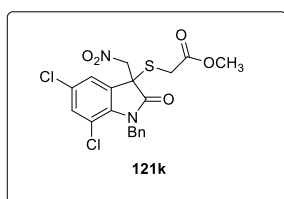
**HPLC:** Daicel IA column, 70:30 (*n*-hexane:*i*-PrOH), flow rate 1.0 mL/min, 254 nm, temp=25 °C, *t*<sub>major</sub>=8.2 min *t*<sub>minor</sub>=14.5 min

**IR(neat):** 3270, 2750, 1760, 1685, 1546, 1456, 1373, 1075, 779, 746, 670 cm<sup>-1</sup>

### 3.8.11 Addition of Methyl Thioglycolate (120) to *N*-Benzyl 5,7-*di*Chloro Isatin derived Nitroalkene 117k

General procedure starting from *N*-benzyl 5,7-*dichloro* isatin derived nitroalkene **117k** and methyl thioglycolate (**120**) was applied. After 22 h, the desired product **121k** was afforded with 80% yield and 39% ee.

Optical rotation was detected as  $[\alpha]_{589}^{29} = +5.04^{\circ}$  (*c* = 0.01 g/mL, CH<sub>2</sub>Cl<sub>2</sub>).



**mp:** 142 °C

**<sup>1</sup>H NMR** (400 MHz, CDCl<sub>3</sub>): δ 7.51 (s, 1H), 7.31 (s, 1H), 7.31 – 7.27 (m, 3H), 7.25 – 7.19 (m, 1H), 5.74 – 5.08 (dd, *J* = 18.9, 3.0 Hz, 2H), 4.82 – 4.78 (d, *J* = 6.7 Hz, 2H), 3.79 (s, 3H).

**<sup>13</sup>C NMR** (100 MHz, CDCl<sub>3</sub>): δ 166.2, 137.5, 136.9, 132.7, 131.9, 128.7, 128.3, 127.4, 127.2, 126.5, 124.1, 123.4, 116.1, 66.0, 50.2, 44.9, 29.7.

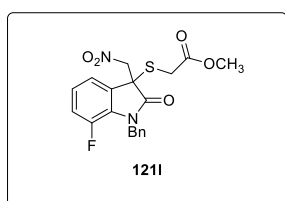
**HPLC:** Daicel ODH column, 90:10 (*n*-hexane:*i*-PrOH), flow rate 1.0 mL/min, 254 nm, temp=25 °C, *t*<sub>major</sub>=17.8 min *t*<sub>minor</sub>=23.5 min

**IR(neat):** 2750, 1760, 1707, 1550, 1374, 1103, 807, 781 cm<sup>-1</sup>.

### 3.8.12 Addition of Methyl Thioglycolate (**120**) to *N*-Benzyl 7-Fluoro Isatin derived Nitroalkene **117l**

General procedure starting from *N*-benzyl 7-fluoro isatin derived nitroalkene **117l** and methyl thioglycolate (**120**) was applied. After 1 h, the desired product **121l** was afforded with 75% yield and 29% ee.

Optical rotation was detected as  $[\alpha]_{589}^{29} = +1.3^{\circ}$  ( $c = 0.01$  g/mL,  $\text{CH}_2\text{Cl}_2$ ).



**mp:** 140 °C

**<sup>1</sup>H NMR** (400 MHz,  $\text{CDCl}_3$ ):  $\delta$  7.38 – 7.30 (m, 2H), 7.28 – 7.26 (m, 2H), 7.21 – 7.19 (m, 2H), 7.13 – 7.09 (m, 1H), 5.75 – 4.96 (dd,  $J = 18.6, 9.7$  Hz, 2H), 4.84 – 4.82 (d,  $J =$

7.4 Hz, 2H), 3.77 (s, 3H), 2.52 – 2.48), (d,  $J = 21.0$  Hz, 2H).

**<sup>13</sup>C NMR** (100 MHz,  $\text{CDCl}_3$ ):  $\delta$  192.4, 187.8, 166.6, 146.3, 141.7, 134.9, 132.4, 129.0, 127.9, 127.3, 122.9, 117.9, 115.7, 114.5, 110.4, 61.2, 43.9.

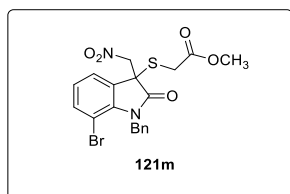
**HPLC:** Daicel ASH column, 80:20 (*n*-hexane:*i*-PrOH), flow rate 1.0 mL/min, 254 nm, temp=25 °C,  $t_{\text{major}}=17.9$  min  $t_{\text{minor}}=23.5$  min

**IR(neat):** 3292, 2740, 1750, 1708, 1550, 1490, 1457, 1374, 1267, 1097, 813, 783, 676  $\text{cm}^{-1}$

### 3.8.13 Addition of Methyl Thioglycolate (**120**) to *N*-Benzyl 7-Bromo Isatin derived Nitroalkene **117m**

General procedure starting from *N*-benzyl 7-bromo isatin derived nitroalkene **117m** and methyl thioglycolate (**120**) was applied. After 3 h, the desired product **121m** was afforded with 66% yield and 47% ee.

Optical rotation was detected as  $[\alpha]_{589}^{29} = +9.25^{\circ}$  ( $c = 0.01$  g/mL,  $\text{CH}_2\text{Cl}_2$ ).



**mp:** 144 °C

**<sup>1</sup>H NMR** (400 MHz, CDCl<sub>3</sub>): δ 7.54 – 7.48 (dd, *J* = 8.5 Hz, 2H), 7.38 – 7.32 (m, 2H), 7.31 – 7.27 (m, 2H), 7.25 – 7.19 (m, 2H), 5.37 – 5.11 (dd, *J* = 12.4, 6.2 Hz, 2H), 4.88 – 4.72 (d, *J* = 10.0 Hz, 2H), 3.77 (s, 1H), 2.40 – 2.32 (d, *J* = 38.2, 2H).

**<sup>13</sup>C NMR** (100 MHz, CDCl<sub>3</sub>): δ 177.9, 166.8, 137.2, 136.2, 130.9, 130.8, 129.0, 128.6, 127.7, 127.2, 126.5, 126.4, 126.1, 123.8, 123.7, 102.8, 44.6.

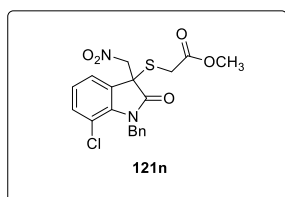
**HPLC:** Daicel ASH column, 90:10 (*n*-hexane:*i*-PrOH), flow rate 1.0 mL/min, 254 nm, temp=25 °C, *t*<sub>major</sub>=18.0 min *t*<sub>minor</sub>=25.0 min

**IR(neat):** 2750, 1760, 1715, 1556, 1489, 1374, 1096, 741 cm<sup>-1</sup>

### 3.8.14 Addition of Methyl Thioglycolate (120) to *N*-Benzyl 7-Chloro Isatin derived Nitroalkene 117n

General procedure starting from *N*-benzyl 7-chloro isatin derived nitroalkene **117n** and methyl thioglycolate (**120**) was applied. After 6 h, the desired product **121n** was afforded with 71% yield and 25% ee.

Optical rotation was detected as  $[\alpha]_{589}^{29} = +6.7^\circ$  (*c* = 0.01 g/mL, CH<sub>2</sub>Cl<sub>2</sub>).



**mp:** 144 °C

**<sup>1</sup>H NMR** (400 MHz, CDCl<sub>3</sub>): δ 7.39 – 7.31 (m, 1H), 7.29 – 7.27 (m, 2H), 7.23 – 7.17 (m, 3H), 7.16 – 7.08 (m, 1H), 5.12 – 4.98 (dd, *J* = 13.2, 6.0 Hz, 2H), 4.82 – 4.80 (d, *J* = 1.2 Hz, 2H), 3.76 (s, 3H) 1.69 – 1.67 (d, *J* = 81. Hz, 2H).

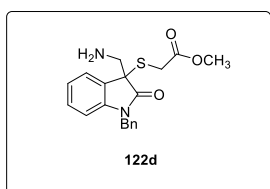
**<sup>13</sup>C NMR** (100 MHz, CDCl<sub>3</sub>): δ 176.0, 166.2, 137.5, 136.9, 132.7, 131.9, 128.7, 128.3, 127.4, 127.2, 126.5, 124.1, 123.4, 116.1, 57.5, 44.9.

**HPLC:** Daicel ODH column, 90:10 (*n*-hexane:*i*-PrOH), flow rate 1.0 mL/min, 254 nm, temp=25 °C, *t*<sub>major</sub>=16.4 min *t*<sub>minor</sub>=21.4 min

**IR(neat):** 2750, 1760, 1707, 1550, 1374, 1103, 807, 781 cm<sup>-1</sup>

### 3.8.15 Reduction of Nitro Group of Sulfa-Michael Adduct 121d

1 eq sulfa-Michael adduct 121d (0.225 mmol, 86 mg) was dissolved in MeOH. 1.5 eq ammonium formate (0.337 mmol, 21.28 mg) and 50 mg 10% Pd on activated charcoal puriss were added to the solution. The reaction was heated to 50 °C. After 14 h, the reaction mixture was filtered through Celite, the filtrate was concentrated and loaded to column chromatography (*n*-Hex:EtOAc). The product was obtained with 60 % yield.



**mp:** 132 °C

**<sup>1</sup>H NMR** (400 MHz, CDCl<sub>3</sub>): δ 7.57 – 7.53 (m, 1H), 7.38 – 7.32 (m, 1H), 7.30 – 7.27 (m, 4H), 7.24 – 7.22 (d, *J* = 7.09 Hz, 1H), 7.21 – 7.19 (m, 1H), 7.12 – 7.10 (dd, *J* = 8.7, 1.3 Hz, 1H), 4.88 – 4.70 (dd, *J* = 88.7, 1.3 Hz, 2H), 3.78 – 3.70 (m, 6H), 3.48 – 3.46 (d, *J* = 1.8 Hz, 1H).

**<sup>13</sup>C NMR** (100 MHz, CDCl<sub>3</sub>): δ 166.7, 160.2, 142.5, 139.2, 134.4, 129.7, 129.1, 128.2, 127.2, 121.4, 121.2, 118.2, 118.0, 117.6, 110.5, 110.4, 53.4, 51.8, 48.0, 47.4, 34.9.

**IR(neat):** 3282, 2928, 2750, 1760, 1692, 1609, 1561, 1372, 1089, 884, 795, 749, 695 cm<sup>-1</sup>

## CHAPTER 4

### CONCLUSION

Throughout this work, a new synthetic methodology was studied for the asymmetric synthesis of methyl 2-((1-methyl-3-(nitromethyl)-2-oxindolin-3-yl)thio)acetate (**121a**) by the bifunctional acid/base organocatalysts developed by our research group.

In the first part, sulfa-Michael addition of methyl thioglycolate (**120**) to *N*-methyl substituted isatin derived nitroalkene **117a** was tested with bifunctional organocatalysts. Since 1-adamantyl squaramide-quinine (**I**) was the best working organocatalyst, the solvent, temperature, catalyst loading and concentration screenings were done with this organocatalyst. The solvent screening revealed that THF is the proper solvent for the reaction because of elevating the yield and enantioselectivity to 53% and 59% respectively in drastically reduced reaction duration (10 min). Although we could not improve enantioselectivity via changing temperature or catalyst loading changing, we caught a slight increase in enantioselectivity when methyl thioglycolate (**120**) concentration was doubled. Different groups were substituted to 3-position substituted isatin derived nitroalkene **117** in the second part. The optimized conditions were tested on *N*-ethyl, allyl, benzyl substituted **117b-c** and unsubstituted **116** isatin derived nitroalkenes. *N*-benzyl substituted isatin derived nitroalkene **117d** led to the highest enantioselectivity (70 % ee). The side reactions were also observed to be diminished and the yield was increased to 75 %. Derivatization studies continued with ten different *N*-benzyl substituted isatin derived nitroalkenes **117e-n**. Sulfa-Michael reaction of these derivatives were carried out, but we could not obtain a

more advanced result. Lastly, the sulfa-Michael adduct **121d** underwent catalytic reduction and the nitro group was reduced into amine group. As aforementioned in Aim of The Work (Section 1.5), the reduced product **122d** was planned to attack on ester carbonyl group in order to yield thiomorpholine-3-one based compound **123d** which can be biologically active and unique skeleton. Unfortunately, the protocols we applied for the cyclization reaction did not yield the target molecule **123d**.

## REFERENCES

1. Gawley, R. E.; Aubé, J. *Principles of Asymmetric Synthesis*. Elsevier Science Ltd. **1996**, 1<sup>st</sup> ed.
2. Walshe, J.M. *Mov. Disord.* **2003**, *18*, 853.
3. Black, J.W.; Crowther, A.F.; Shanks, R.G.; Smith, L.H.; Dornhorst, A.C. *The Lancet* **1964**, *283*, 1080.
4. Blaschke, G.; Kraft, H. P.; Markgraf, H. *Chem. Ber.* **1980**, *113*, 2318.
5. Blaser, H. *Chem. Rev.* **1992**, *92*, 935.
6. Guerlavais, V.; Carroll, P. J.; Jouillie, M. M. *Tetrahedron: Asymmetry* **2002**, *13*, 675.
7. M. M.; Zadsirjan, V.; Farajpour, B. *RSC Adv.*, **2016**, *6*, 30498
8. Schreiner, P. R. *Chem. Soc. Rev.* **2003**, *32*.
9. Santaniello, E.; Ferraboschi, P.; Grisenti, P.; Manzocchi, A. *Chem. Rev.* **1992**, *92*, 1071.
10. Rachwalski, M.; Vermue, N.; Rutjes, F. P. J. T. *Chem. Soc. Rev.* **2013**, *42*, 9268.
11. Knowles, W.S. *Acc. Chem. Res.* **1983**, *16*, 106.
12. Katsuki, T.; Sharpless, K. B. *J. Am. Chem. Soc.* **1980**, *102*, 5976.
13. Noyori, R. *Angew. Chem. Int. Ed.* **2002**, *41*, 2008.
14. a. Manginon, I.K.; Northrup, A. B.; MacMillan, D.W. *Angew. Chem. Int. Ed.* **2004**, *43*, 6722.  
b. Franzen, J.; Marigo, M.; Fielenbach, D.; Wabnitz, T.C.; Kjaersgaard, A.; Jørgensen, K.A. *J. Am. Chem. Soc.* **2005**, *127*, 18296.  
c. Wenzel, A.G.; Lalonde, M. P.; Jacobsen, E. N. *Synlett* **2003**, *12*, 1919.  
d. List, B.; Lerner, R. A.; Barbas, C. F. III *J. Am. Chem. Soc.* **2000**, *122*, 2395.
15. MacMillan, D. W. C. *Nature*, **2008**, *455*, 304.
16. Pellisier, H. *Tetrahedron* **2007**, *63*, 9267.
17. Etzenbach-Effers, K.; Berkessel, A. *Top-Curr. Chem* **2010**, *291*, 1.
18. Jacobsen, E. N.; Taylor, M. S. *Angew. Chem. Int. Ed.* **2006**, *45*, 1520.

19. Berkessel, A.; Gröger, H. *Asymmetric Organocatalysis: From Biomimetic Concepts to Applications in Asymmetric Synthesis*. 1<sup>st</sup> ed.; Wiley-VCH, Germany, 2005.
20. Curran, D. P.; Kuo, L. H. *J. Org. Chem.* **1994**, *59*, 3259.
21. Vachal, P.; Jacobsen, E. N. *J. Am. Chem. Soc.* **2002**, *124*, 10012.
22. Ojima, I. *Catalytic Asymmetric Synthesis*. 3<sup>rd</sup> ed.; Wiley, New Jersey, **2010**.
23. Malerich, J. P.; Hagihara, K.; Rawal, V. H. *J. Am. Chem. Soc.* **2008**, *130*, 14416.
24. Alemon, J.; Parra, A.; Jiong, H.; Jørgensen, K. A. *Chem. Eur. J.* **2011**, *17*, 6890.
25. Quiñonero, D.; Prohens, R.; Garau, C.; Frontera, A.; Ballester, P.; Costa, A.; Dey, P. M. *Chem. Phys. Lett.* **2002**, *351*, 115.
26. Zhou, L.-X.; Zhang, Y.-F.; Wu, L.-M.; Li, J.-Q. *J. Mol. Struct.* **2000**, *137*, 516.
27. Choong E. S. *Cinchona Alkaloids in Synthesis and Catalysis: Ligands, Immobilization and Organocatalysis*, 1<sup>st</sup> ed.; Wiley-VCH, Germany, 2009.
28. Wynberg, H. R. *Journal of the Royal Netherlands Chemical Society* **1981**, *100*, 11.
29. Houk, K.N.; Grayson, M. N. *J. Am. Chem. Soc.* **2016**, *138*, 1170.
30. Marcelli, T. *Organocatalysis: Cinchona Catalysts*. John Wiley & Sons, **2011**; Vol. 1, 142.
31. Berry, D.; DiGiovanna, C.; Metric, S.; Murugan, R. *Arkivoc.* **2001**, *2*, 944.
32. Spivey, A. C.; Arseniyadis, S. *Angew. Chem. Int. Ed.* **2004**, *43*, 5436.
33. Wurz, R. P. *Chem. Rev.* **2007**, *107*, 5570.
34. Hodous, B. L.; Fu, G. C. *J. Am. Chem. Soc.* **2002**, *124*, 10006.
35. Schreiner, P.R. *Chem. Soc. Rev.* **2003**, *32*, 289.
36. Miyabe, H.; Takemoto, Y. *Bull. Chem. Soc. Jap.* **2008**, *81*, 785.
37. Işık, M.; Ünver, M.Y.; Tanyeli, C. *J. Org. Chem.* **2015**, *80*, 828.
38. Kanberoglu, E.; Tanyeli, C. *Asian J. Org. Chem.* **2016**, *5*, 114.
39. Yu, JS.; Huang, HM.; Ding, PG.; Hu, XS., Zhou, F.; Zhou, J. *Am. Chem. Soc. Catal.* **2016**, *6*, 5319.



40. Grayson, M.N.; Houk, K. N. *J. Am. Chem. Soc.* **2016**, *138*.
41. Guo, H.; Wong, M.W. *J. Org. Chem.* **2017**, *82*, 4362.
42. Wang, J.; Chen, N.; Xu, J. *Tetrahedron* **2015**, *71*, 4007.
43. Chauhan, P.; Mahajan, S.; Kaya, U.; Valkonen, A.; Rissanen, K.; Enders, D. *Adv. Synth. Catal.* **2016**, *358*, 3173.
44. Beceno, C.; Chauhan, P.; Rembiak, A.; Wang, A.; Enders, D. *Adv. Synth. Catal.* **2015**, *357*, 672.
45. Wang, XF.; Hua, QL.; Cheng, Y.; An, XL.; Yang, QQ.; Chen, JR.; Xiao, WJ. *Angew. Chem.* **2010**, *122*, 8557.
46. Yang, W.; Yang, Y.; Du, D.-M. *Org. Lett.* **2013**, *15*, 1190.
47. Duan, SW.; Li, Y.; Liu, YL.; Zou, YQ.; Shi, DQ.; Xiao, WJ.; *Chem. Commun.* **2012**, *48*, 5160.
48. Sumpter, W. C., *Chem. Rev.* **1944**, *34*, 993.
49. Shing, G. S.; Desta, Z. Y. *Chem. Rev.* **2012**, *112*, 6104.
50. Pakravan, P.; Kashanian, S.; Khadei, M. M.; Harding, F. *J. Pharmacol. Rep.* **2013**, *65*, 313.
51. Pal, M.; Sharma, N. K.; Priyonka, Jha, K. K. *J. Adv. Sci. Res.* **2011**, *2*, 35.
52. Zhang, H.; Liu, Y.; Chen, R.; Xue, J.; Li, Y.; Tang, Y. *Asian J. Org. Chem.* **2013**, *2*, 307.
53. Chen, G.; Hao, XJ.; Sun, QY.; Ding, J. *Chem. Pap.* **2010**, *64*, 673.
54. Alonso, D.A.; Baeza, A.; Chinchilla, R.; Gómez, C.; Guillena, G.; Pastor, I. M.; Ramón, D. *J. Molecules* **2017**, *22*, 895.
55. Berner, O. M.; Tedeschi, L.; Enders, D. *Eur. J. Org. Chem* **2002**, 1877.
56. Enders, D.; Lüttgen, K.; Narine, A. A. *Synthesis* **2007**, *7*, 959.
57. Frayne, S. H.; Murthy, R. R.; Northrop, B. H. *J. Org. Chem.* **2017**, *82*, 7946.
58. Erker, T.; Schreder, M. E.; Studenik, C. *Arch. Pharm. Pharm. Med. Chem.* **2000**, *333*, 58.
59. Aiello, A.; Fattorusso, E.; Lucaino, P.; Menna, M.; Esposito, G.; Iuvone, T.; Pala, D. *Eur. J. Org. Chem.* **2003**, 898
60. Galanski, M. E.; Erker, T.; Handler, N.; Lemmens-Gruber, R.; Kamyar, M.; Studenik, C. R. *Bioorg. Med. Chem.* **2016**, *14*, 826.

61. Silviya D. Furdas, S. D.; Shekfeh, S.; Kannan, S.; Sippl, W.; Jung, M. *Med. Chem. Commun.* **2012**, *3*, 305.
62. Chen, G.; Xiao-Jiang Hao, X J.; Sun, Q Y.; Ding, J. *Chem. Pap.* **2010**, *5*, 673.
63. Li, Y. M.; Wei, X. H.; Li, X. A.; Yang, S. D. *Chem. Commun.* **2013**, *49*, 11701.
64. a. Clark, P. G., Vieira, L. C., Tallant, C. , Fedorov, O. , Singleton, D. C., Rogers, C. M., Monteiro, O. P., Bennett, J. M., Baronio, R. , Müller, S. , Daniels, D. L., Méndez, J. , Knapp, S. , Brennan, P. E. and Dixon, D. J. *Angew. Chem. Int. Ed.*, **2015**, *54*, 6217.
- b. Grunewald, G. L.; Sall, D. J.; Monn, J. A. *J. Med. Chem.* **1988**, *31*, 433
- c. Wan, Y. , Auberger, N. , Thétiot-Laurent, S. , Bouillère, F. , Zulauf, A. , He, J. , Courtiol-Legourd, S. , Guillot, R. , Kouklovsky, C. , Cote des Combes, S. , Pacaud, C. , Devillers, I. and Alezra, V. *Eur. J. Org. Chem.* **2018**, 329.

## APPENDIX A

### NMR DATA

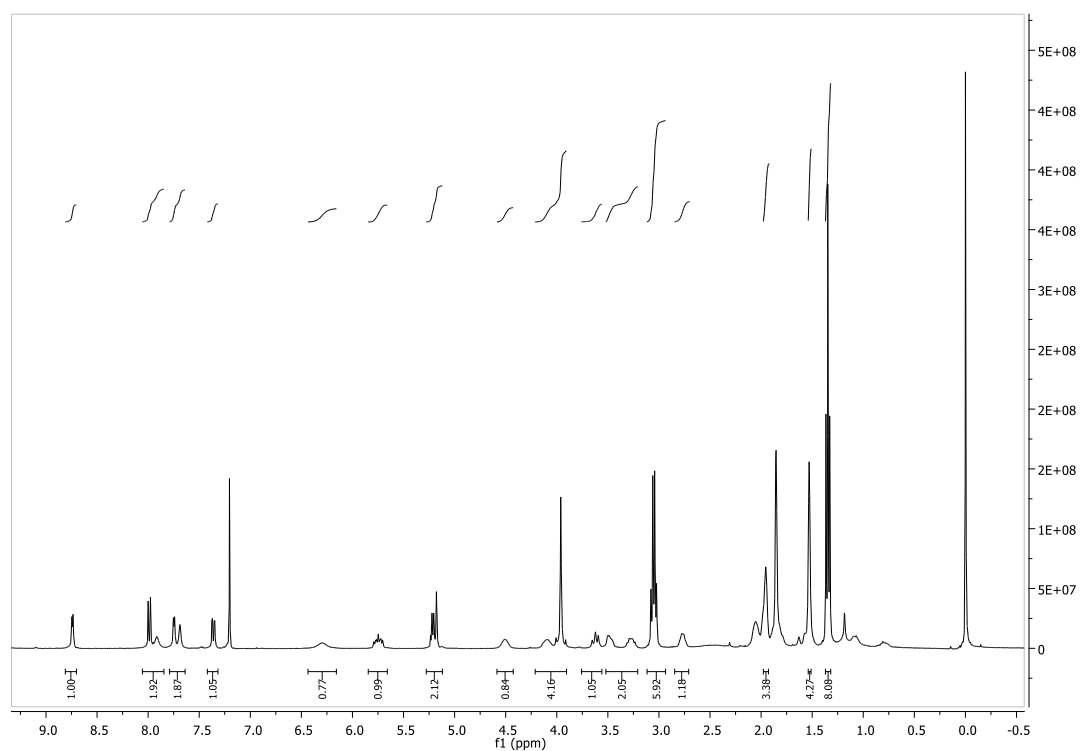
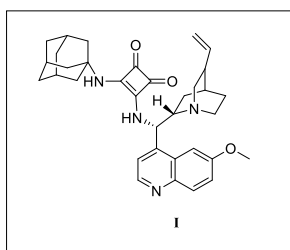


**Figure A. 1**  $^1\text{H}$  NMR spectrum of **I**

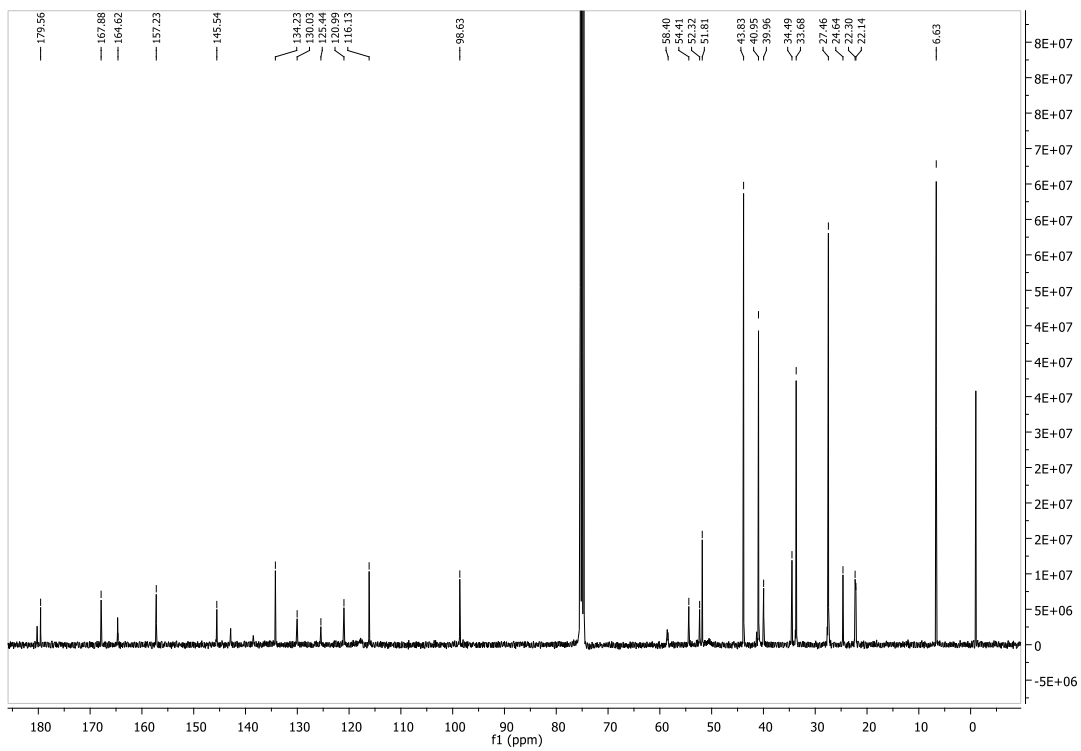


Figure A. 2  $^{13}\text{C}$  NMR spectrum of I

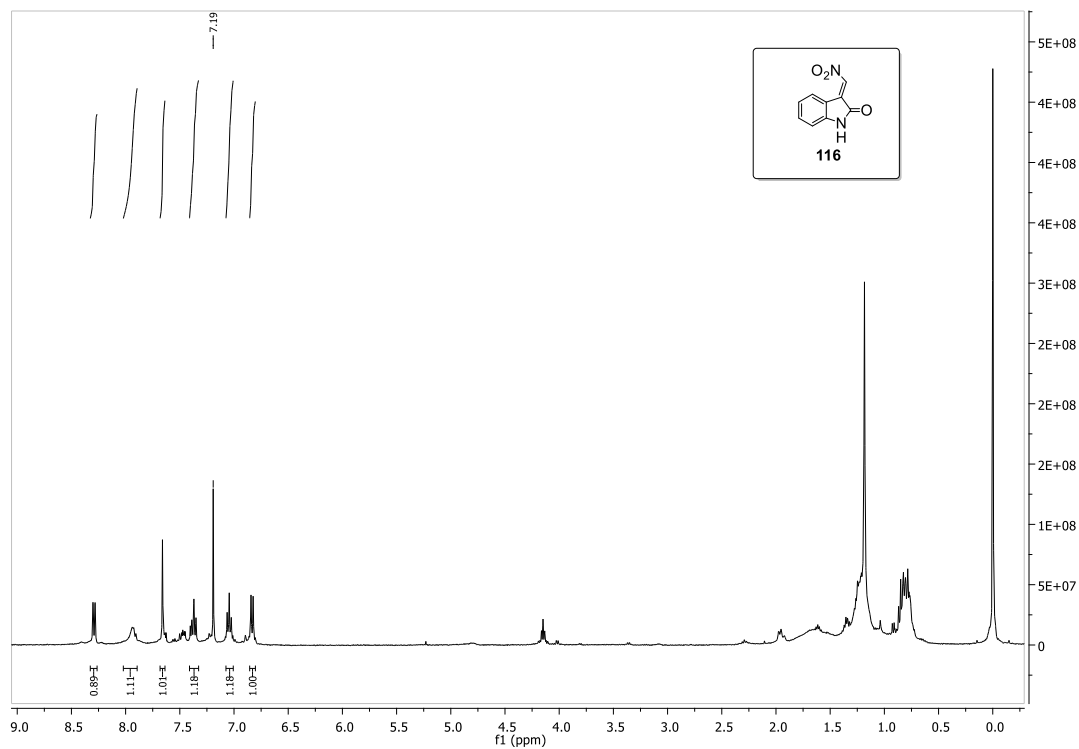


Figure A. 3 <sup>1</sup>H NMR spectrum of 116

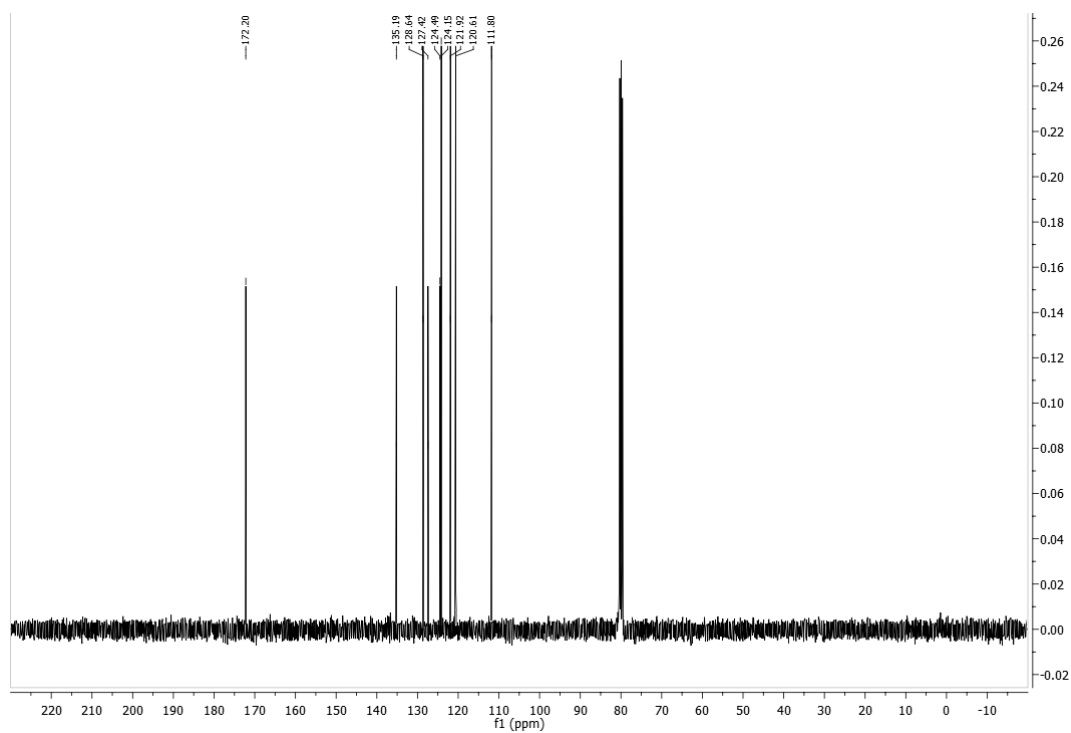
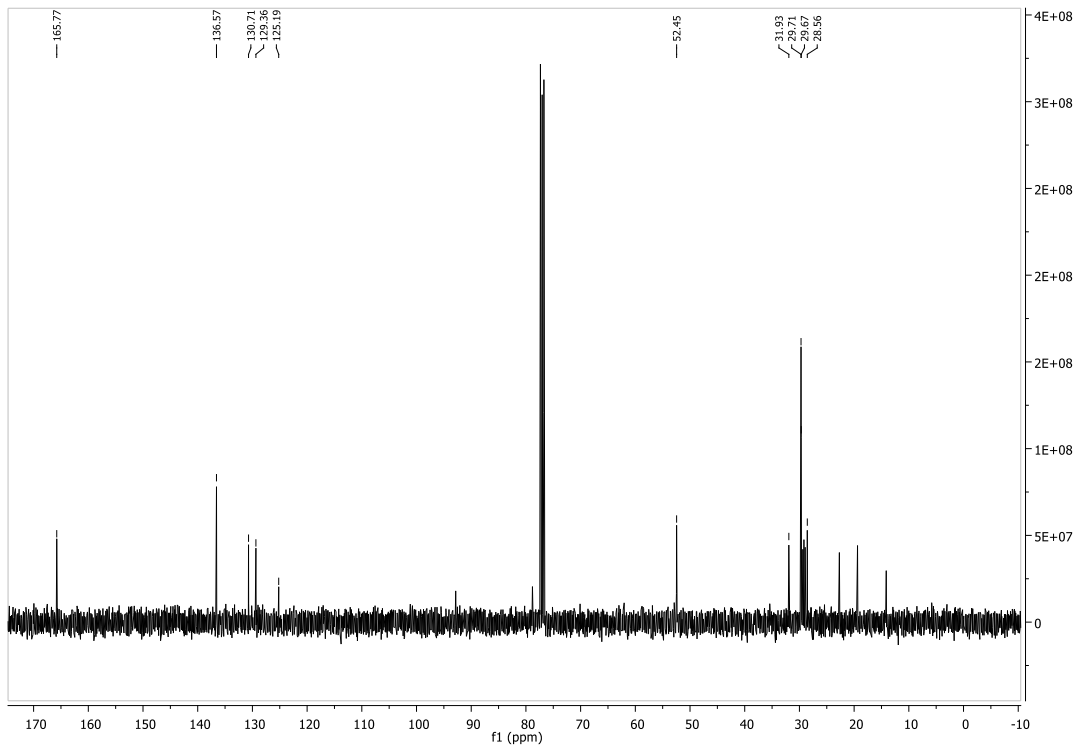
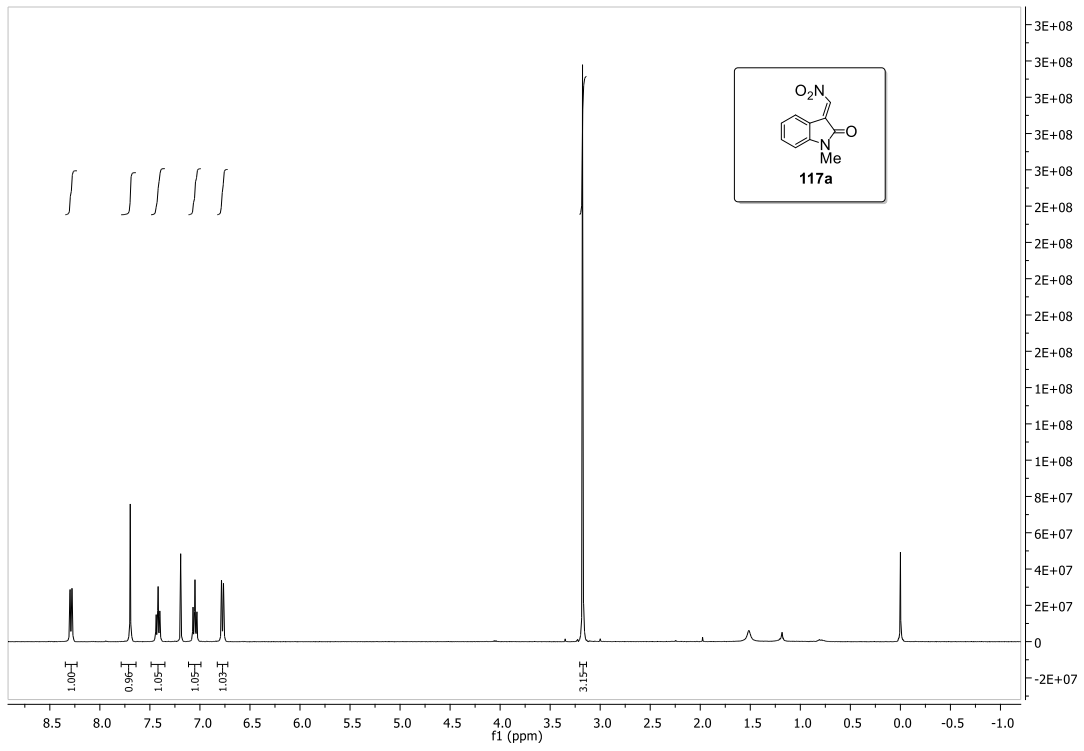
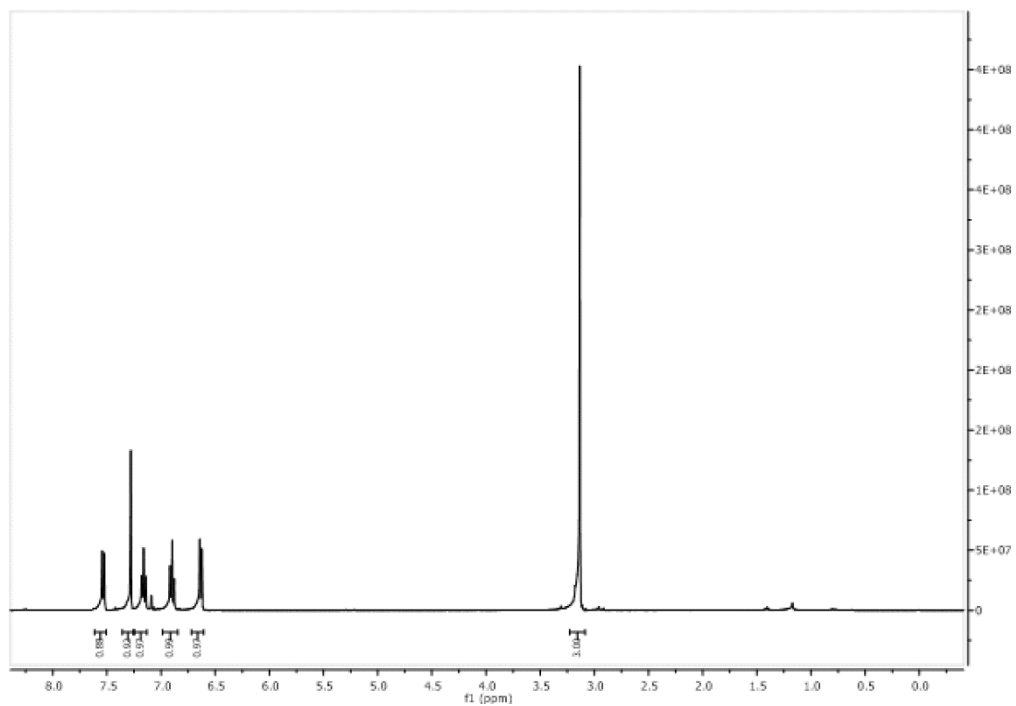
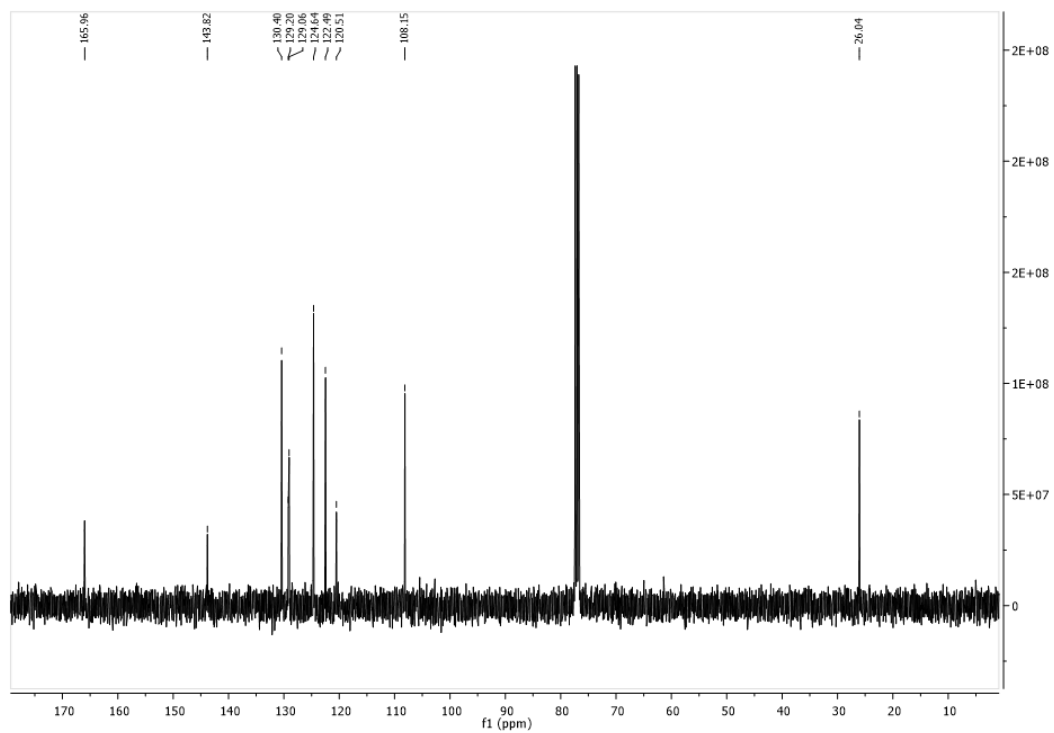


Figure A. 4 <sup>13</sup>C NMR spectrum of 116

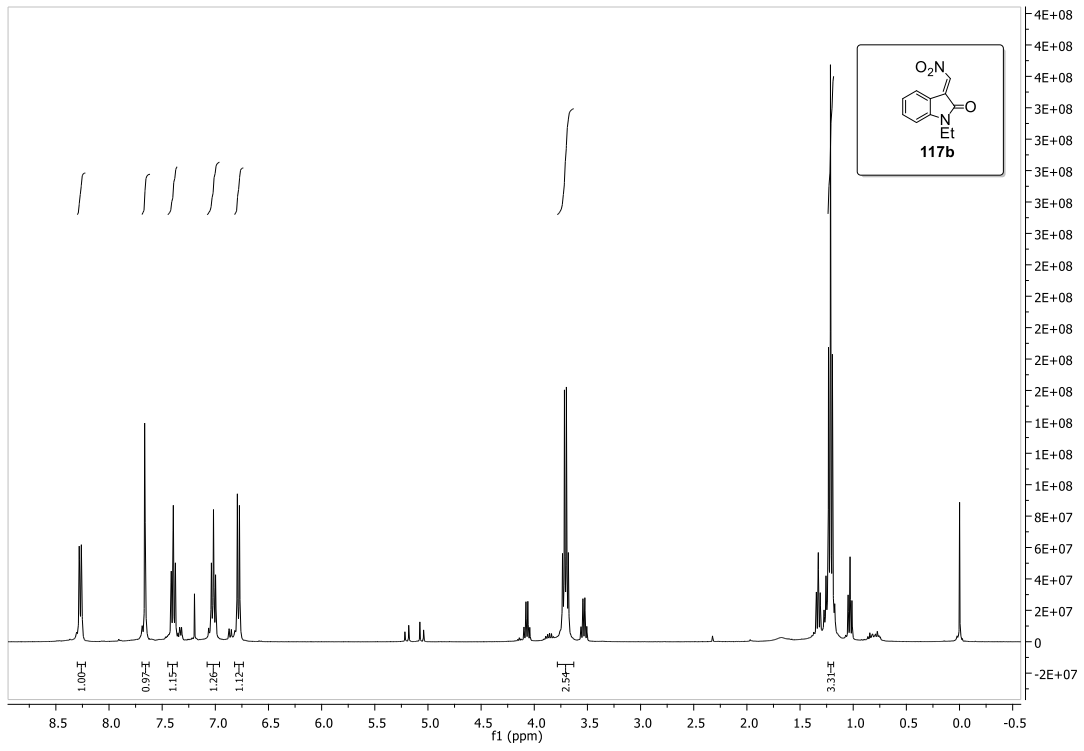




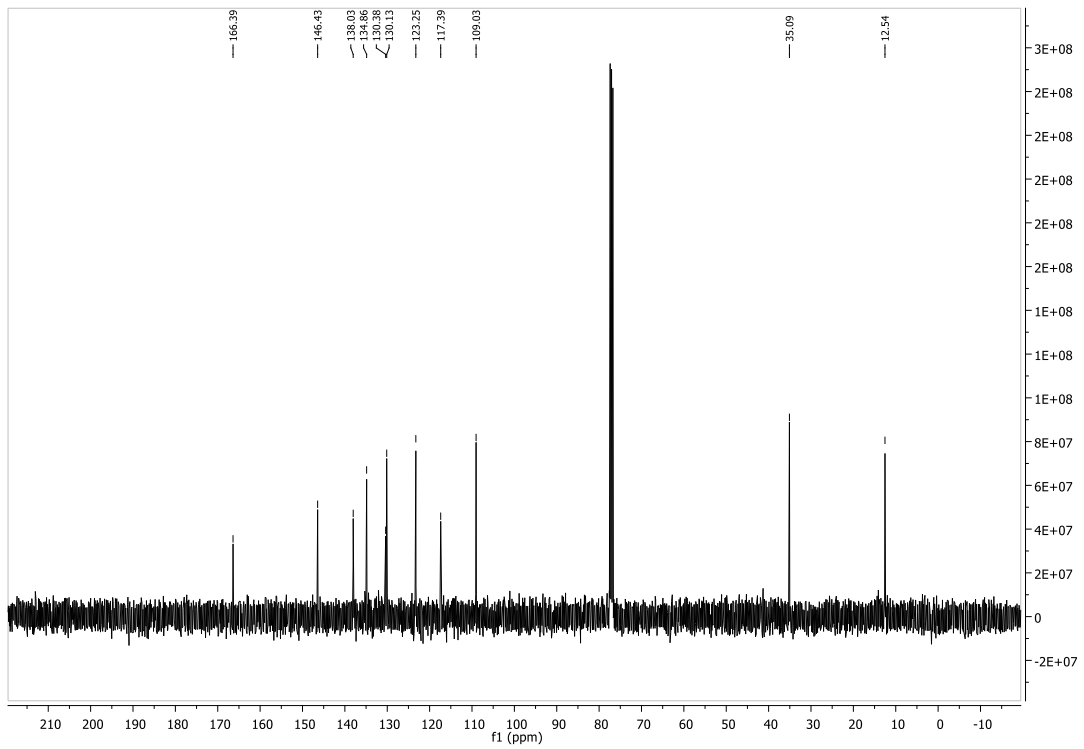
**Figure A. 7**  $^1\text{H}$  NMR spectrum of Z-117a



**Figure A. 8**  $^{13}\text{C}$  NMR spectrum of Z-117a

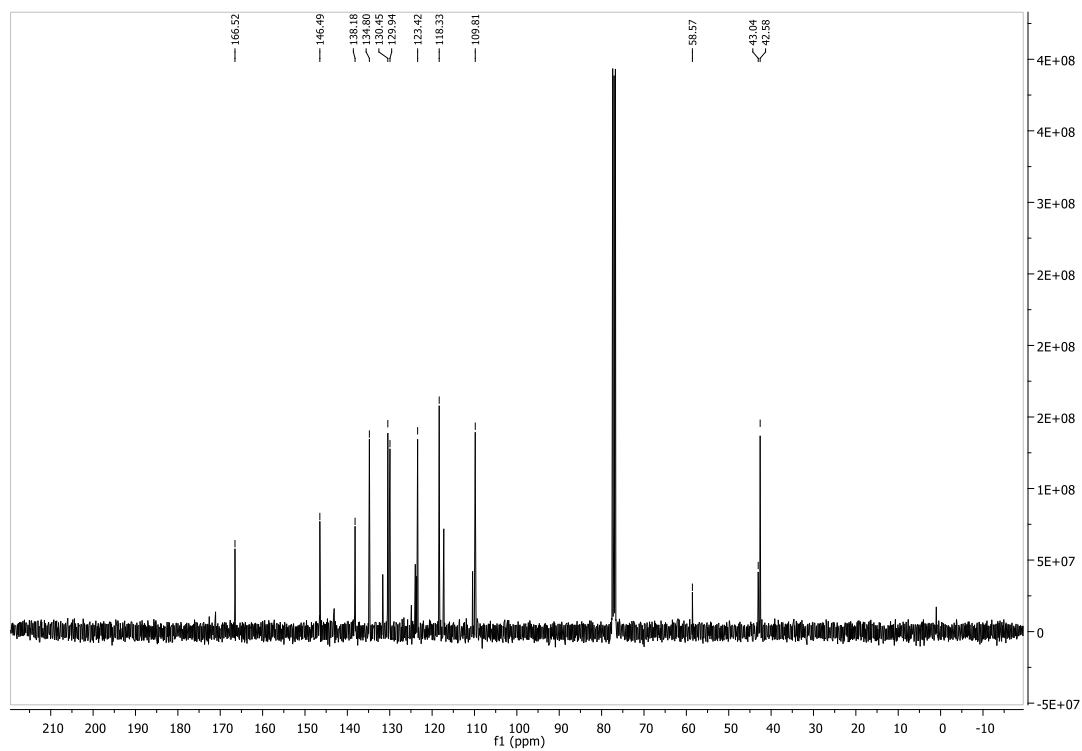
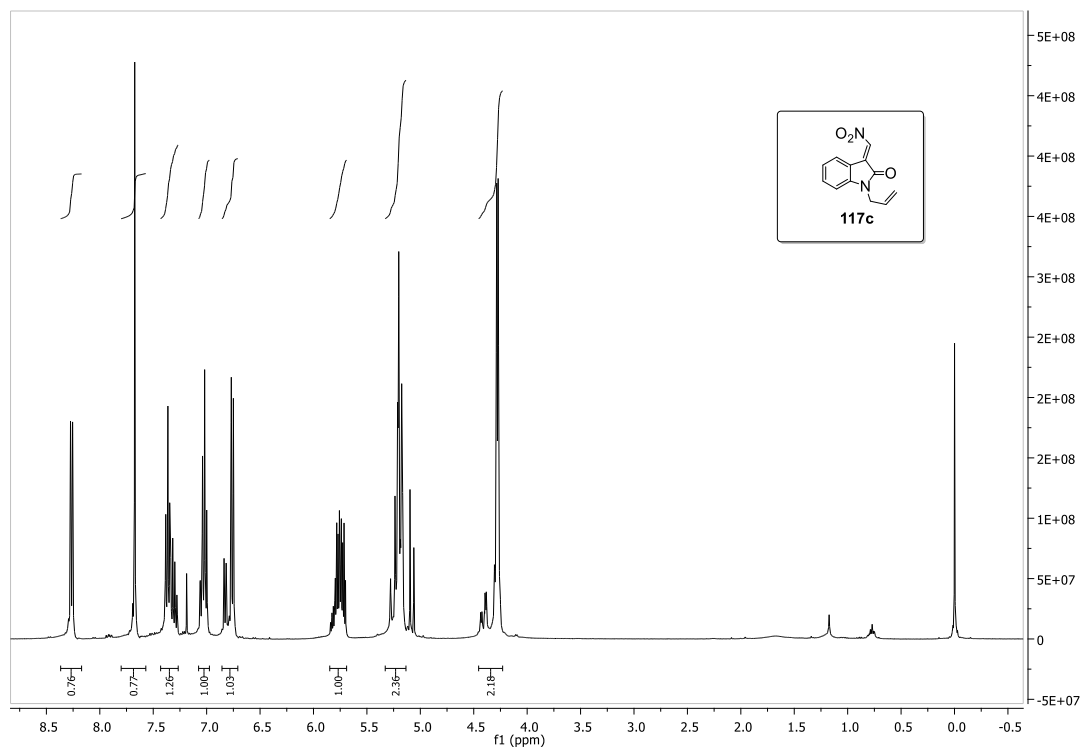


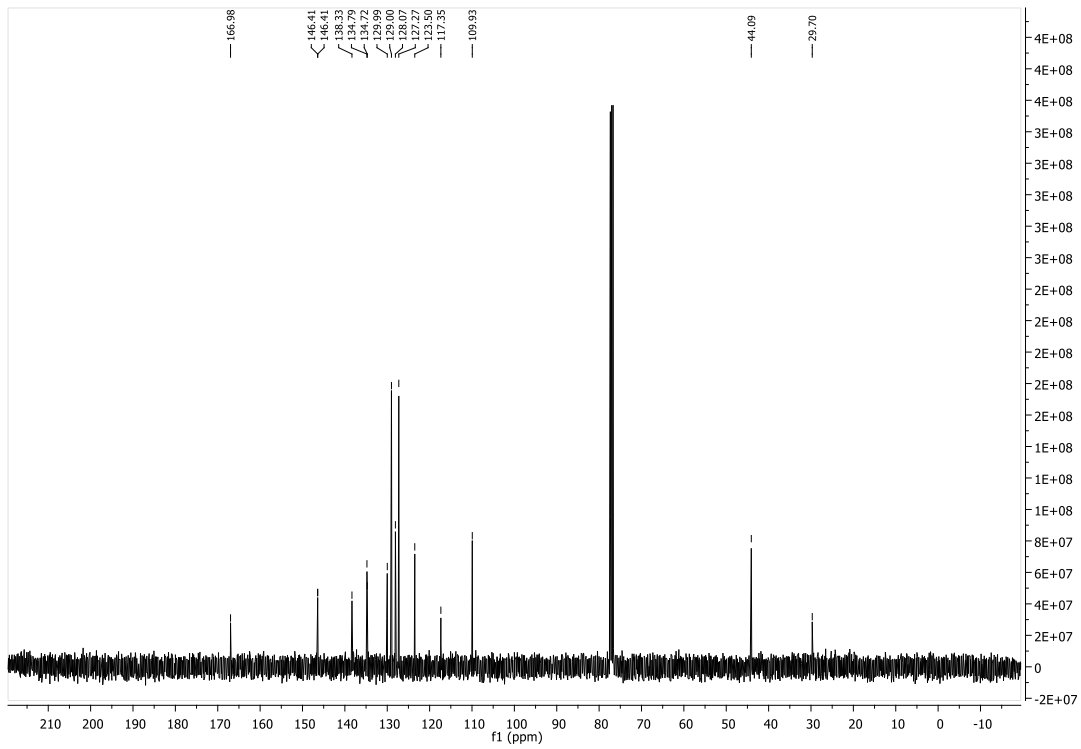
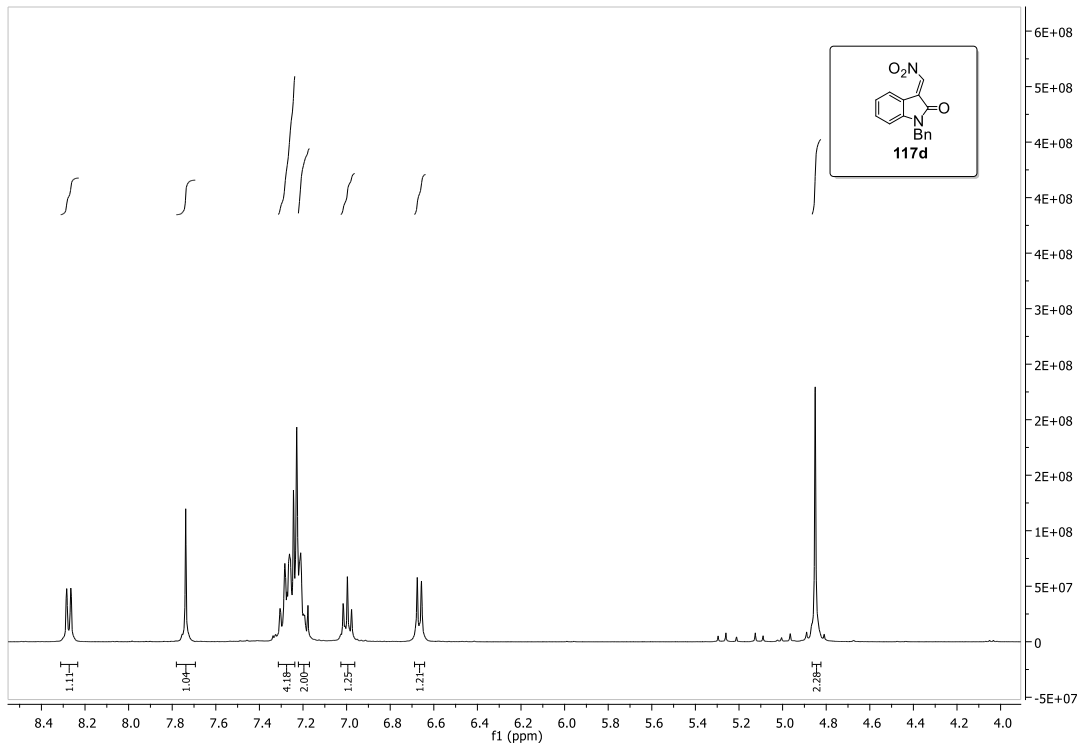
**Figure A. 9**  $^1\text{H}$  NMR spectrum of **117b**

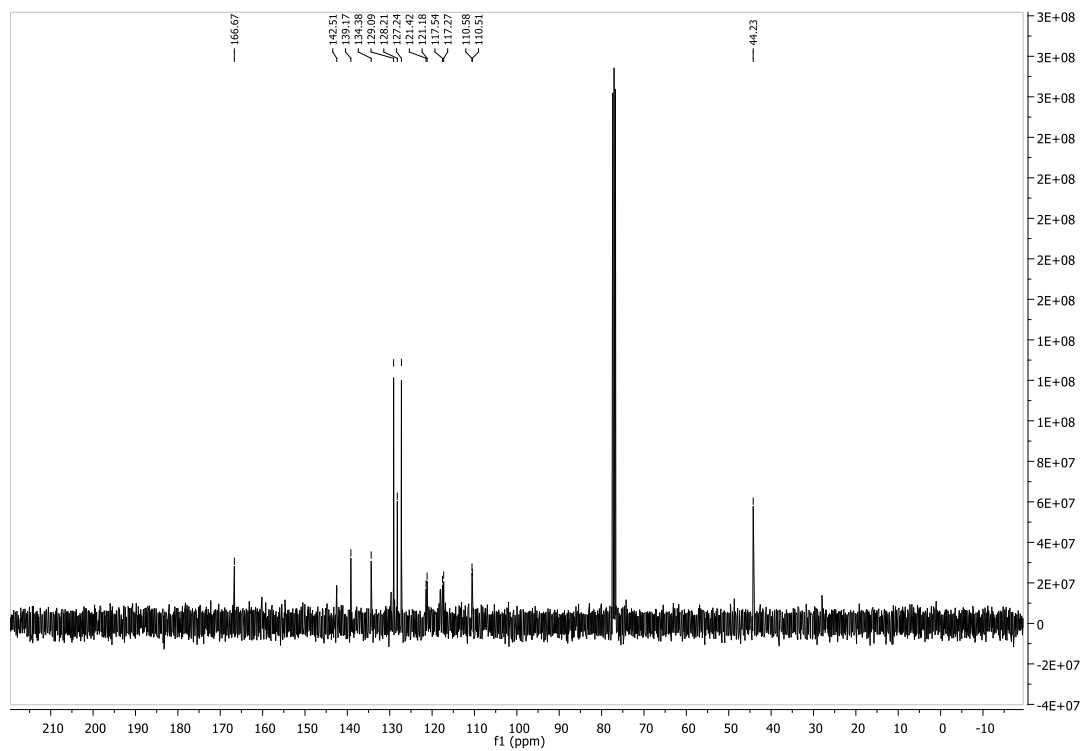
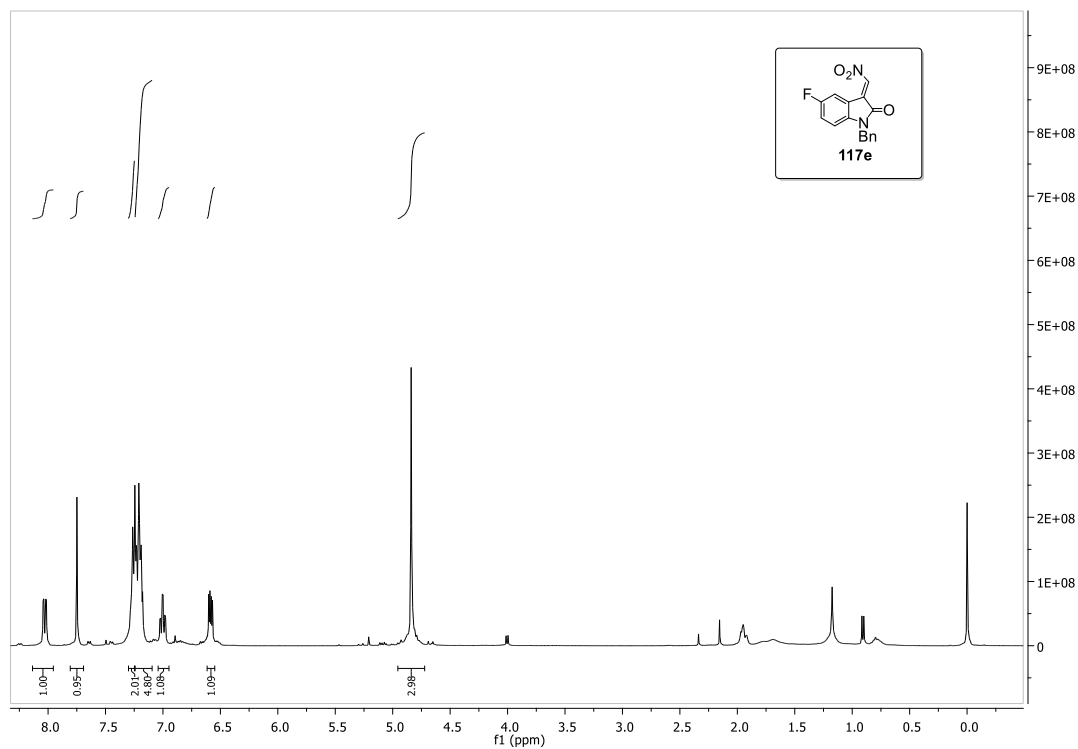


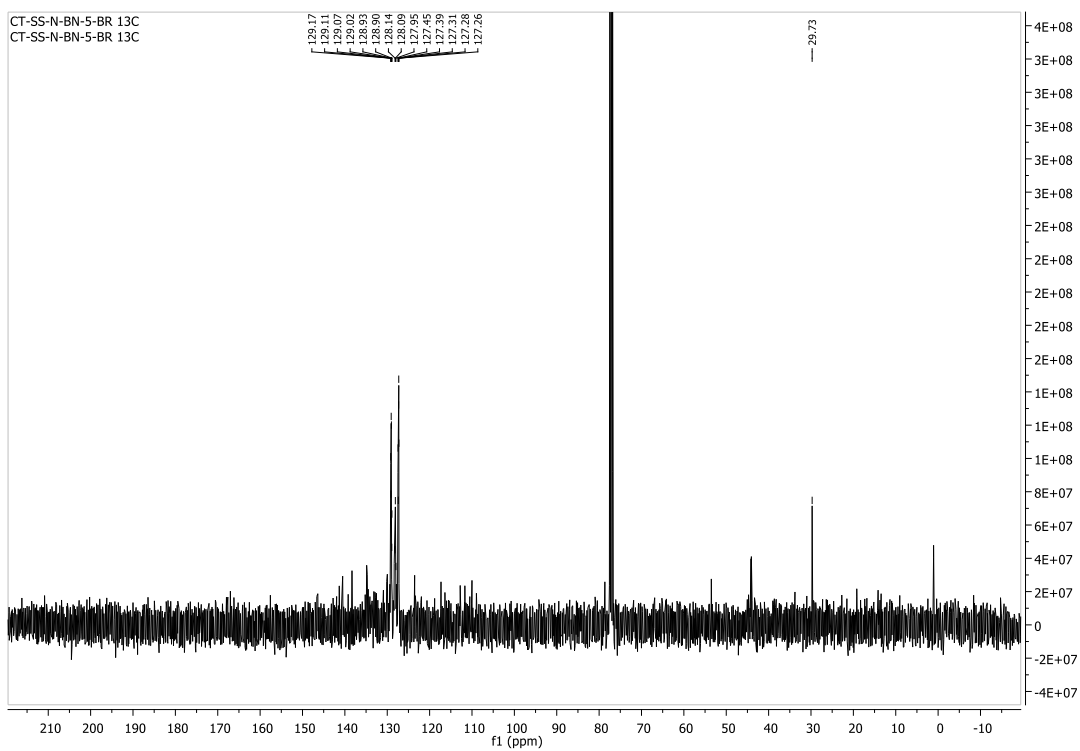
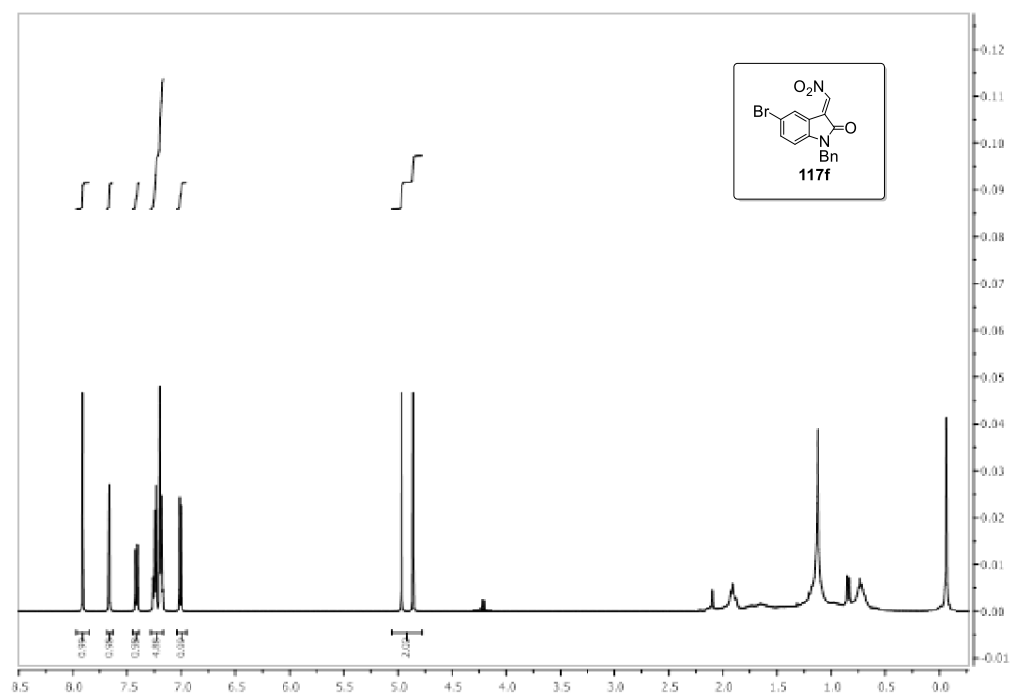
**Figure A. 10**  $^{13}\text{C}$  NMR spectrum of **117b**

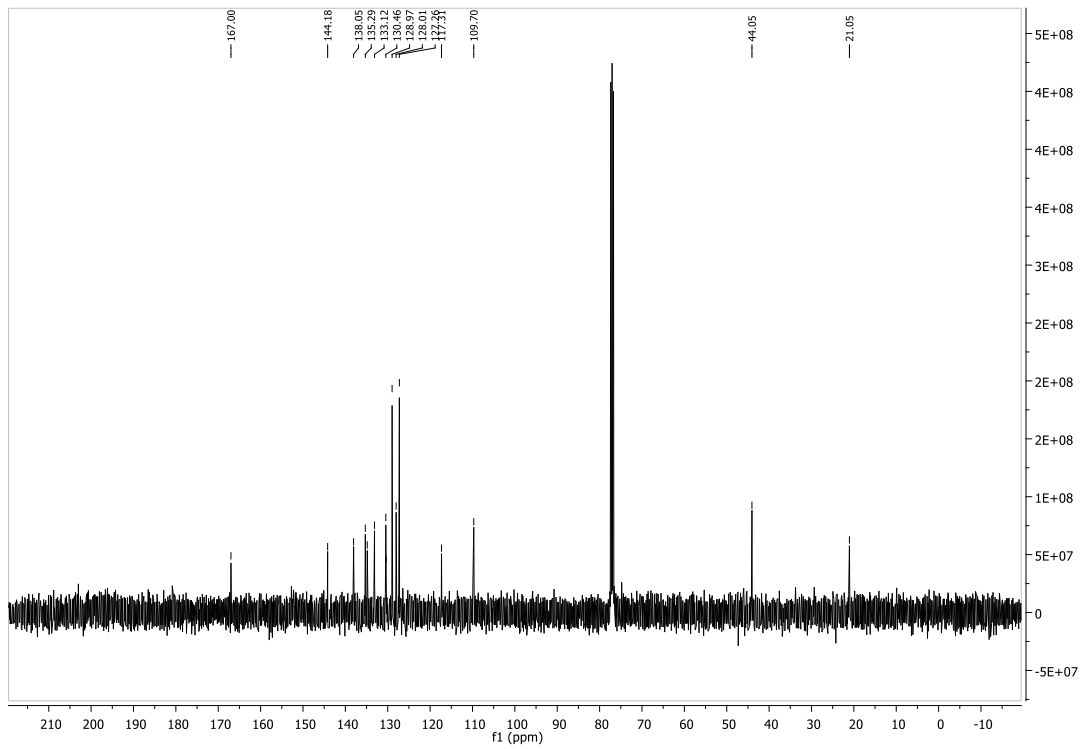
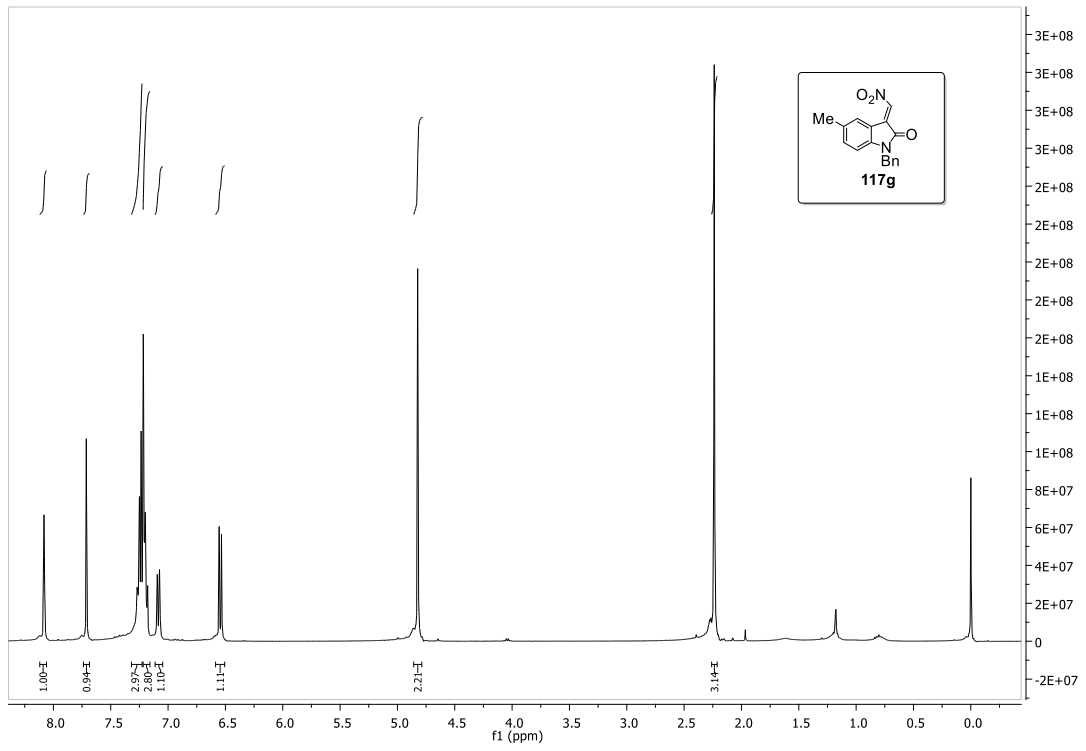












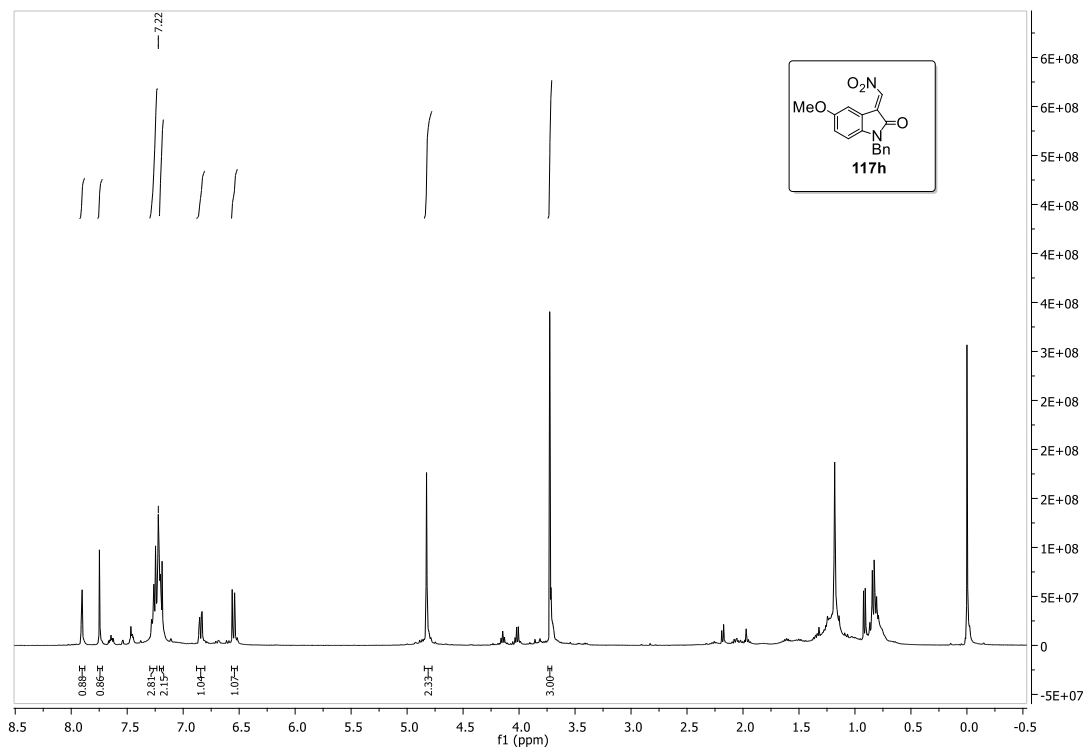


**Figure A. 21** <sup>1</sup>H NMR spectrum of **117h**

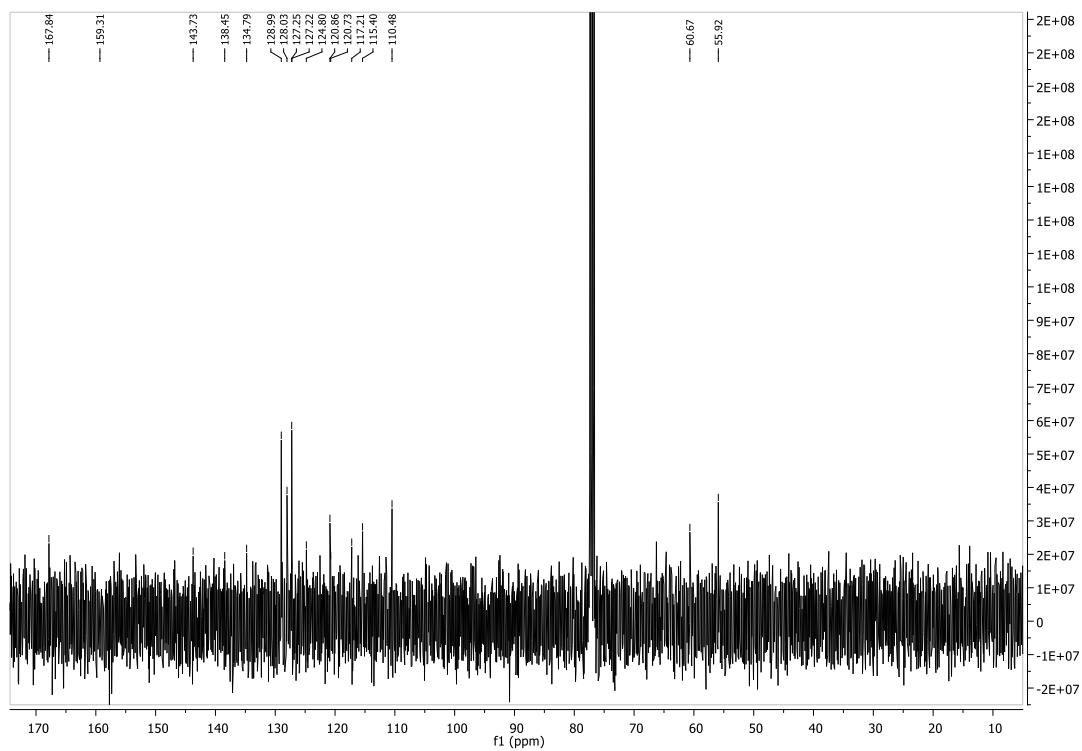


**Figure A. 22** <sup>13</sup>C NMR spectrum of **117h**

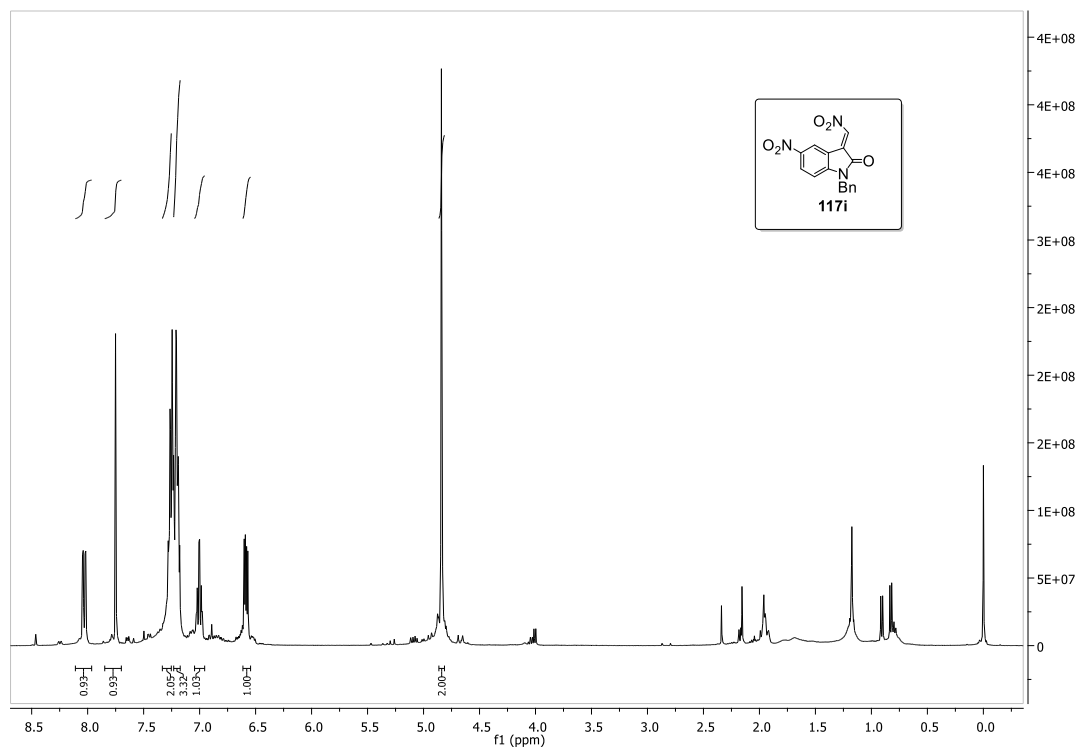


**Figure A. 23**  $^1\text{H}$  NMR spectrum of **117i**

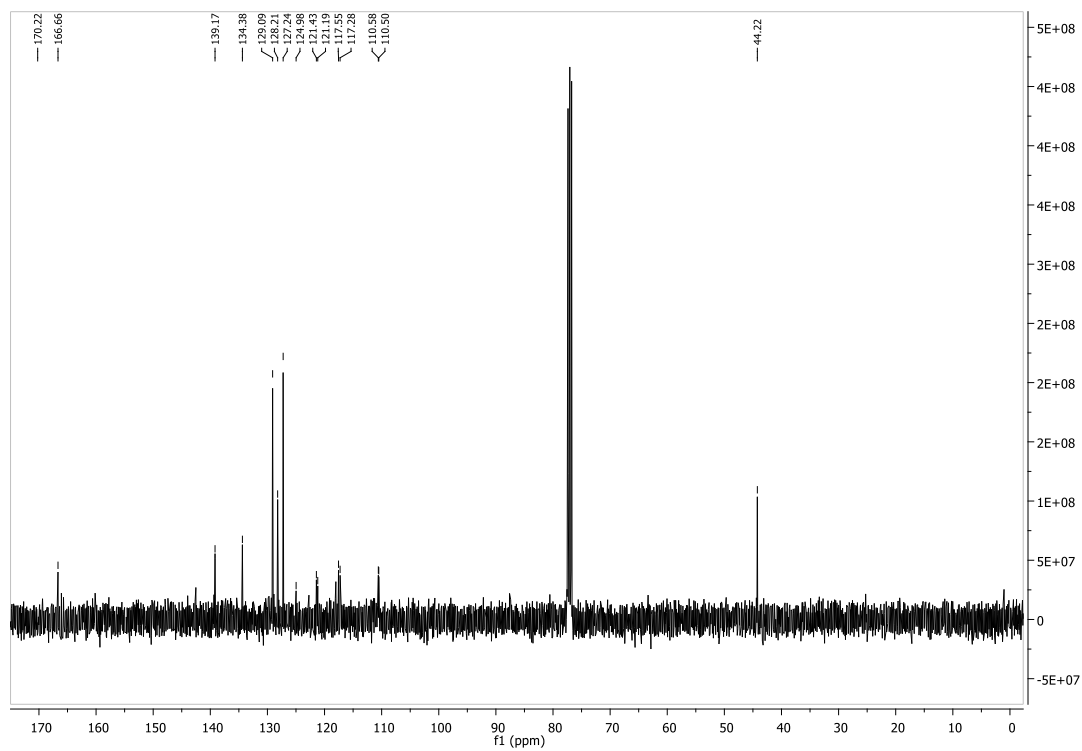


**Figure A. 24**  $^{13}\text{C}$  NMR spectrum of **117i**

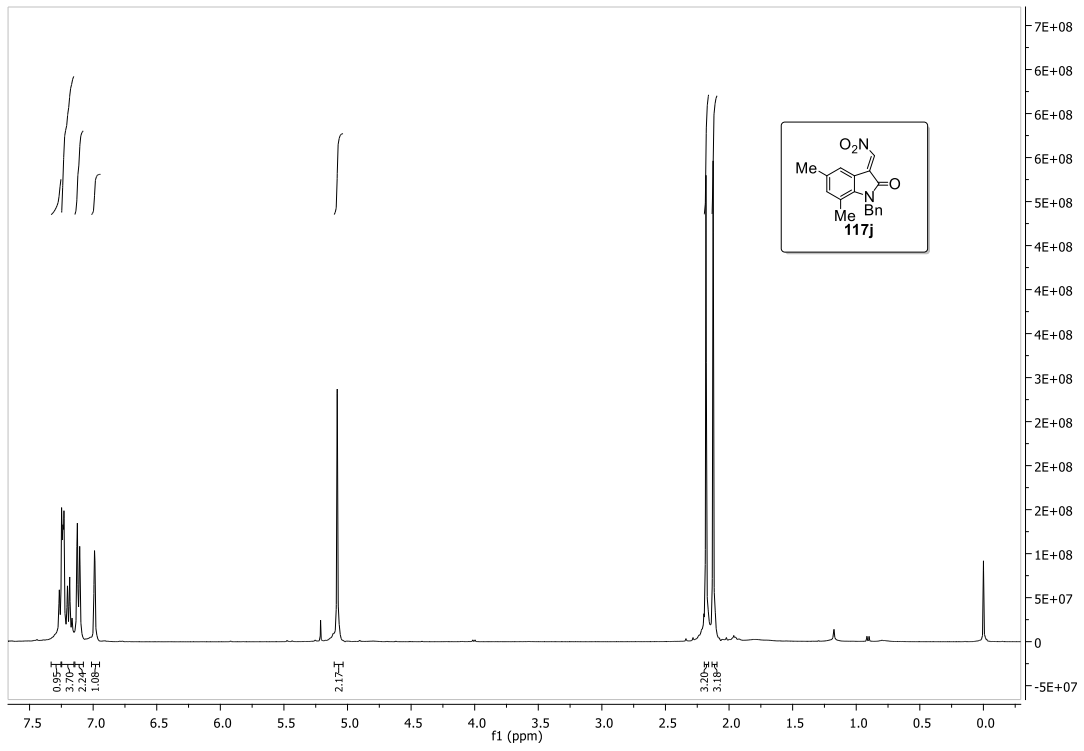


Figure A. 25  $^1\text{H}$  NMR spectrum of **117j**

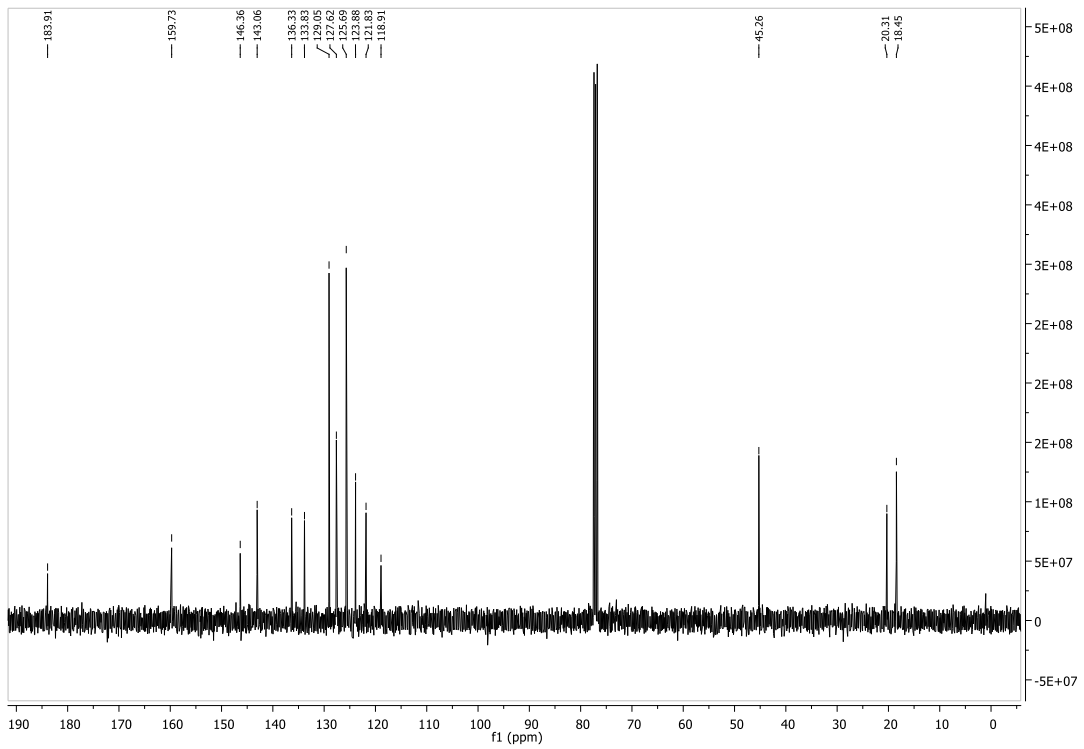


Figure A. 26  $^{13}\text{C}$  NMR spectrum of **117j**



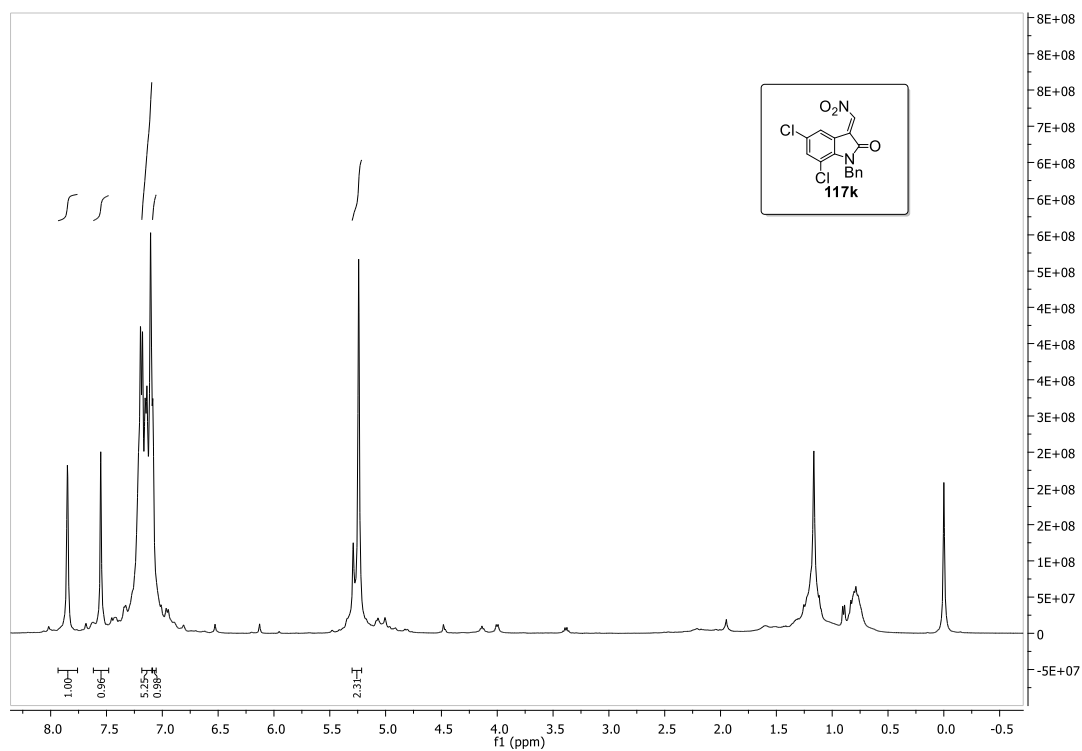


Figure A. 27  $^1\text{H}$  NMR spectrum of **117k**

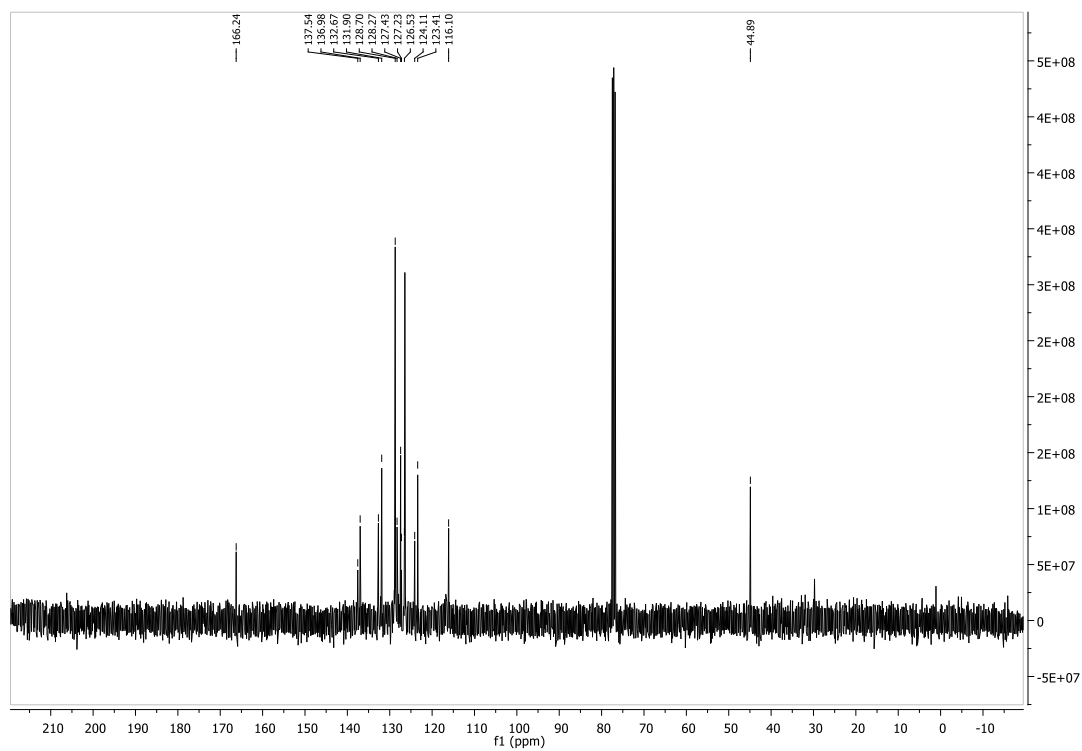


Figure A. 28  $^{13}\text{C}$  NMR spectrum of **117k**

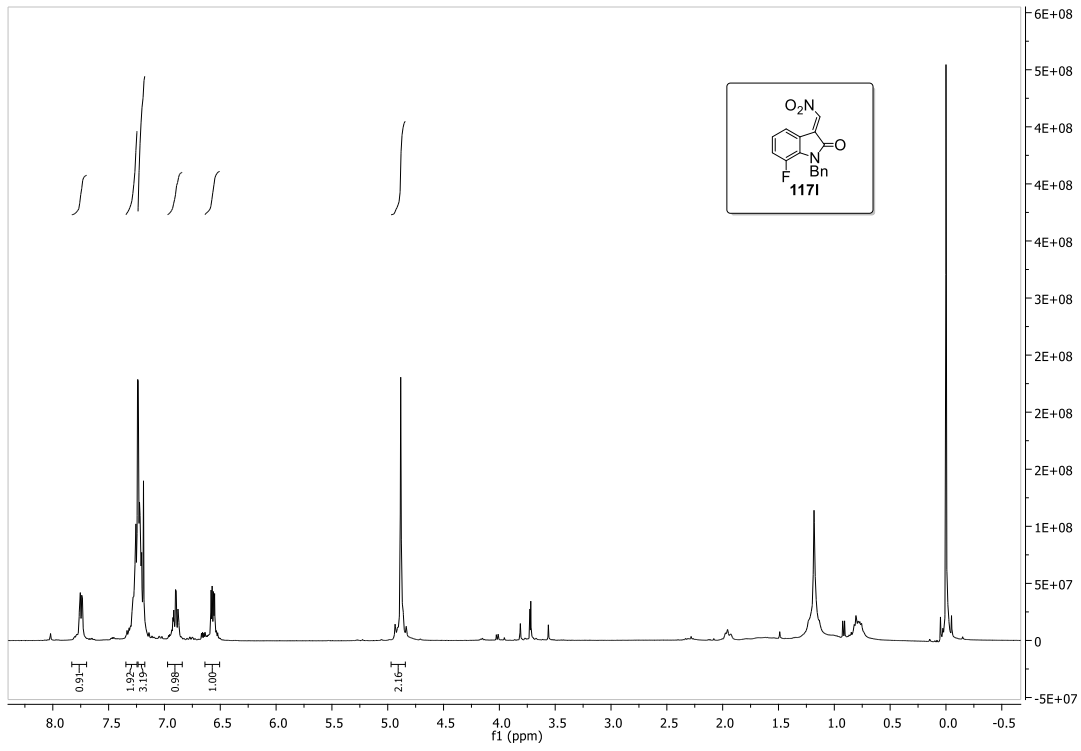


Figure A. 29  $^1\text{H}$  NMR spectrum of 1171

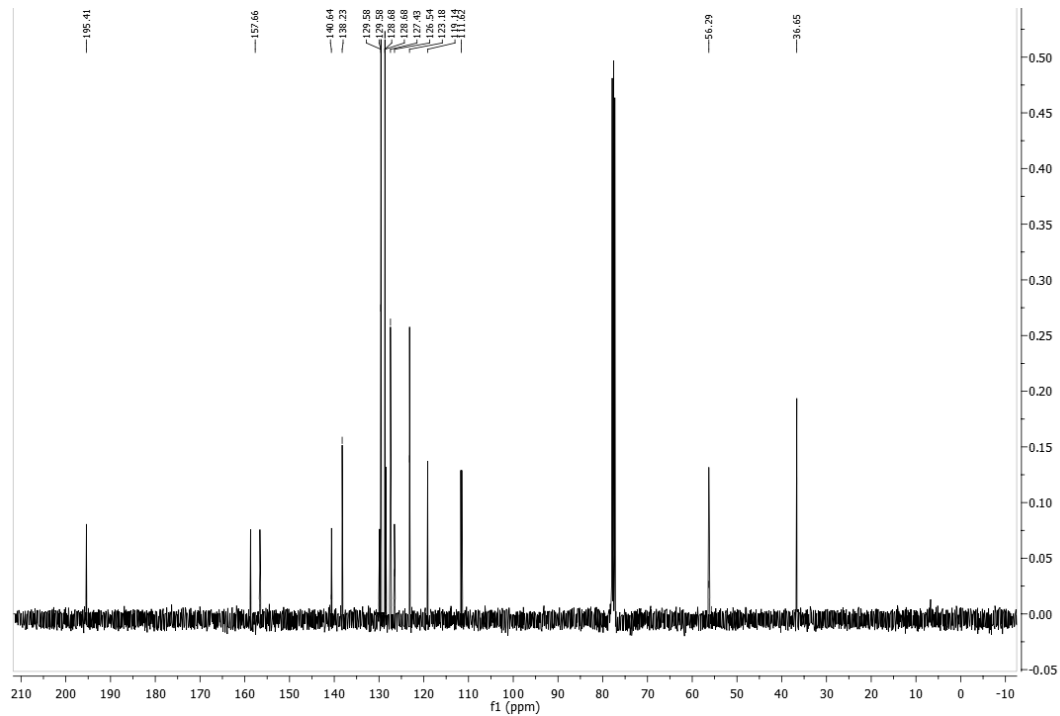
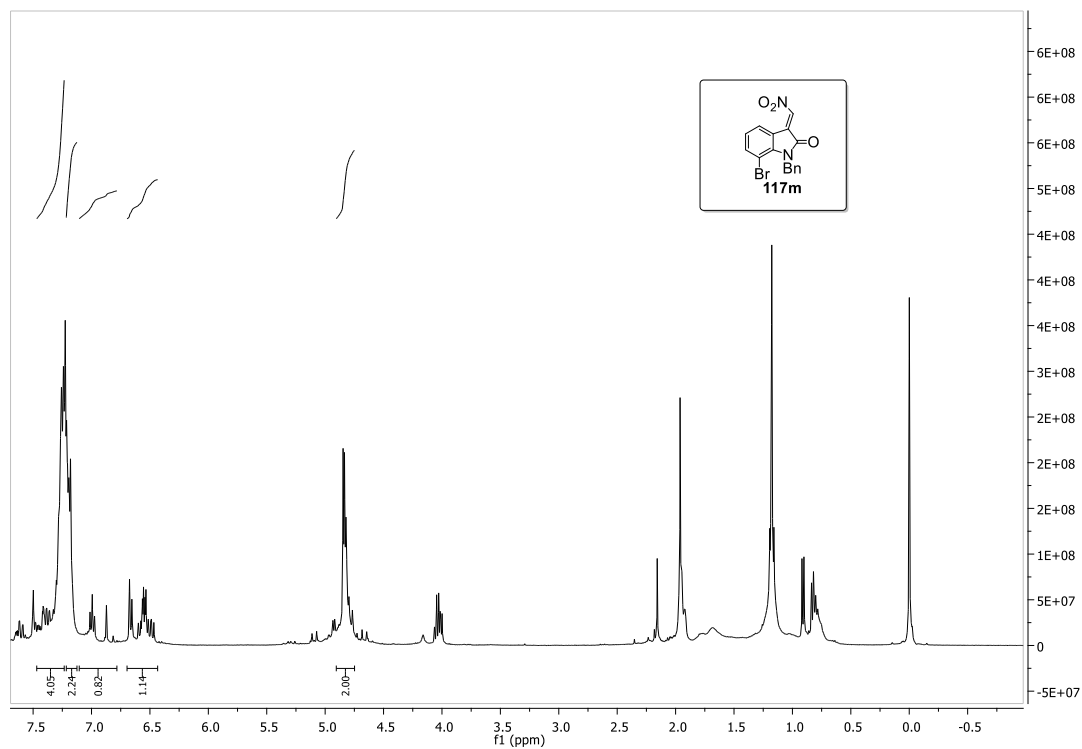
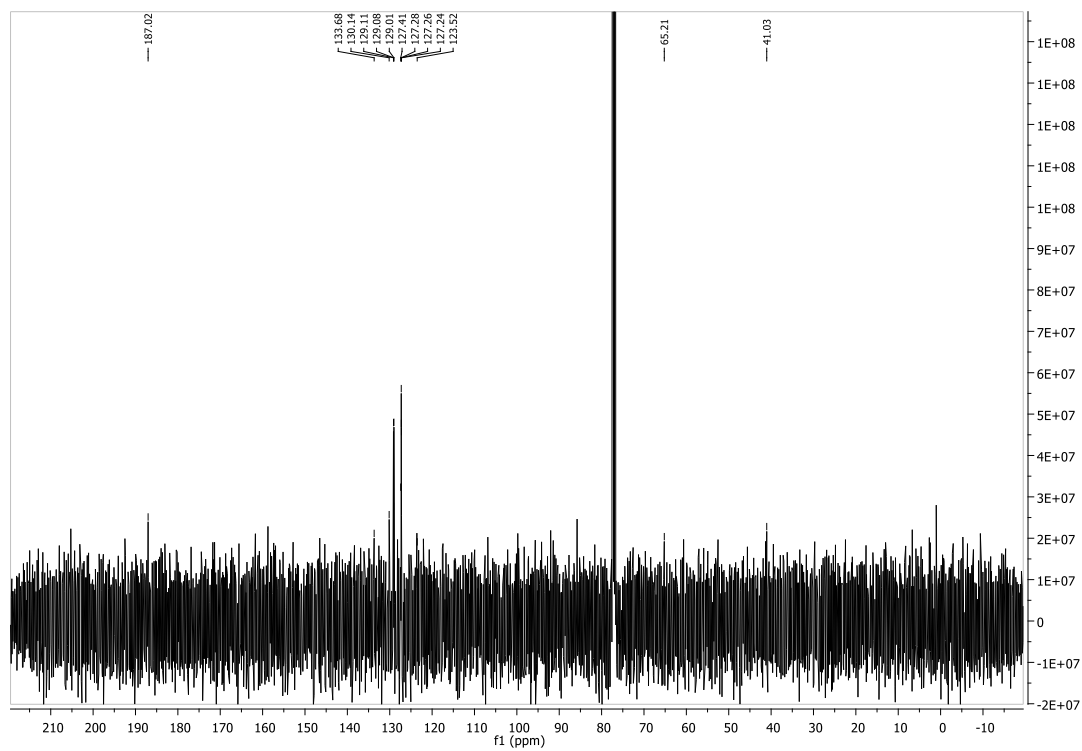


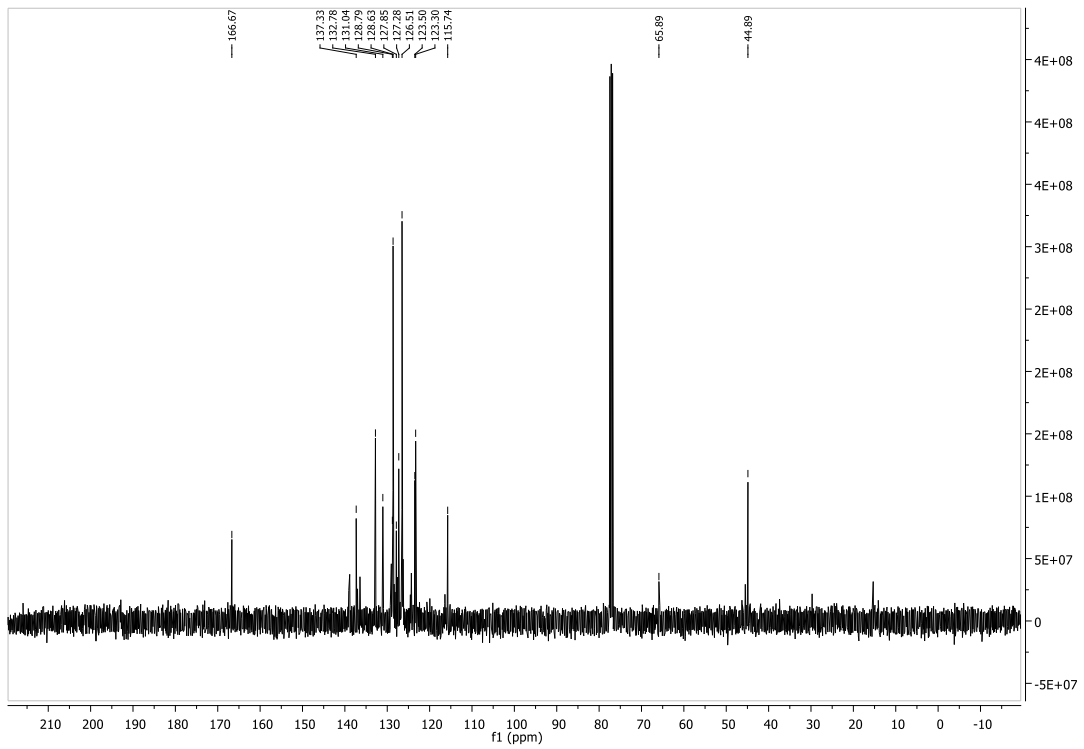
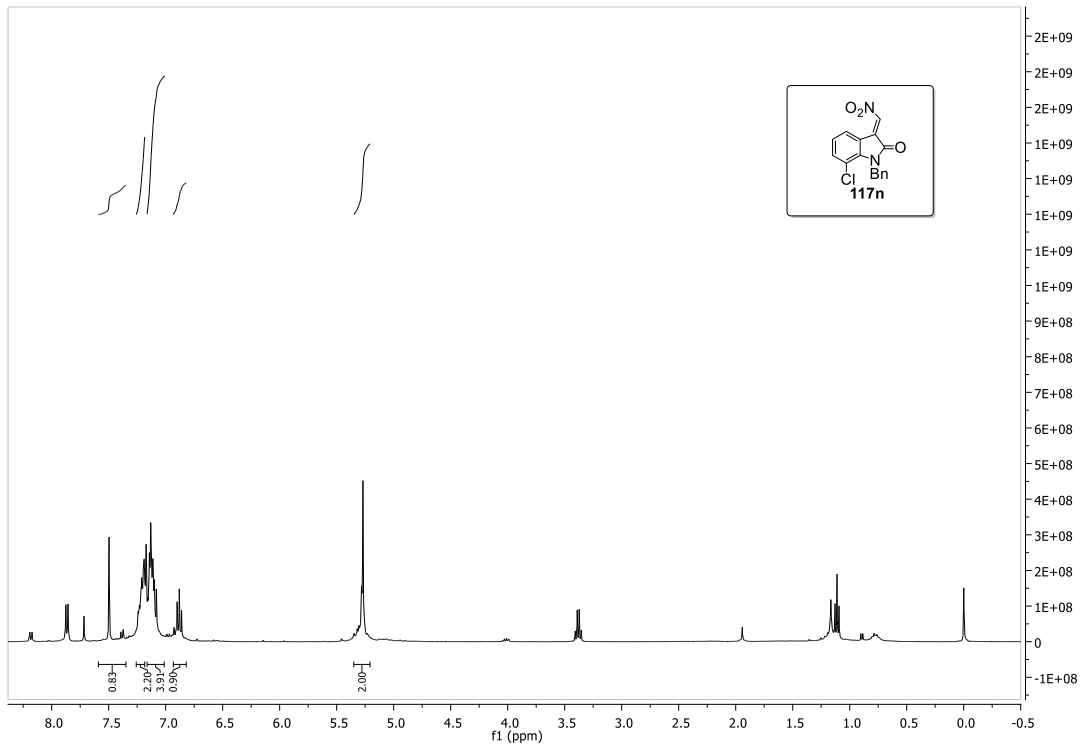
Figure A. 30  $^{13}\text{C}$  NMR spectrum of 1171



**Figure A. 31**  $^1\text{H}$  NMR spectrum of **117m**



**Figure A. 32**  $^{13}\text{C}$  NMR spectrum of **117m**



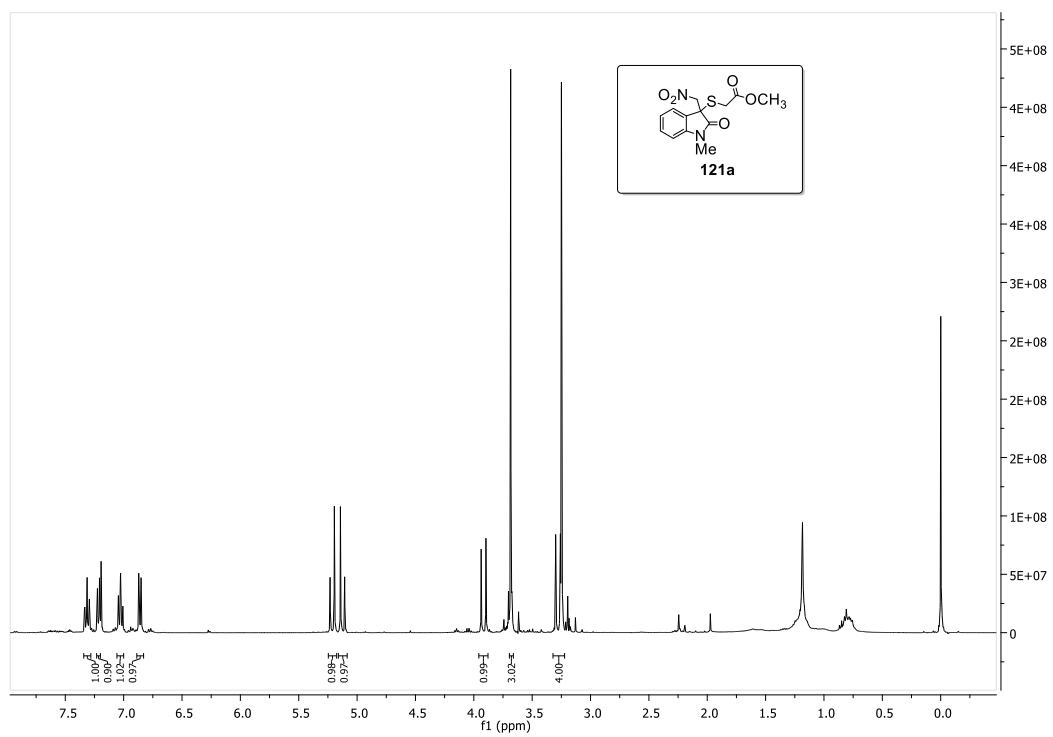


**Figure A. 35** <sup>1</sup>H NMR spectrum of **121a**

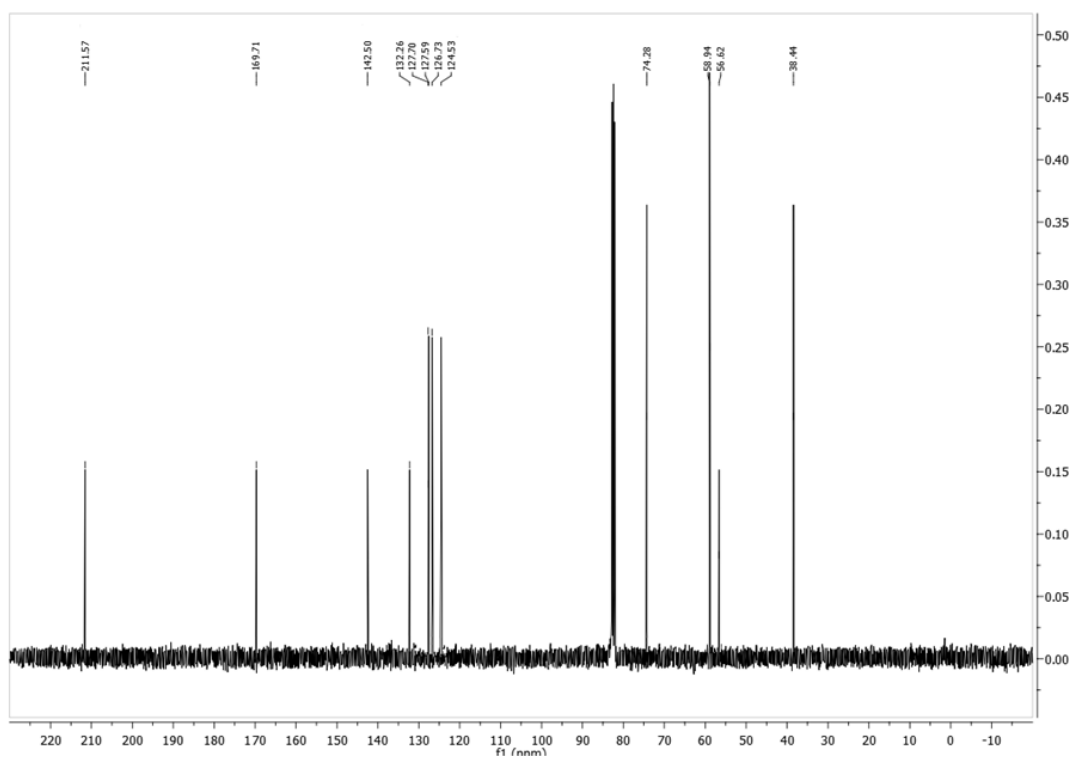


**Figure A. 36** <sup>13</sup>C NMR spectrum of **121a**

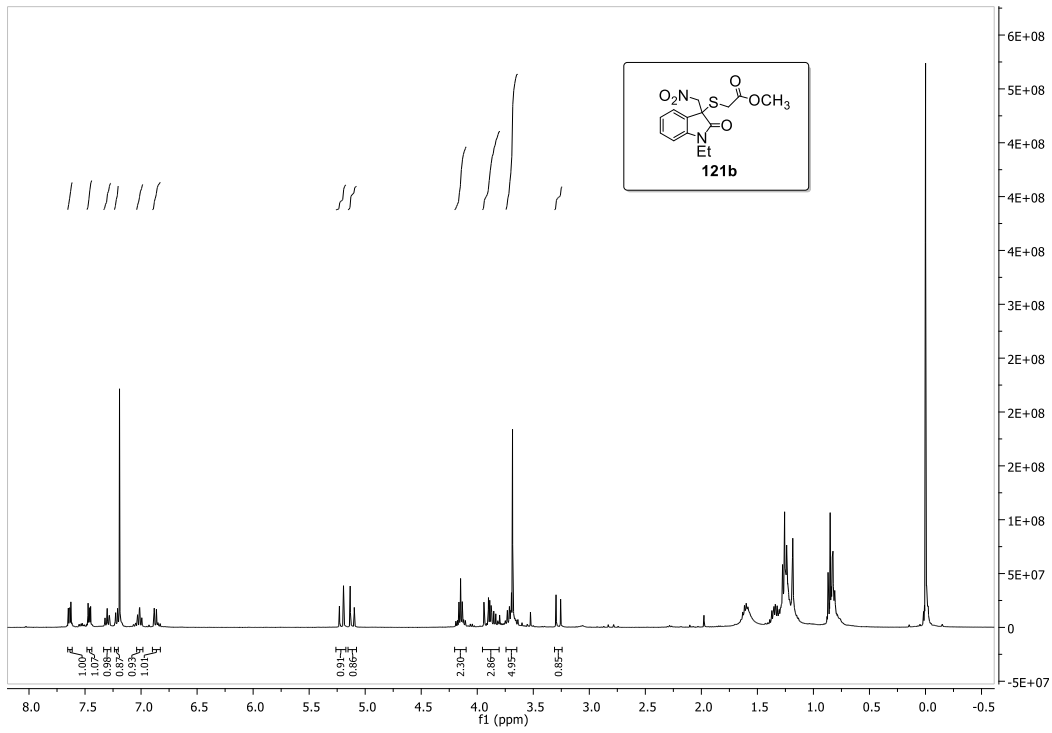


**Figure A. 37** <sup>1</sup>H NMR spectrum of **121b**

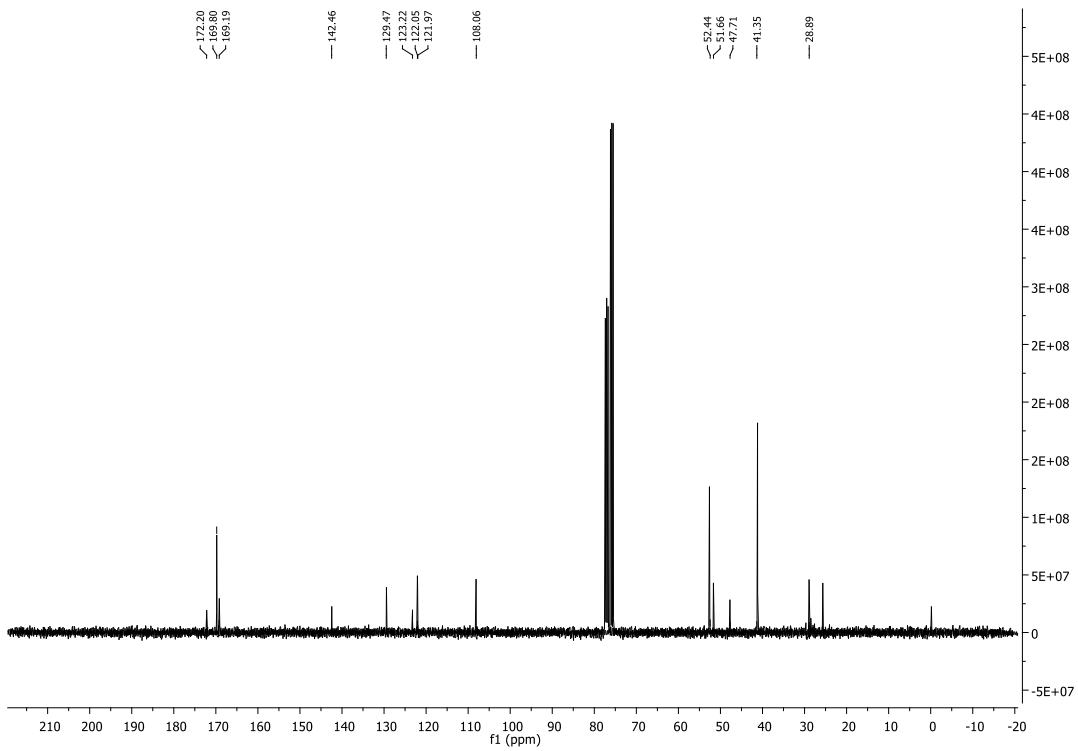


**Figure A. 38** <sup>13</sup>C NMR spectrum of **121b**

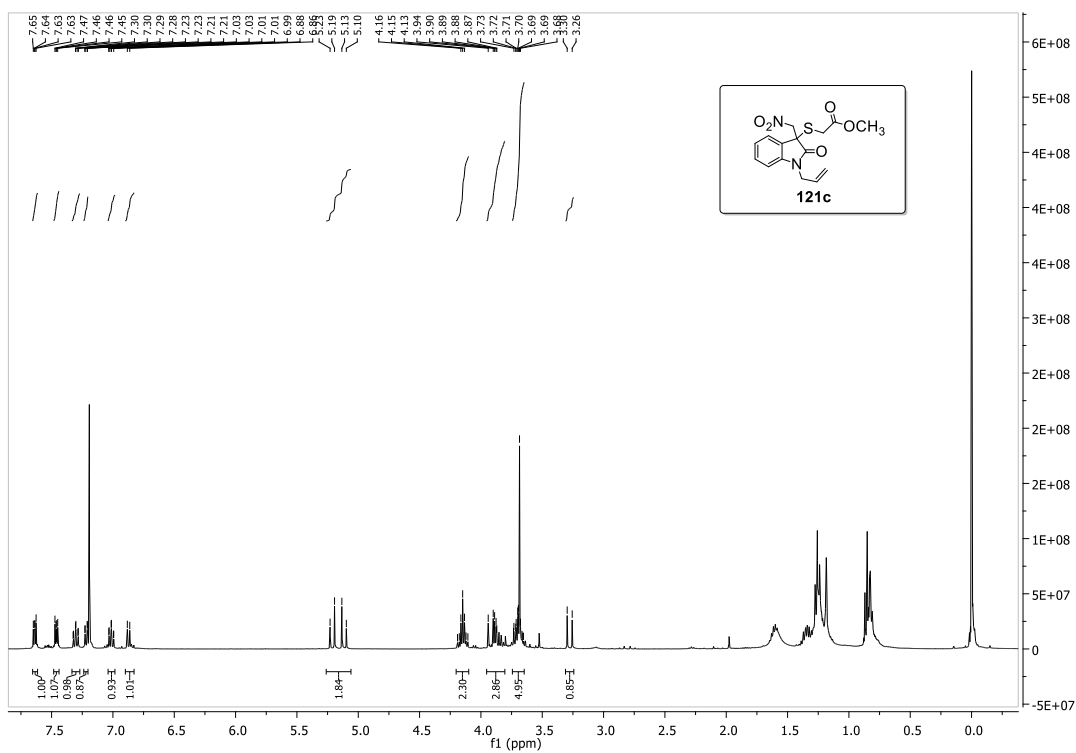


Figure A. 39  $^1\text{H}$  NMR spectrum of **121c**

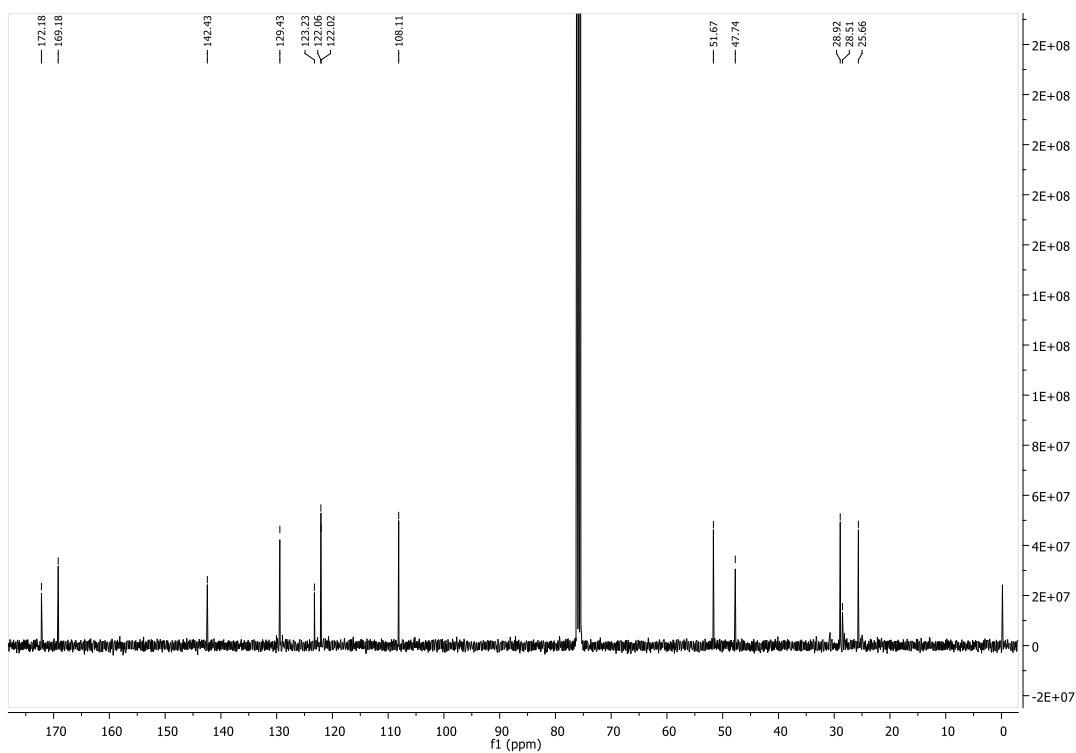


Figure A. 40  $^{13}\text{C}$  NMR spectrum of **121c**

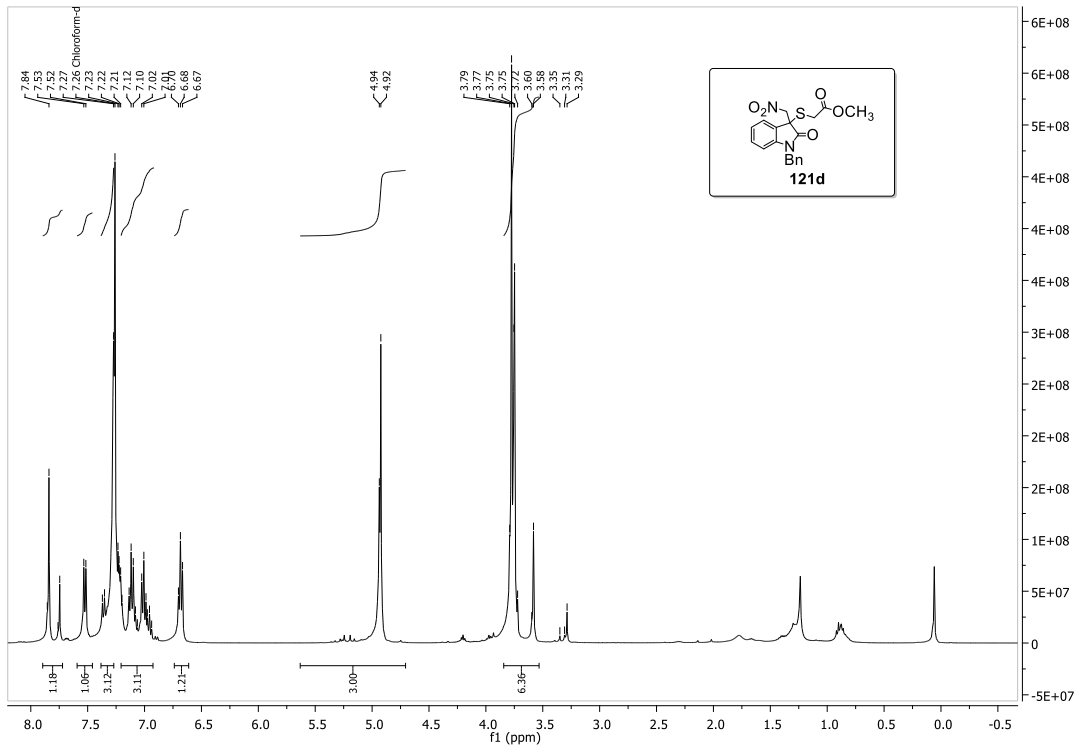


Figure A. 41 <sup>1</sup>H NMR spectrum of **121d**

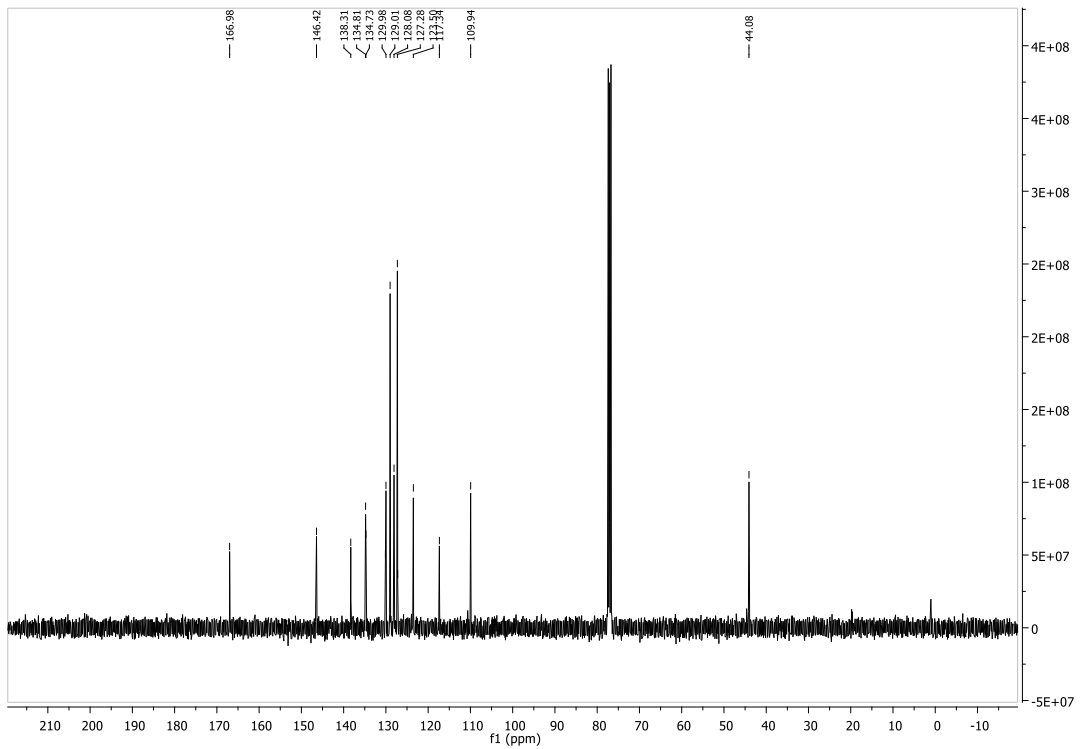
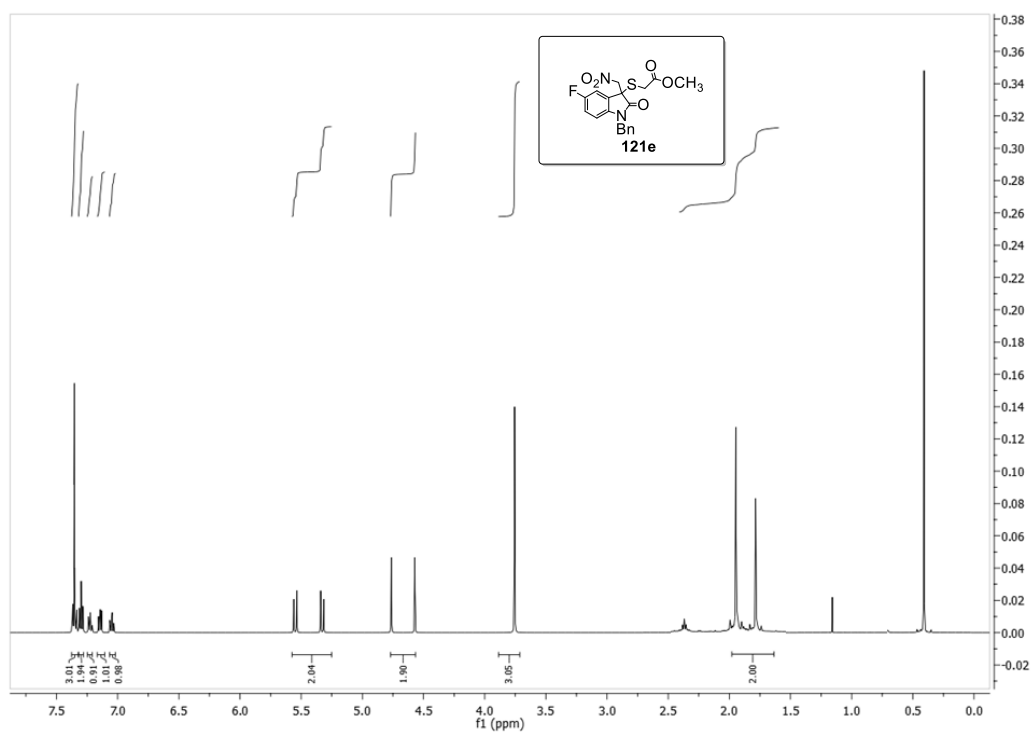
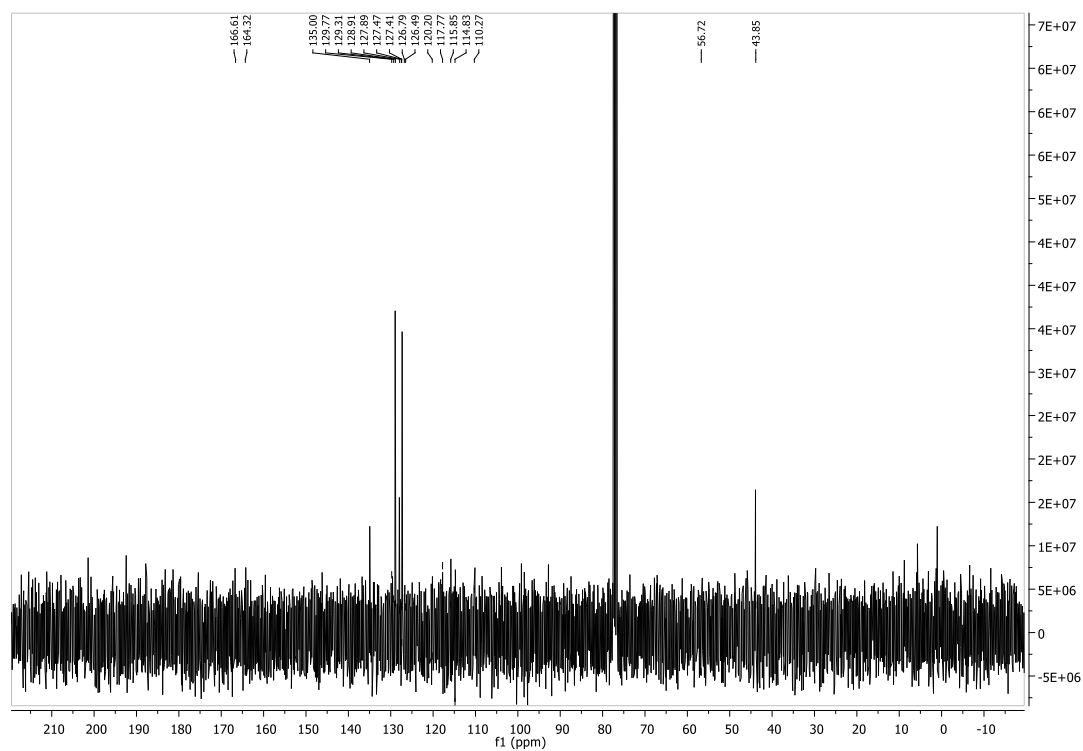


Figure A. 42 <sup>13</sup>C NMR spectrum of **121d**





**Figure A. 43**  $^1\text{H}$  NMR spectrum of **121e**



**Figure A. 44**  $^{13}\text{C}$  NMR spectrum of **121e**

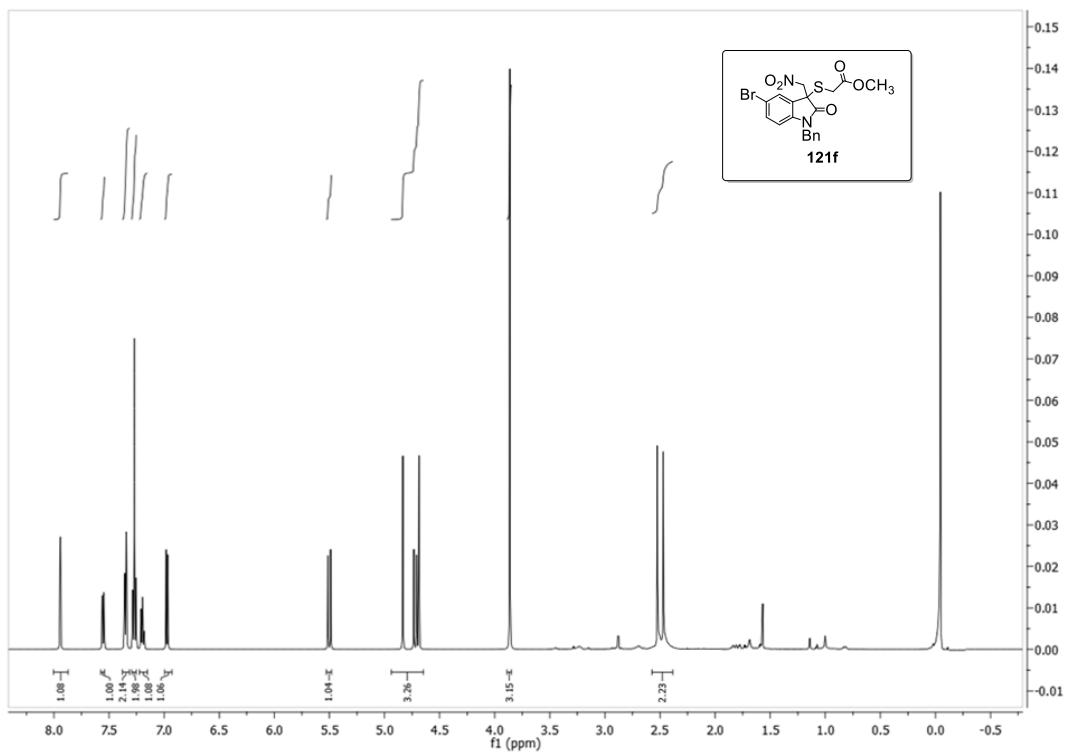


Figure A. 45  $^1\text{H}$  NMR spectrum of **121f**

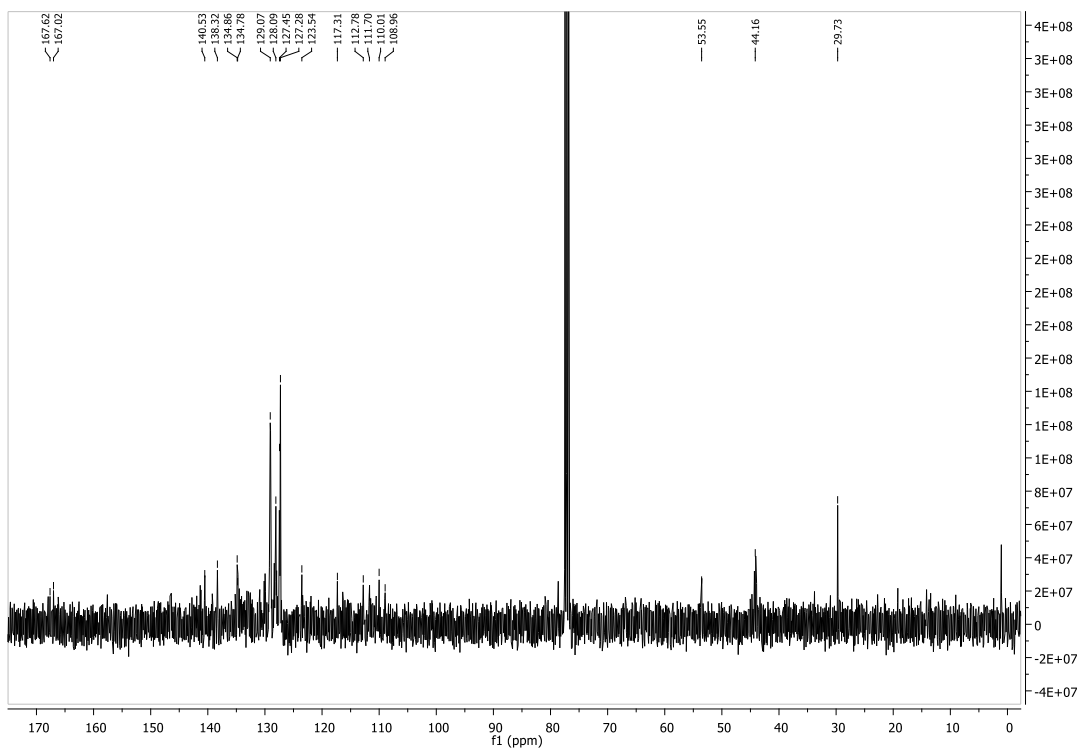
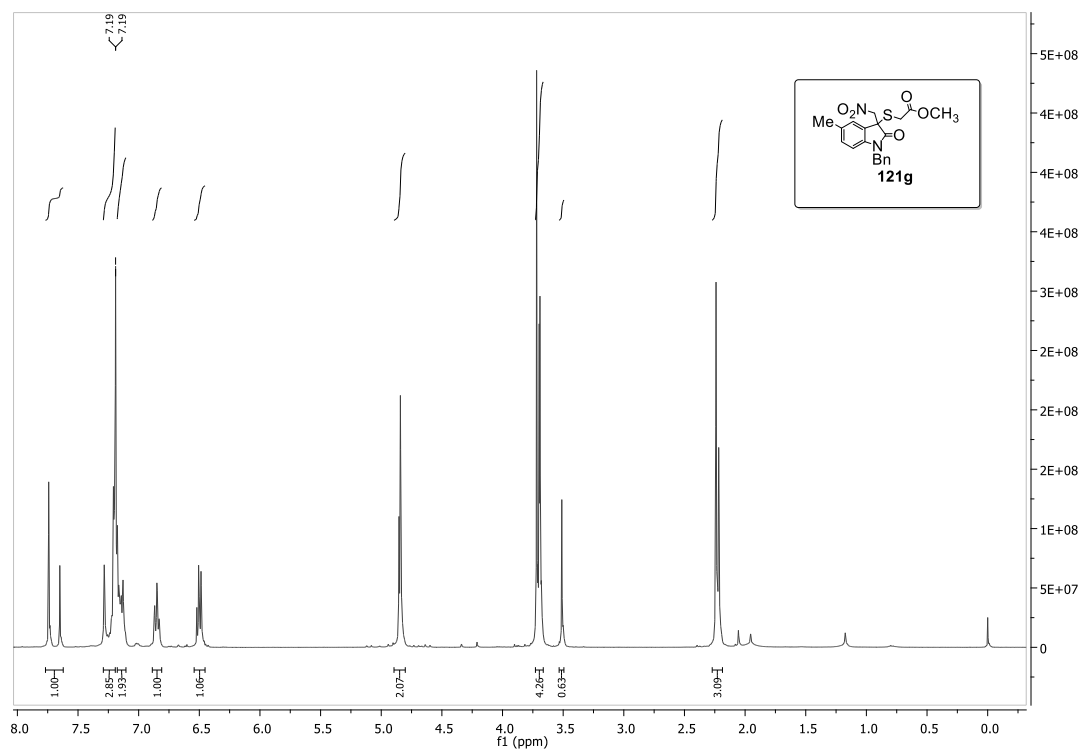
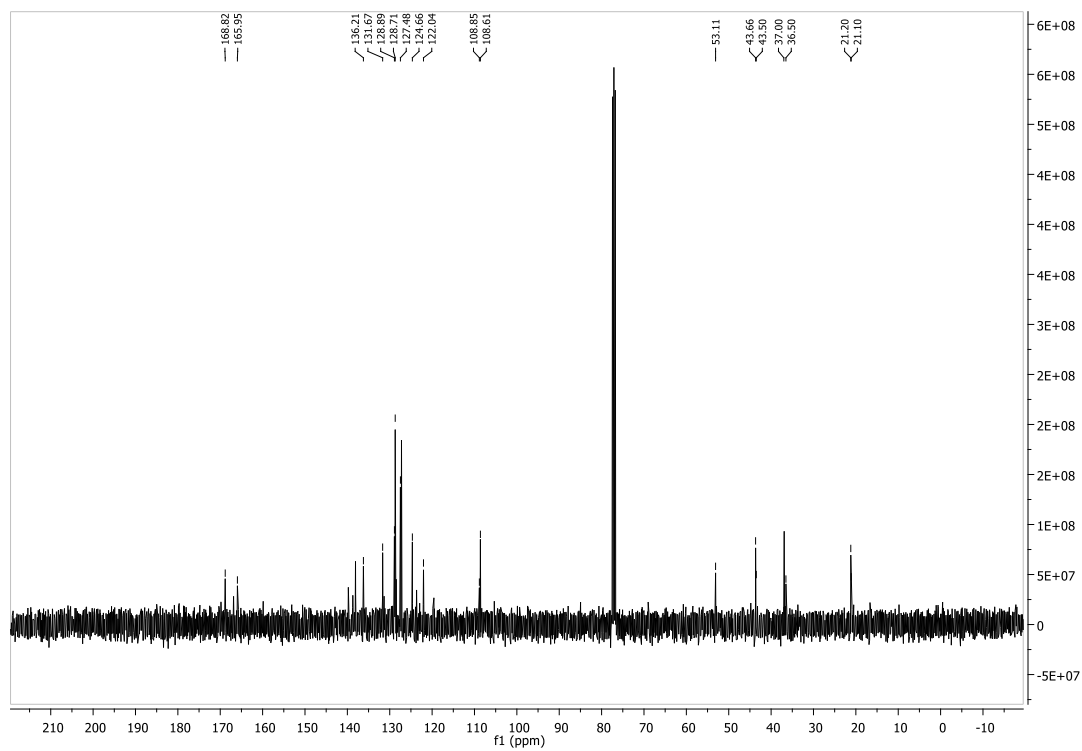


Figure A. 46  $^{13}\text{C}$  NMR spectrum of **121f**



**Figure A. 47**  $^1\text{H}$  NMR spectrum of **121g**



**Figure A. 48**  $^{13}\text{C}$  NMR spectrum of **121g**

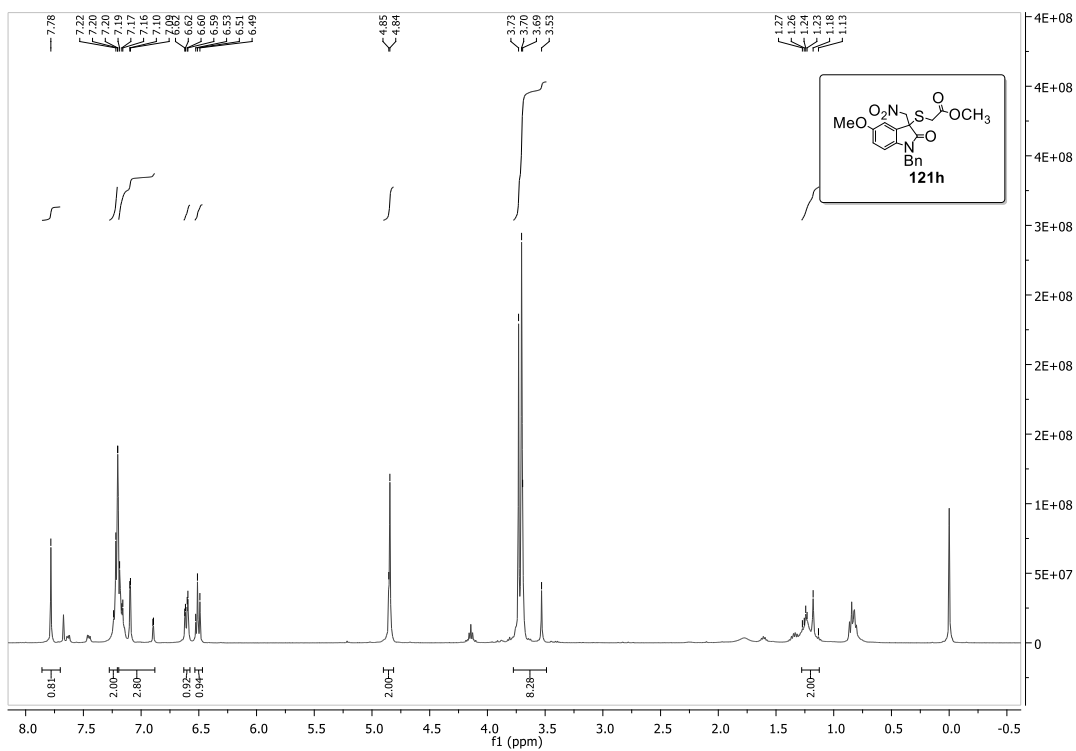


Figure A. 49 <sup>1</sup>H NMR spectrum of **121h**

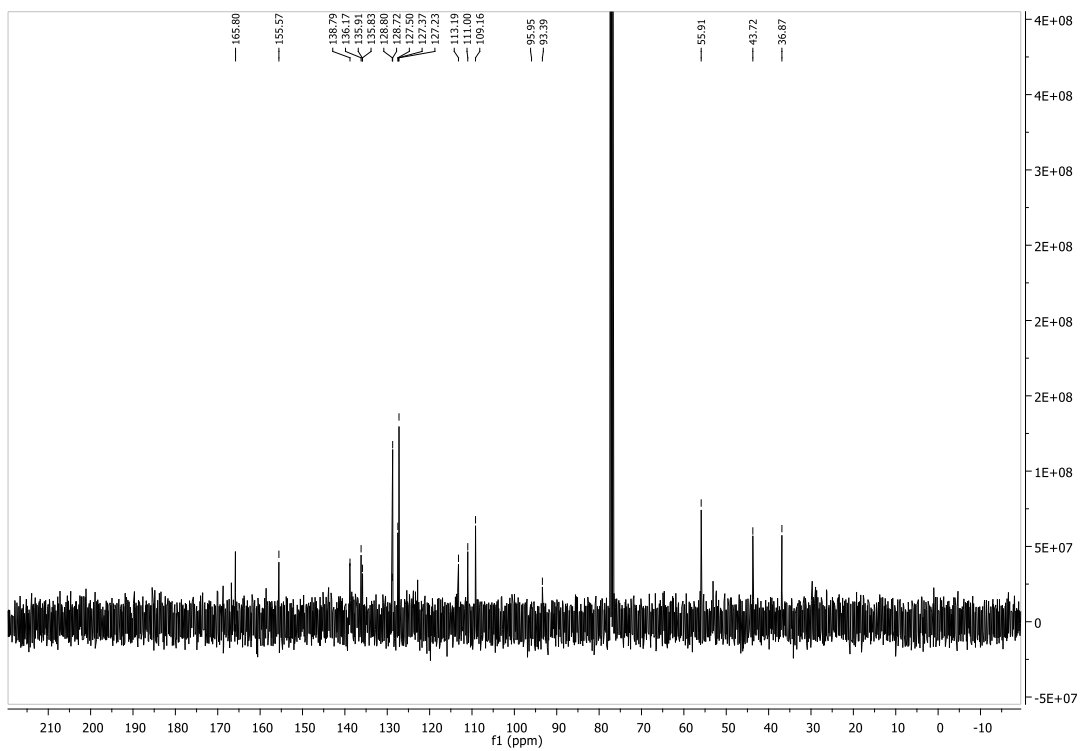
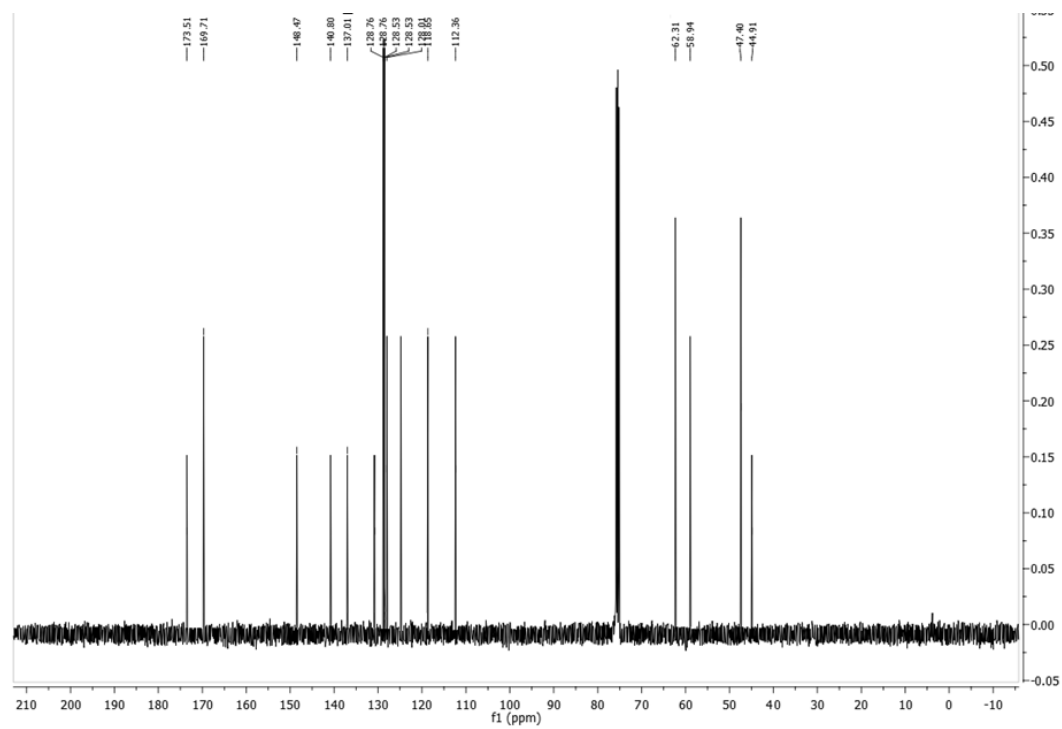
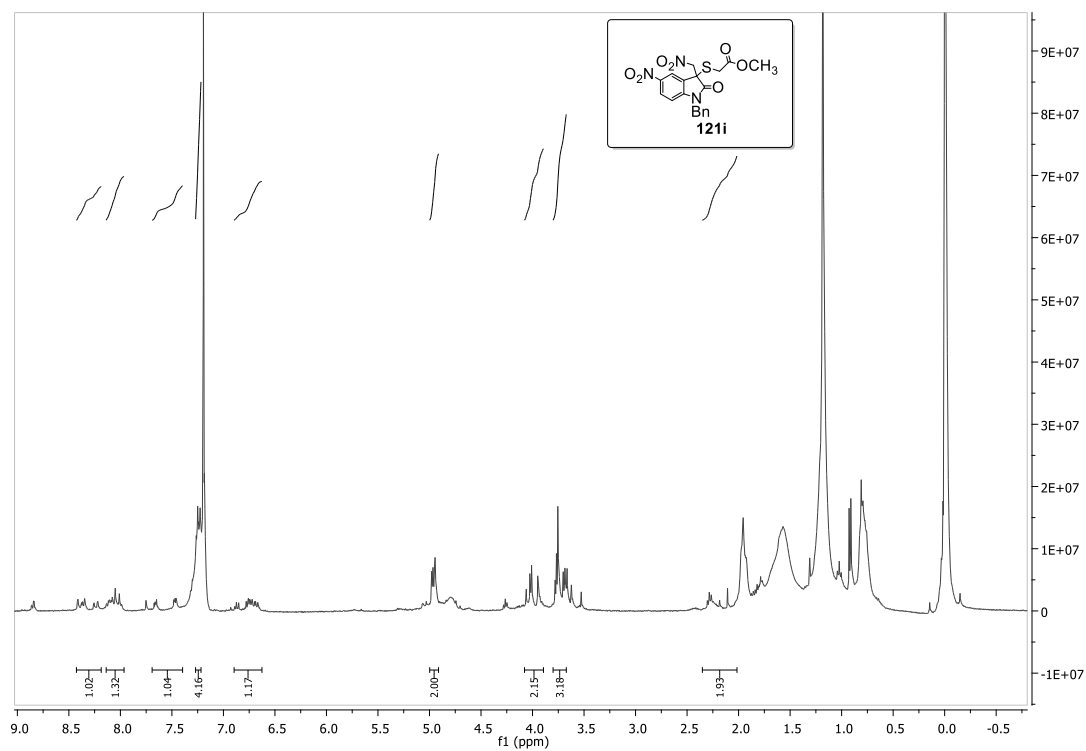
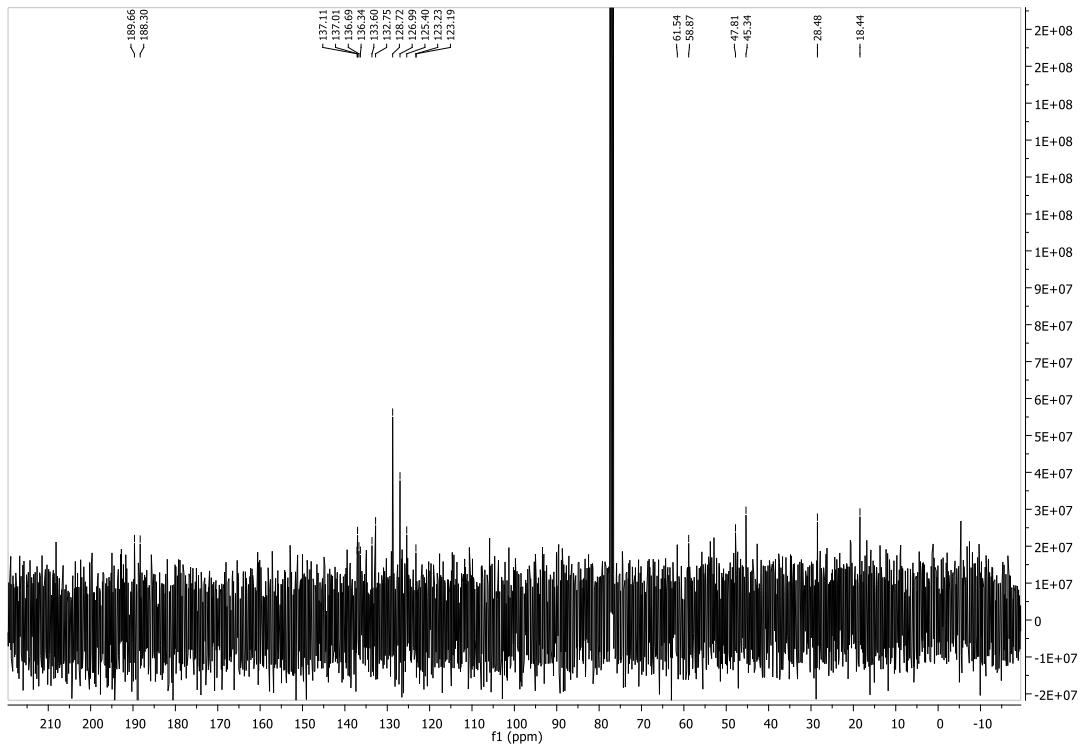
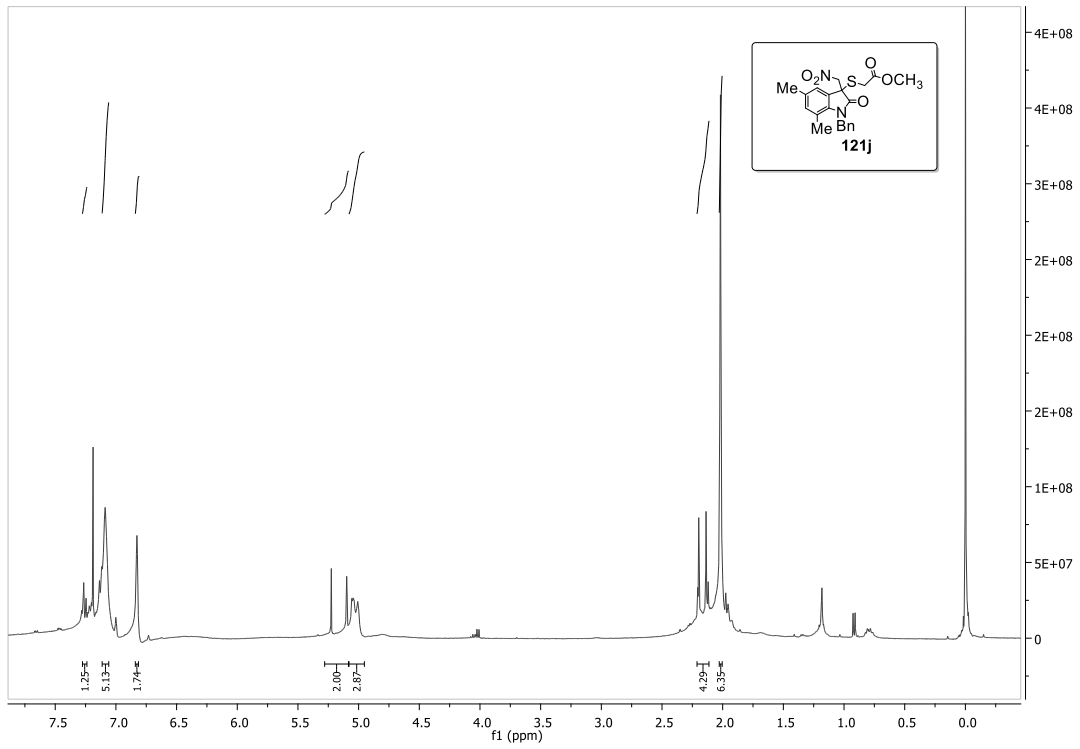
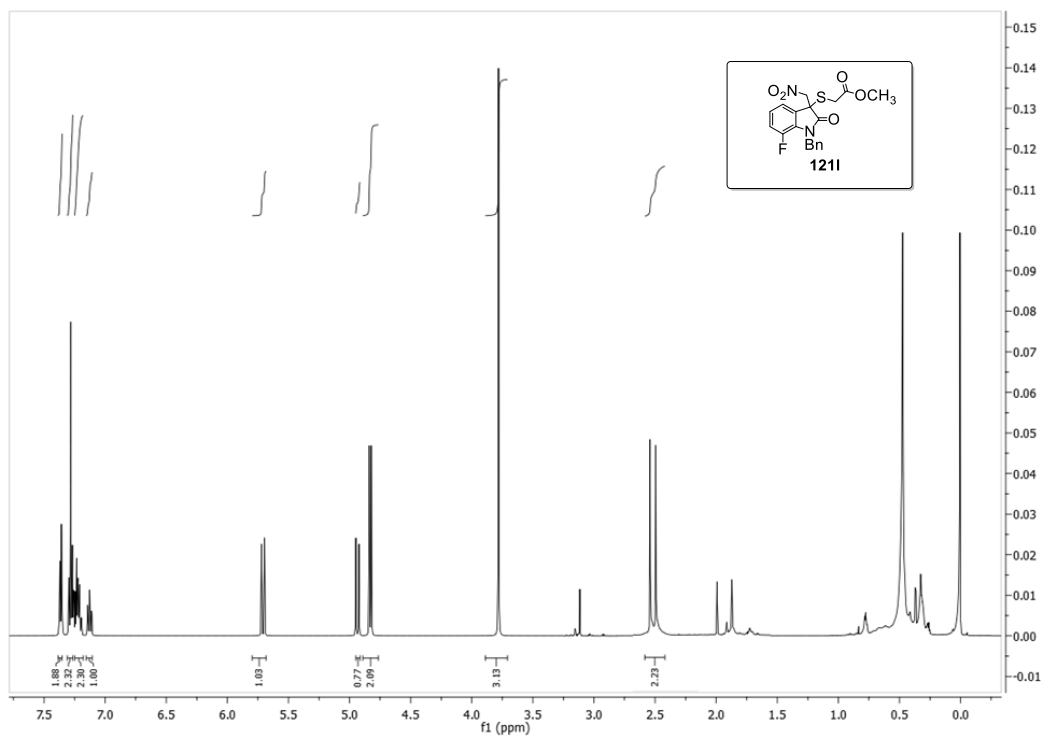


Figure A. 50 <sup>13</sup>C NMR spectrum of **121h**









**Figure A. 57**  $^1\text{H}$  NMR spectrum of **1211**

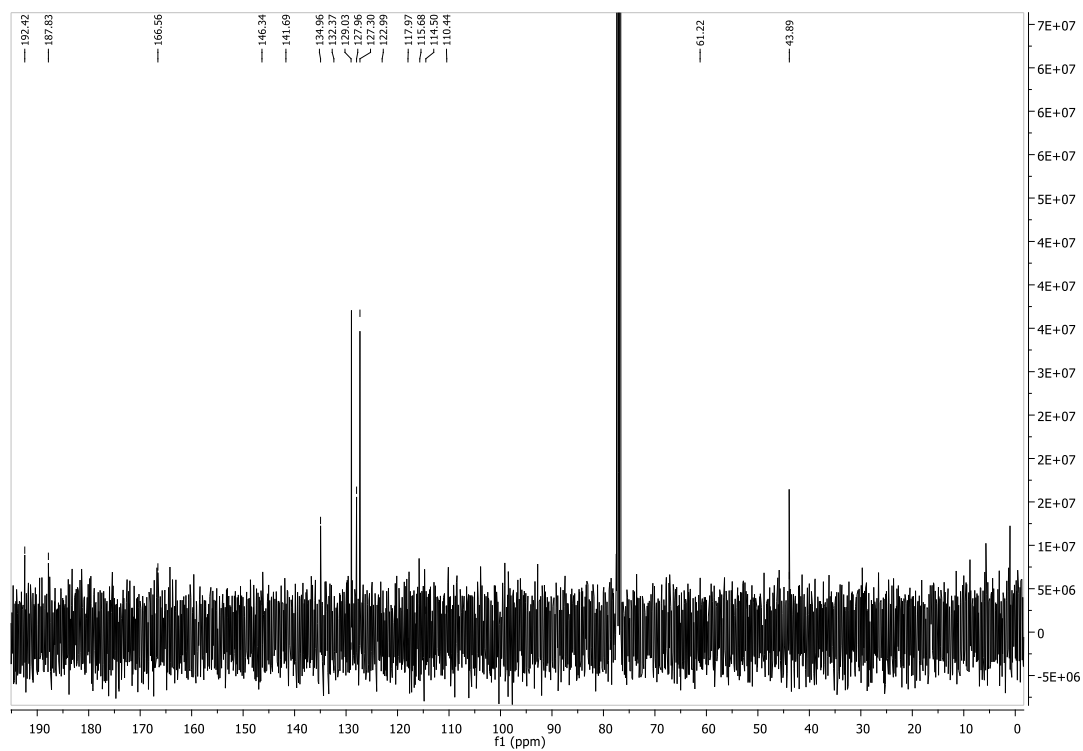


**Figure A. 58**  $^{13}\text{C}$  NMR spectrum of **1211**



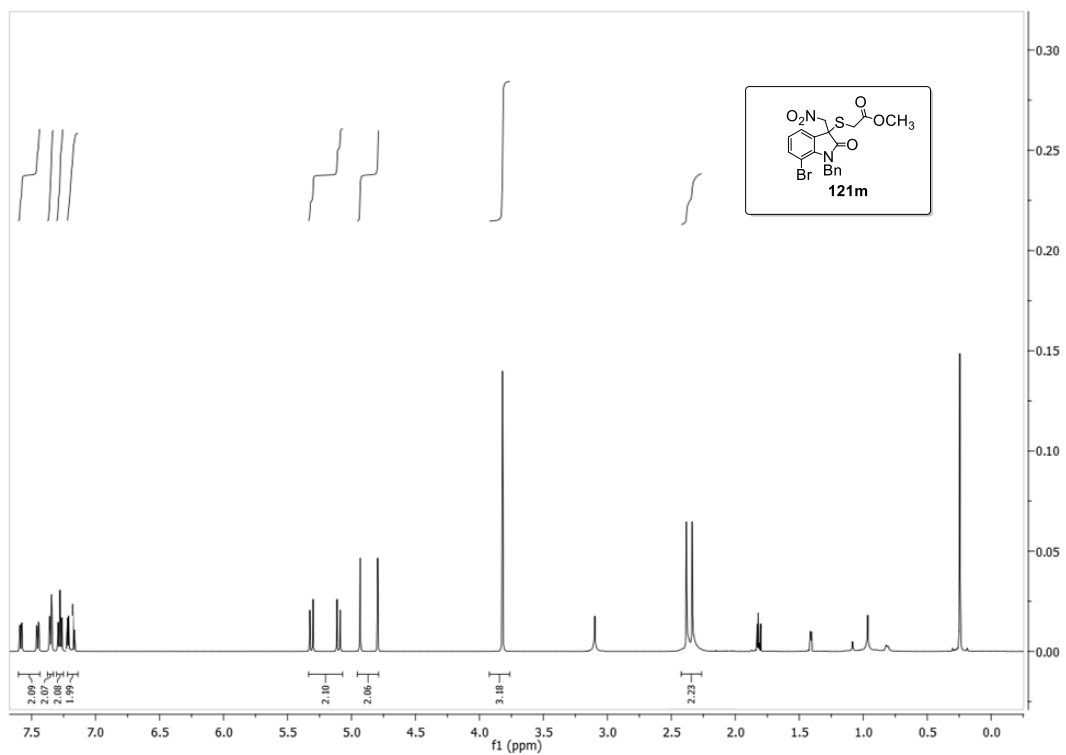


Figure A. 59  $^1\text{H}$  NMR spectrum of **121m**

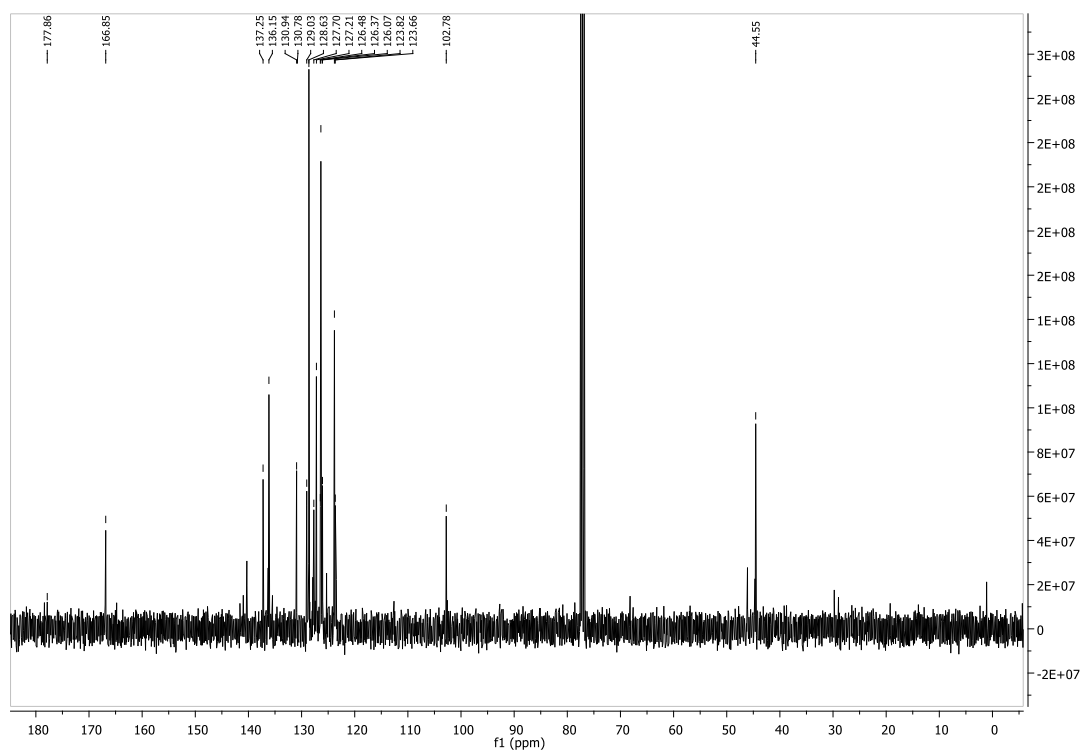
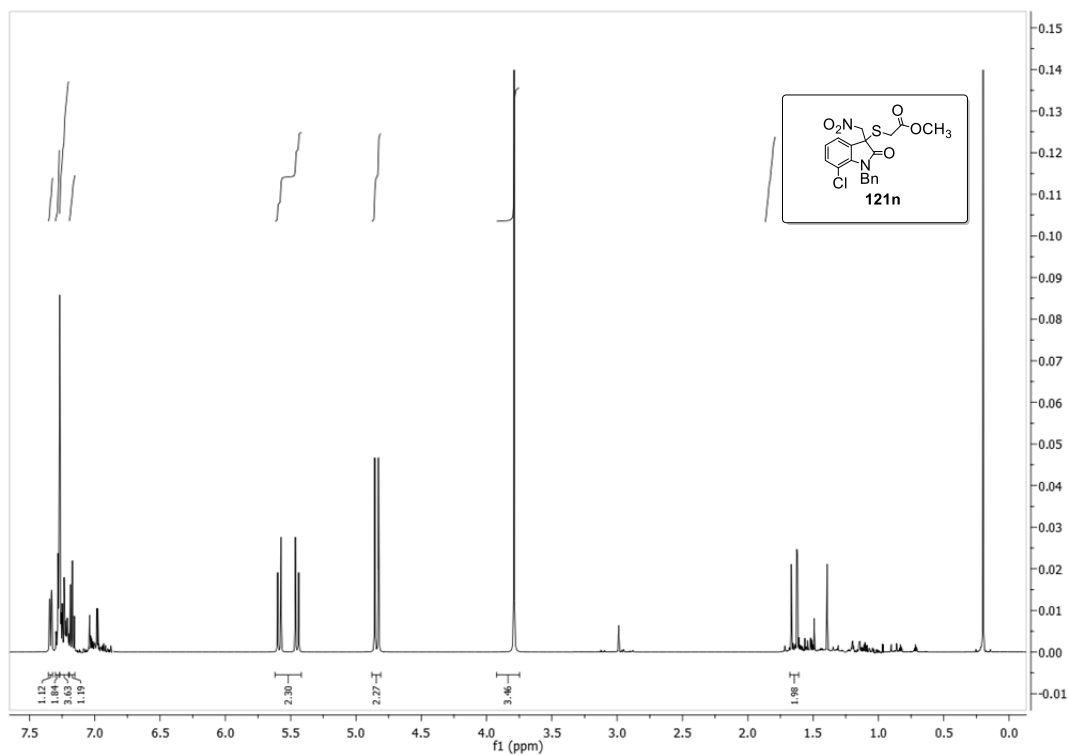
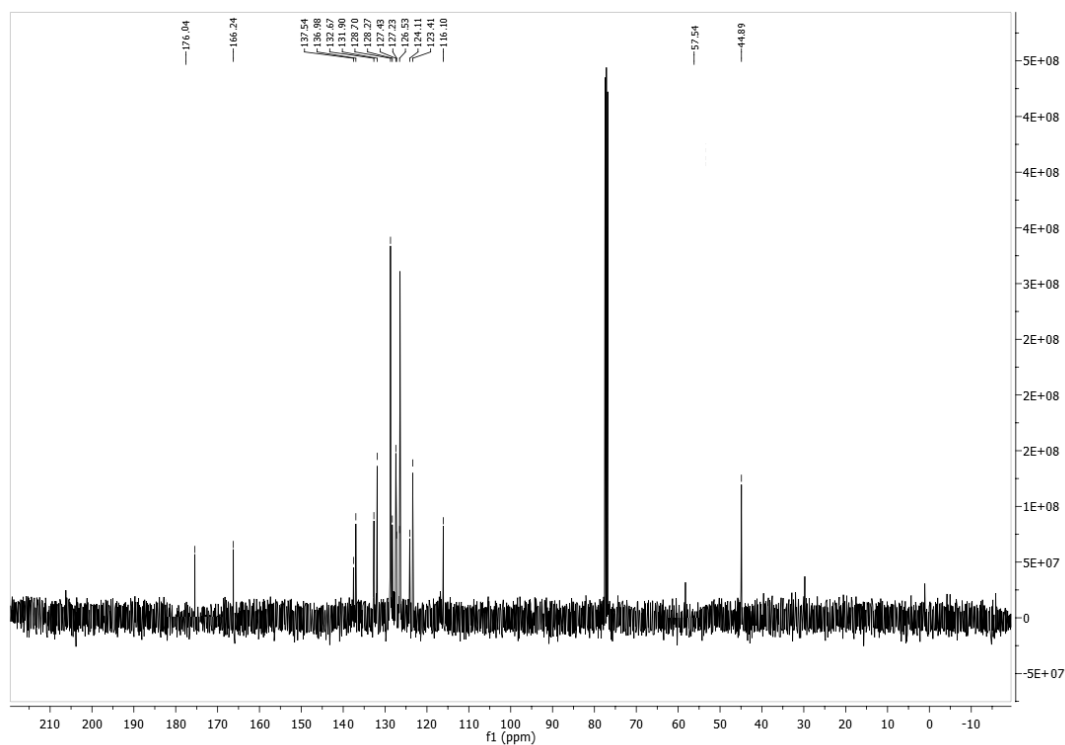


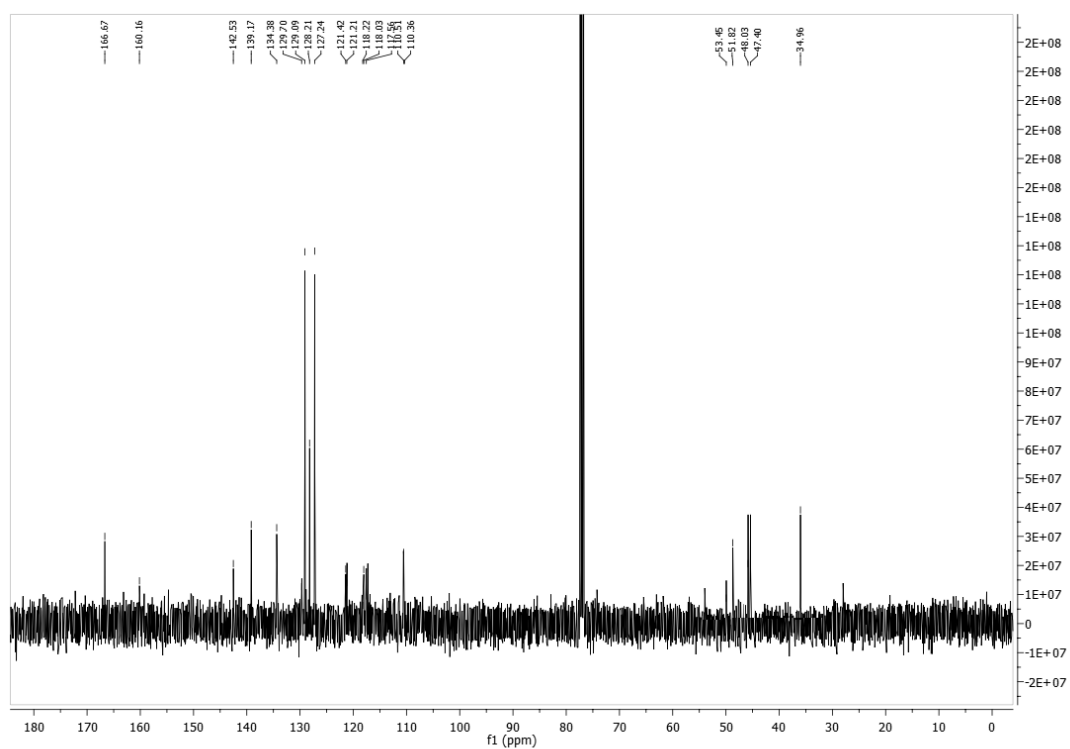
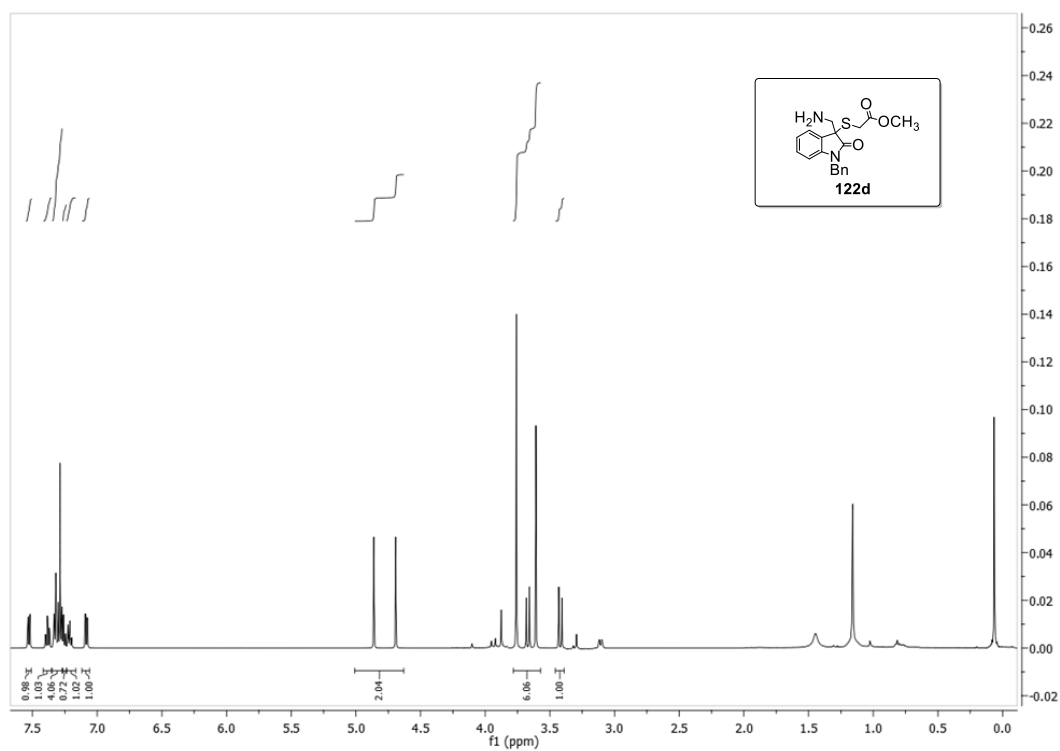
Figure A. 60  $^{13}\text{C}$  NMR spectrum of **121m**



**Figure A. 61**  $^1\text{H}$  NMR spectrum of **121n**



**Figure A. 62**  $^{13}\text{C}$  NMR spectrum of **121n**



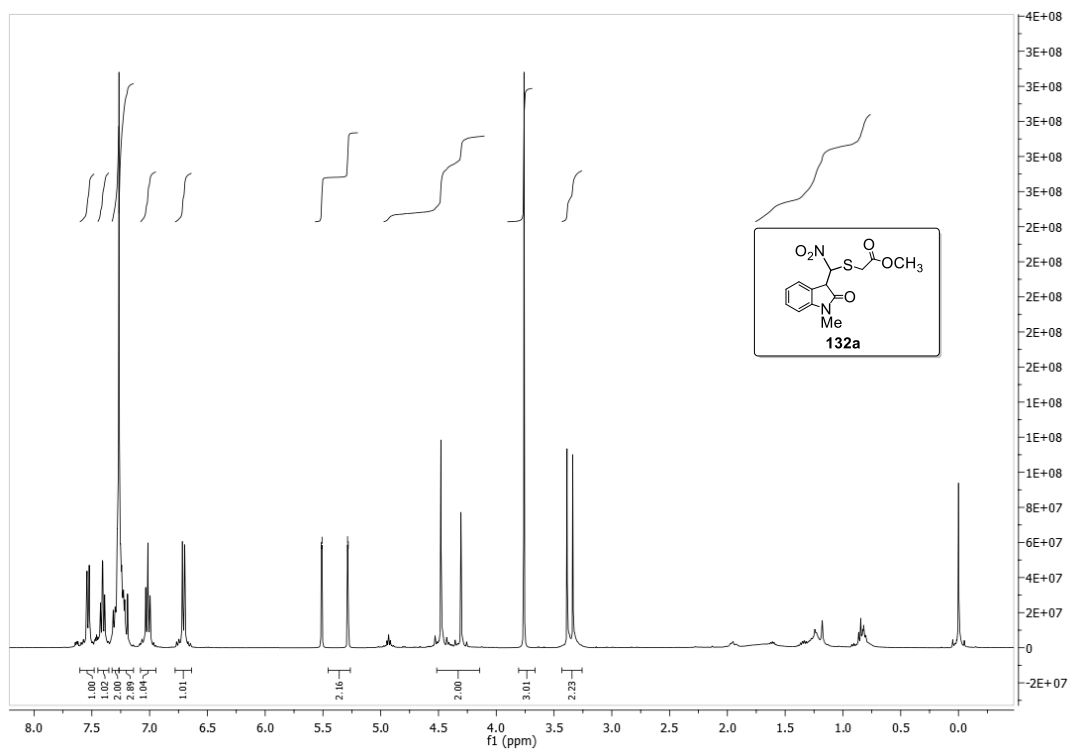


Figure A. 65  $^1\text{H}$  NMR spectrum of **132a**

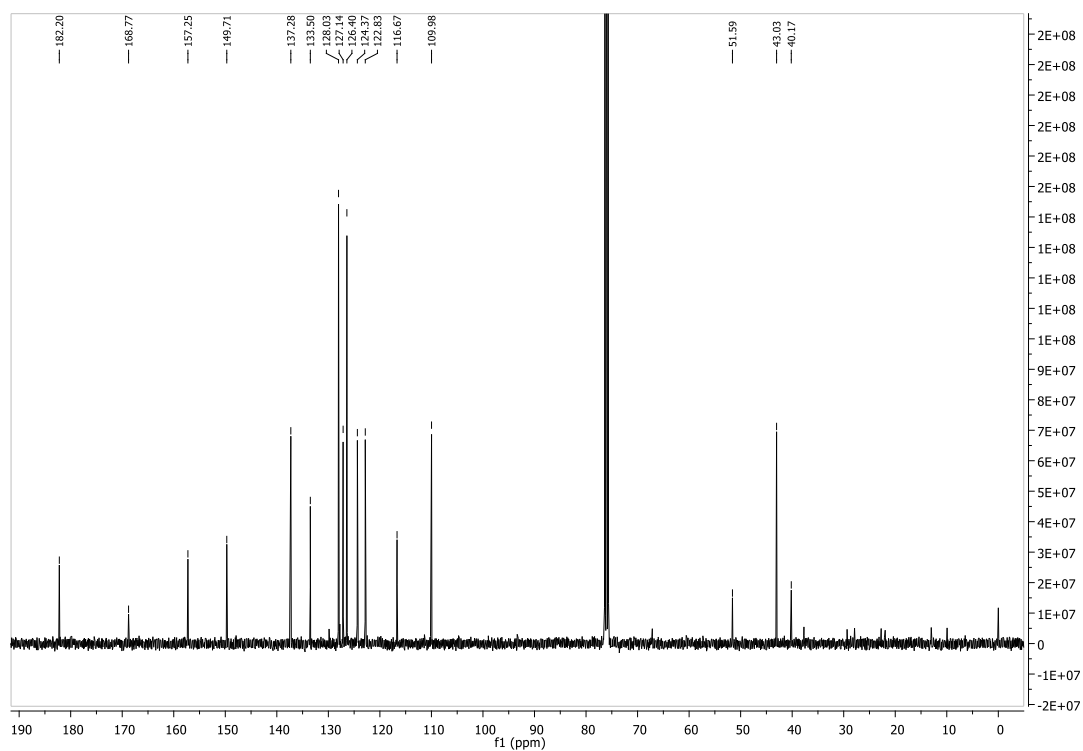


Figure A. 66  $^{13}\text{C}$  NMR spectrum of **132a**

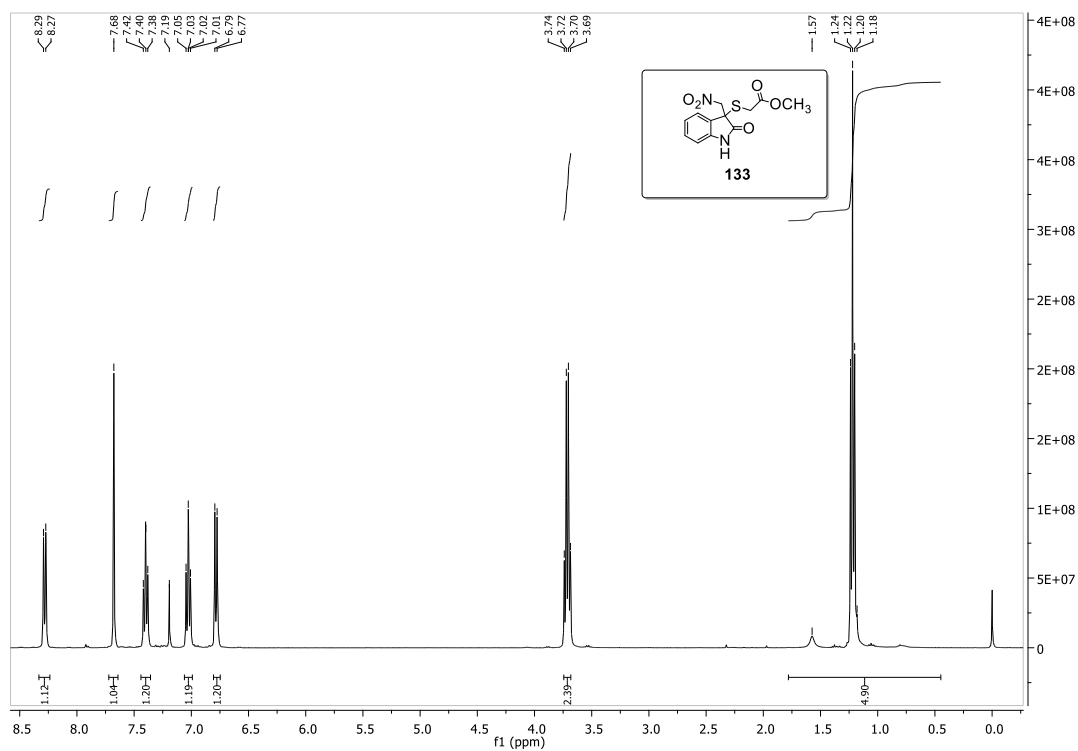


Figure A. 67  $^1\text{H}$  NMR spectrum of 133

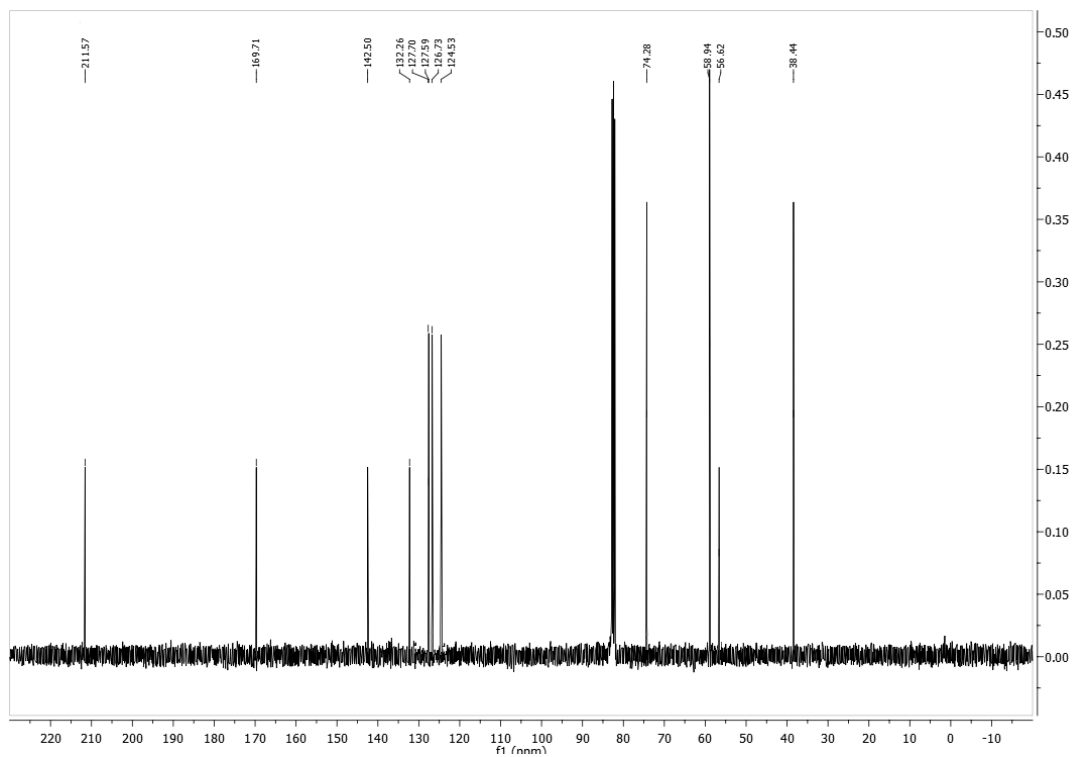


Figure A. 68  $^{13}\text{C}$  NMR spectrum of 133



## APPENDIX B

### HPLC DATA

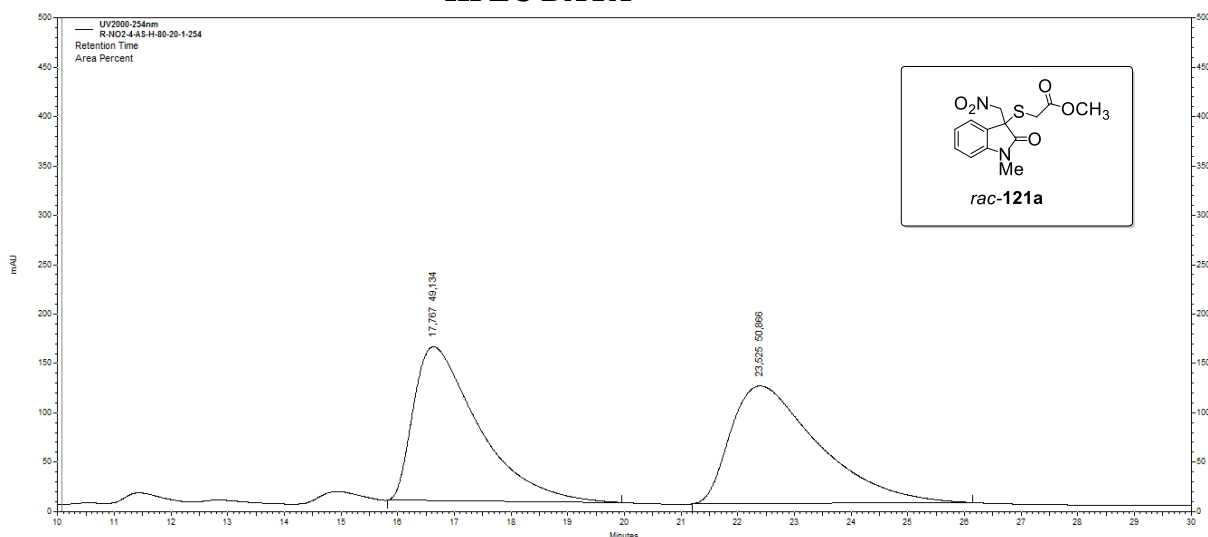


Figure B. 1 HPLC chromatogram of *rac*-121a

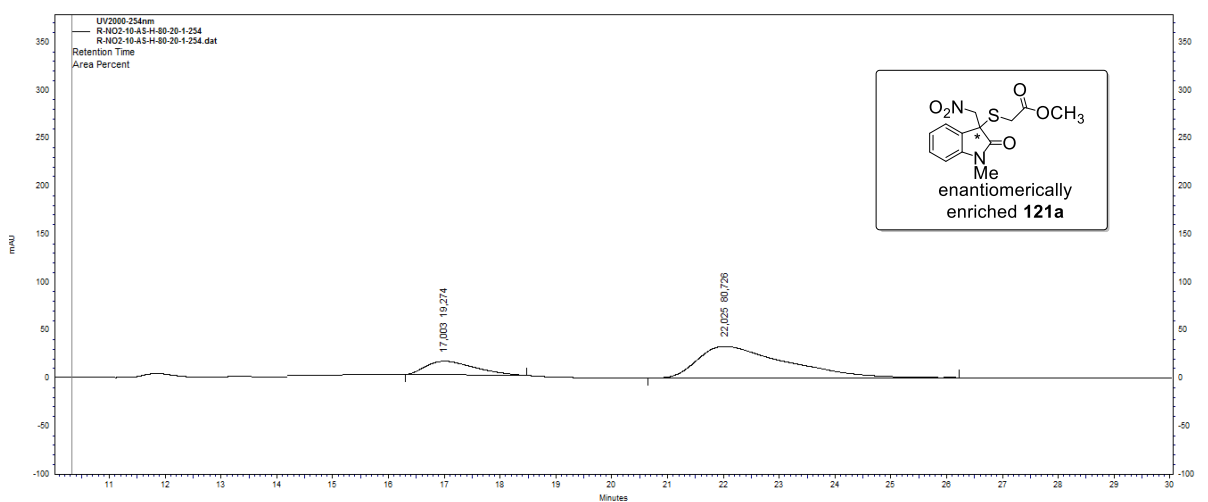
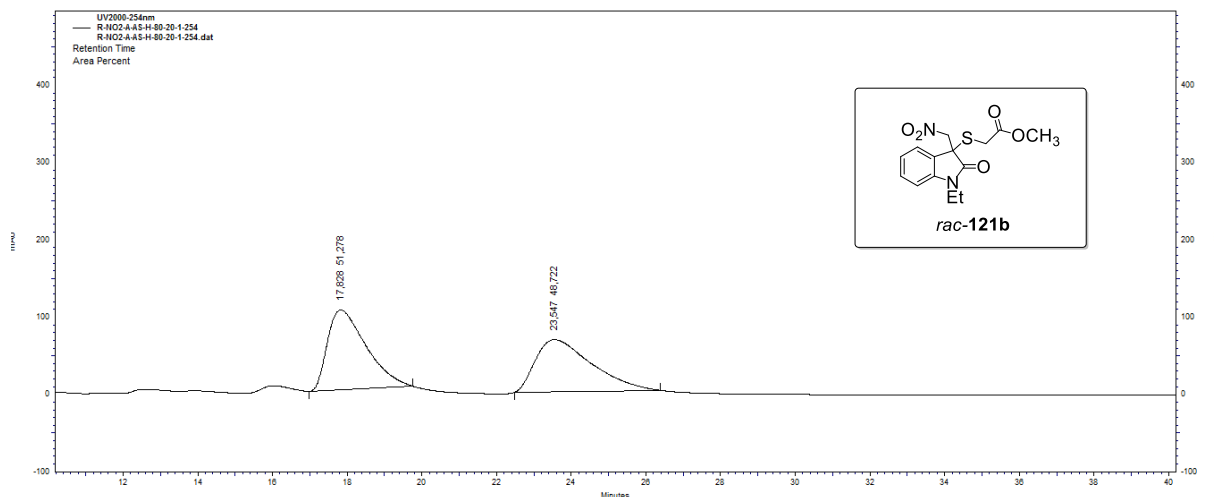
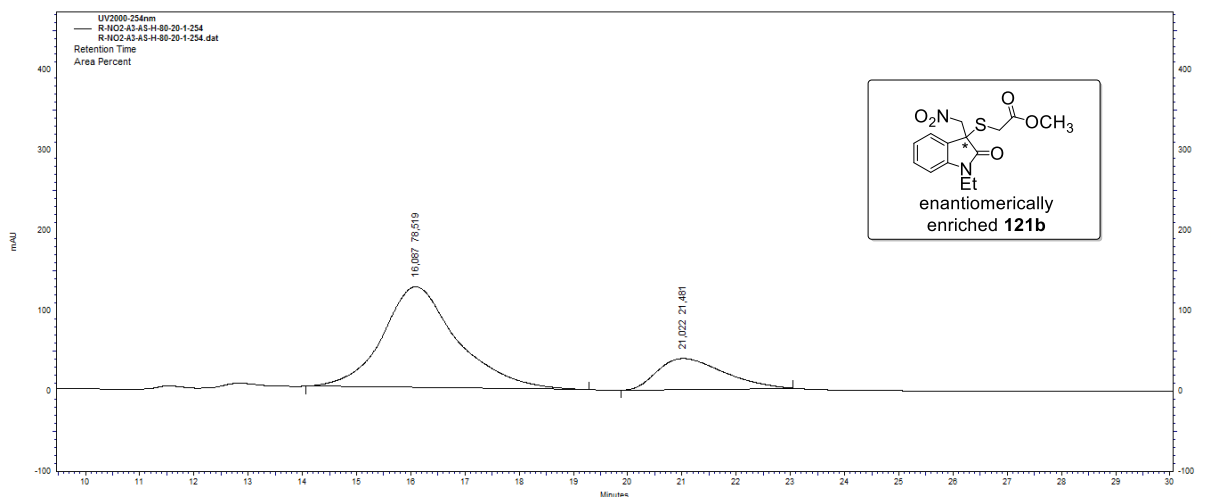


Figure B. 2 HPLC chromatogram of enantiomerically enriched 121a



**Figure B. 3** HPLC chromatogram of *rac*-121b



**Figure B. 4** HPLC chromatogram of enantiomerically enriched 121b



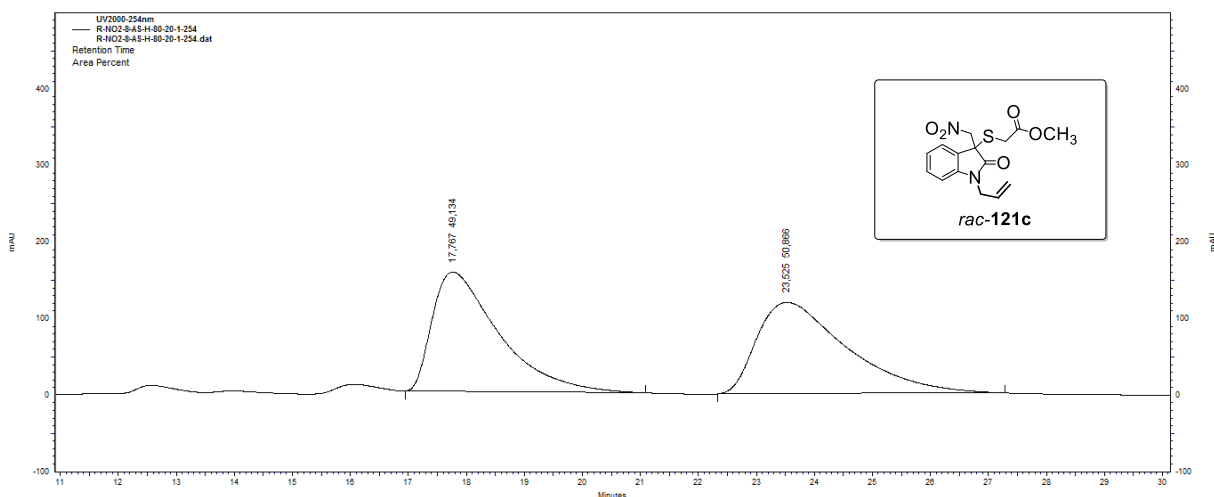


**Figure B. 5** HPLC chromatogram of *rac-121c*

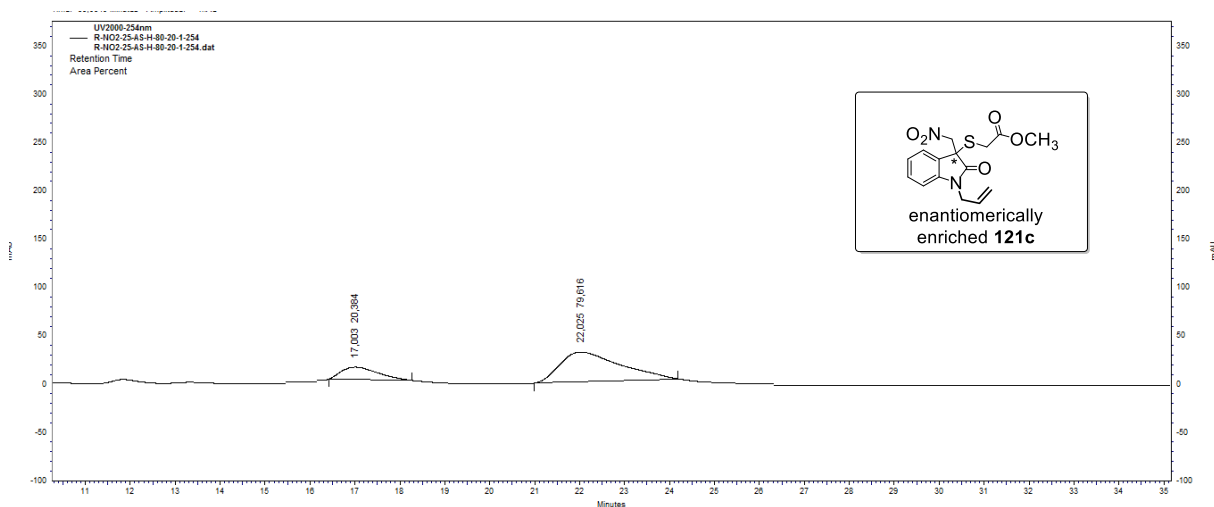


**Figure B. 6** HPLC chromatogram of enantiomerically enriched **121c**

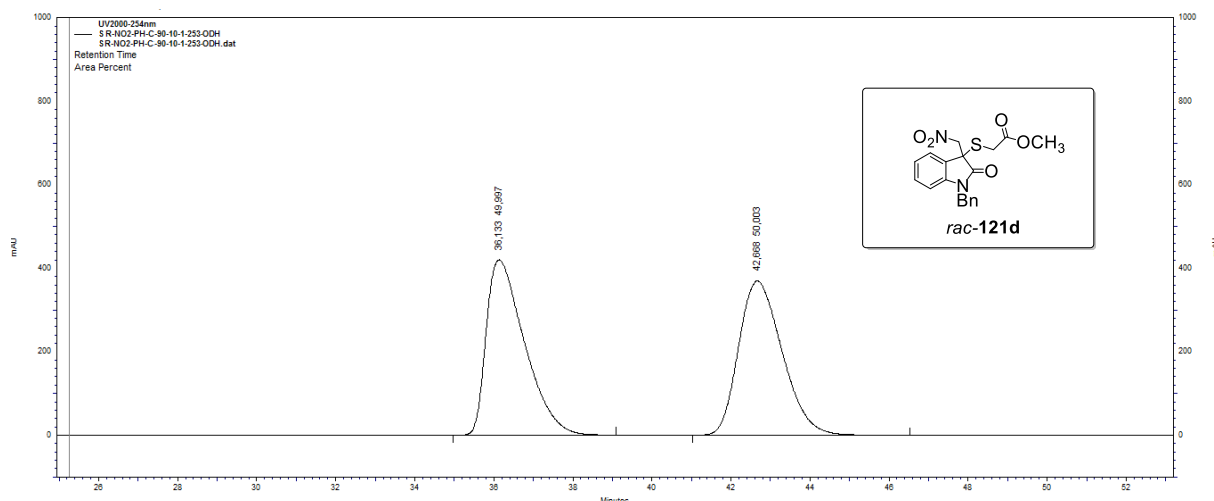


**Figure B. 7** HPLC chromatogram of *rac*-121d

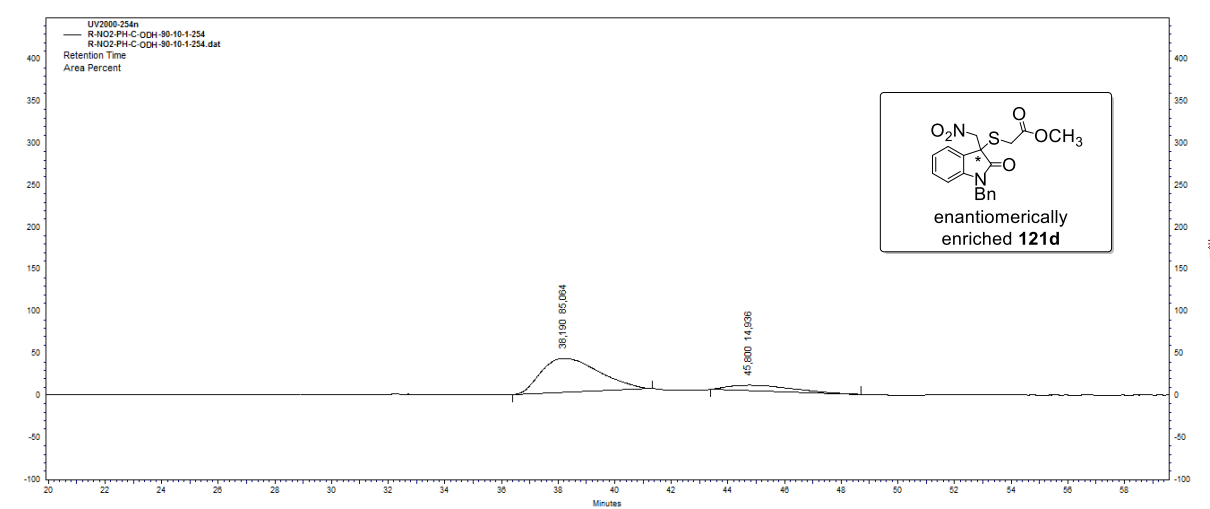


**Figure B. 8** HPLC chromatogram of enantiomerically enriched 121d

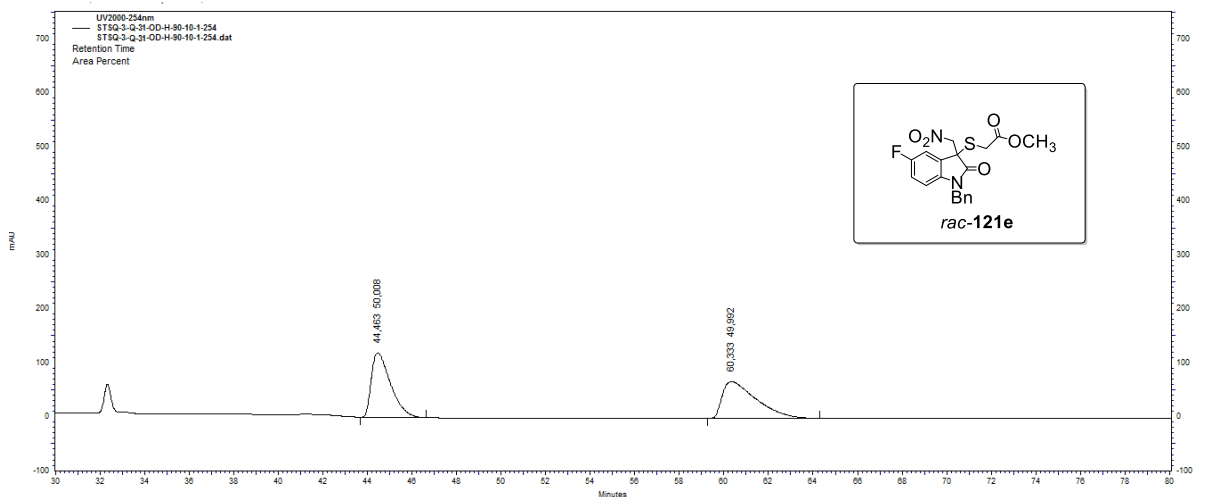


**Figure B. 9** HPLC chromatogram of *rac-121e*

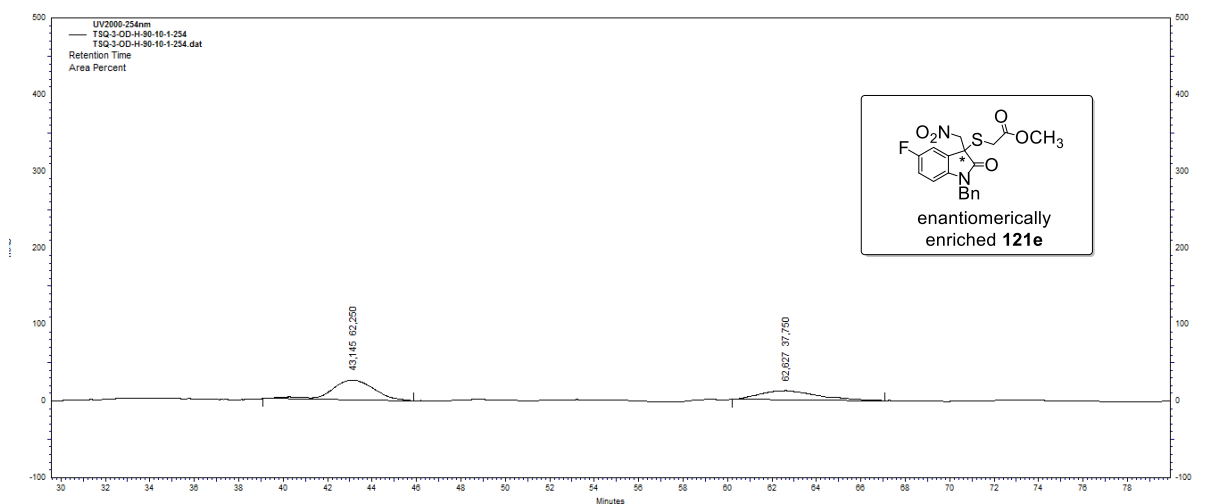


**Figure B. 10** HPLC chromatogram of enantiomerically enriched **121e**

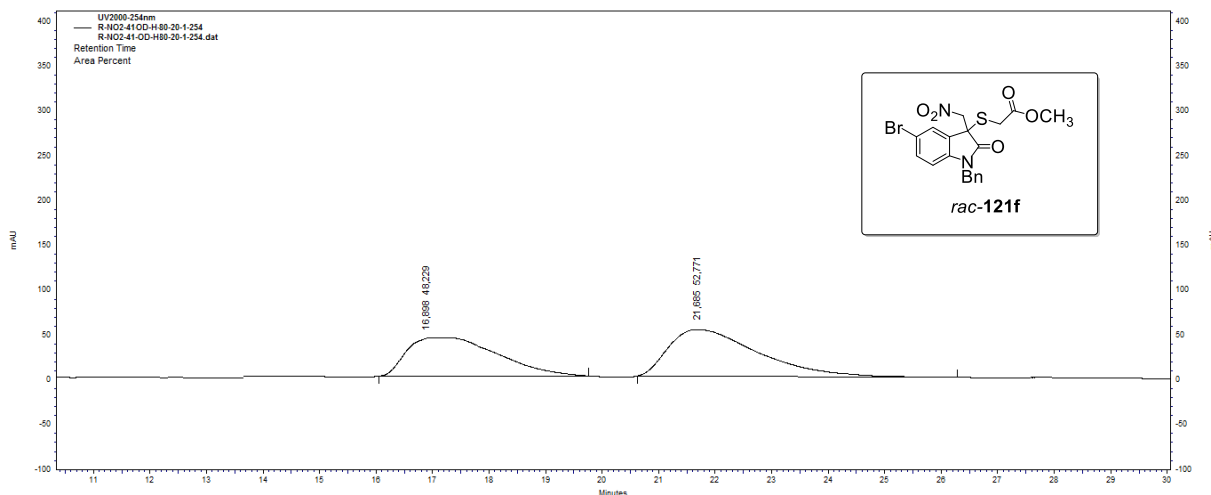


**Figure B. 11** HPLC chromatogram of *rac*-121f

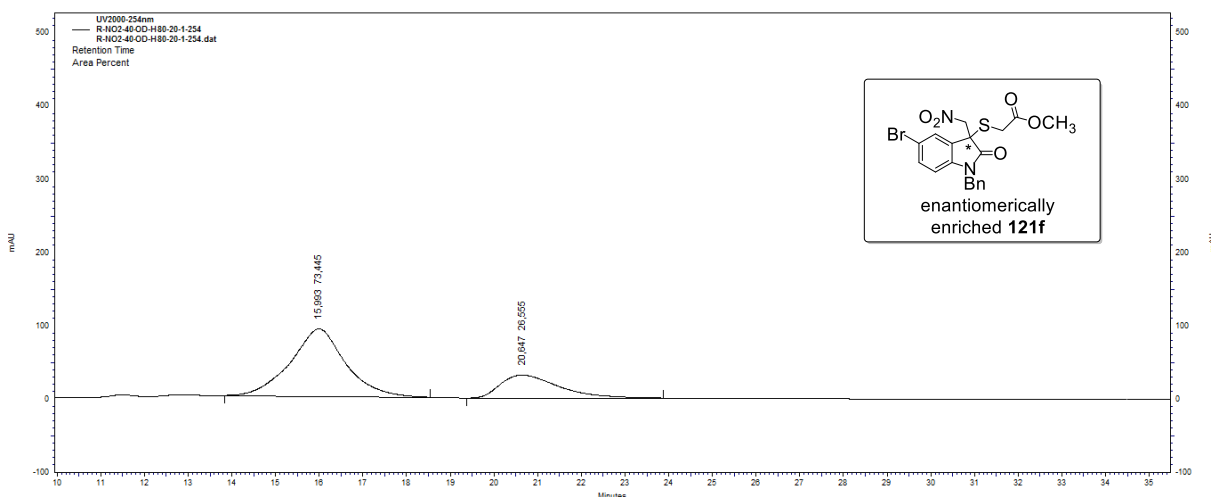


**Figure B. 12** HPLC chromatogram of enantiomerically enriched 121f

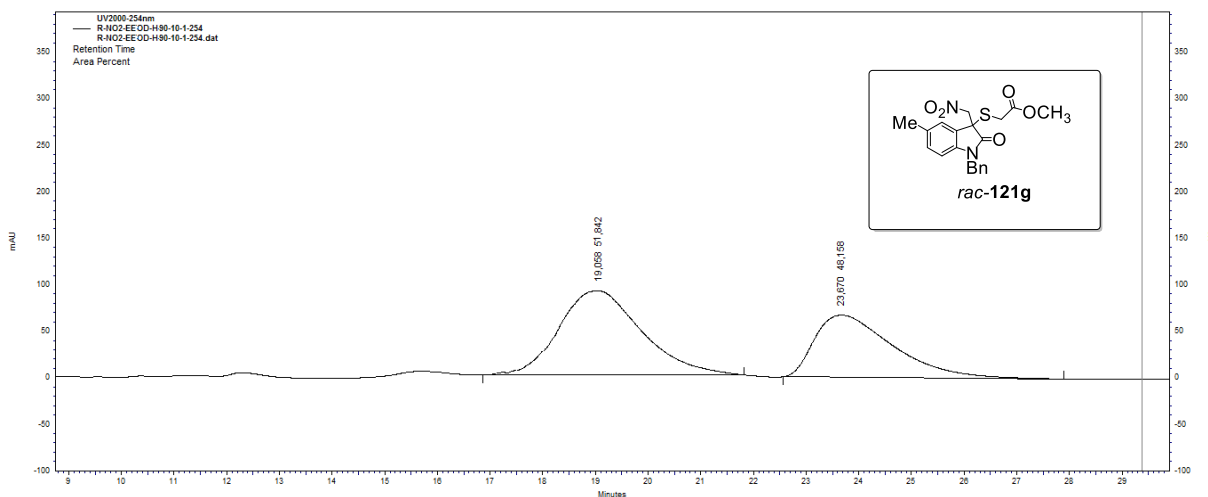


**Figure B. 13** HPLC chromatogram of *rac-121g*

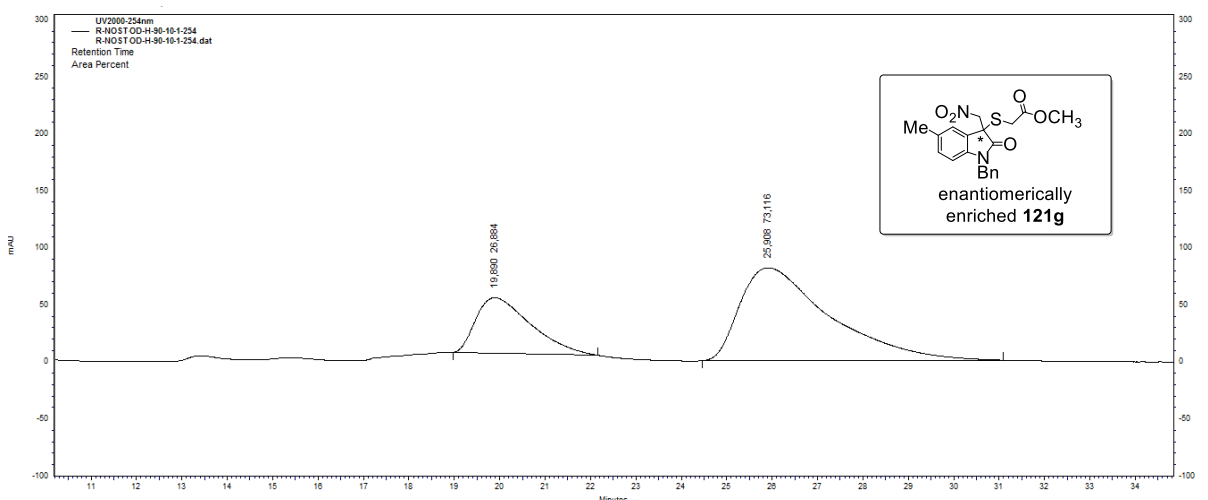


**Figure B. 14** HPLC chromatogram of enantiomerically enriched **121g**

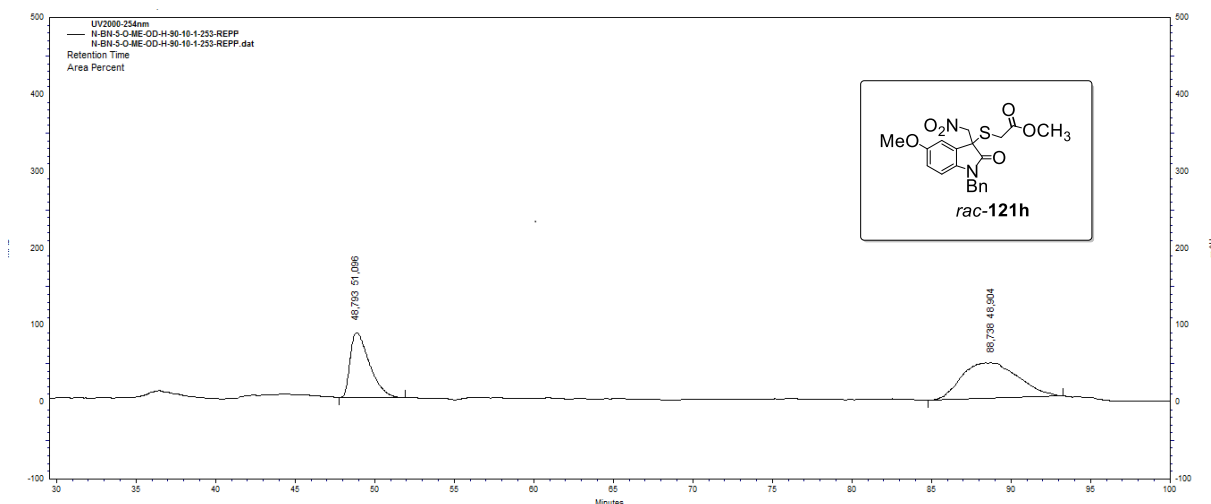


**Figure B. 15** HPLC chromatogram of *rac*-121h

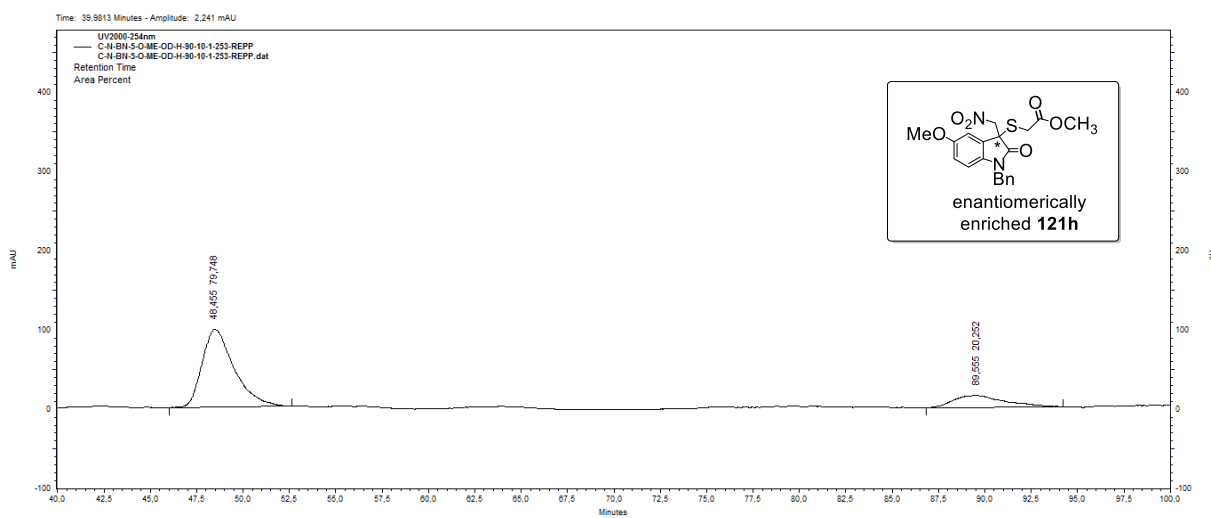


**Figure B. 16** HPLC chromatogram of enantiomerically enriched 121h

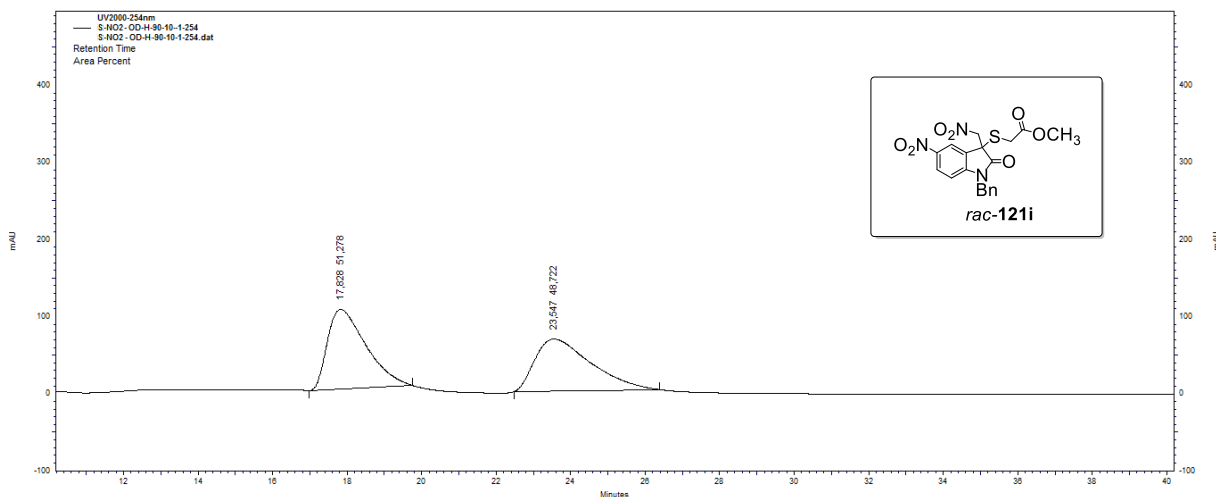


**Figure B. 17** HPLC chromatogram of *rac-121i*

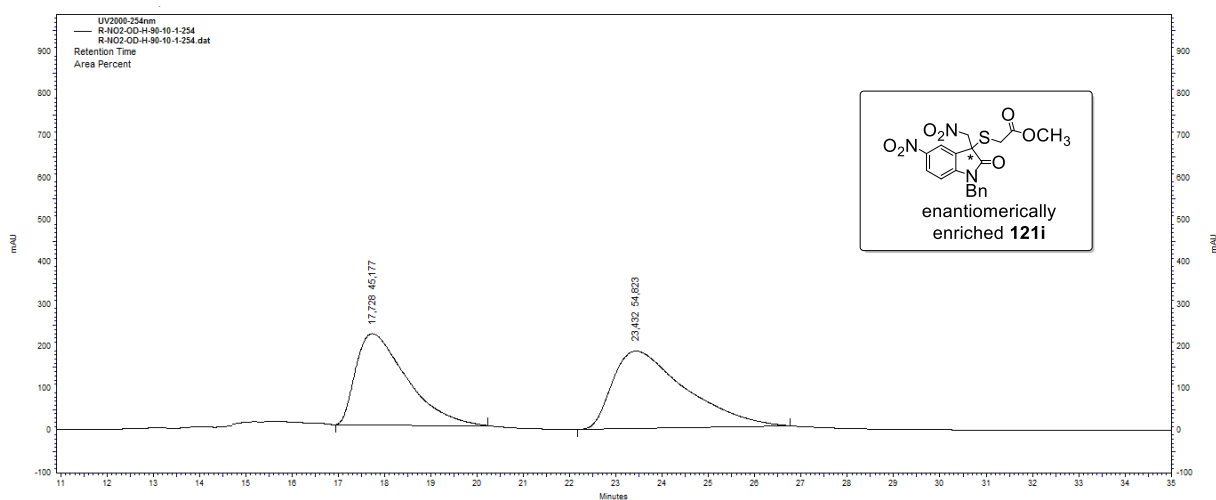


**Figure B. 18** HPLC chromatogram of enantiomerically enriched **121i**

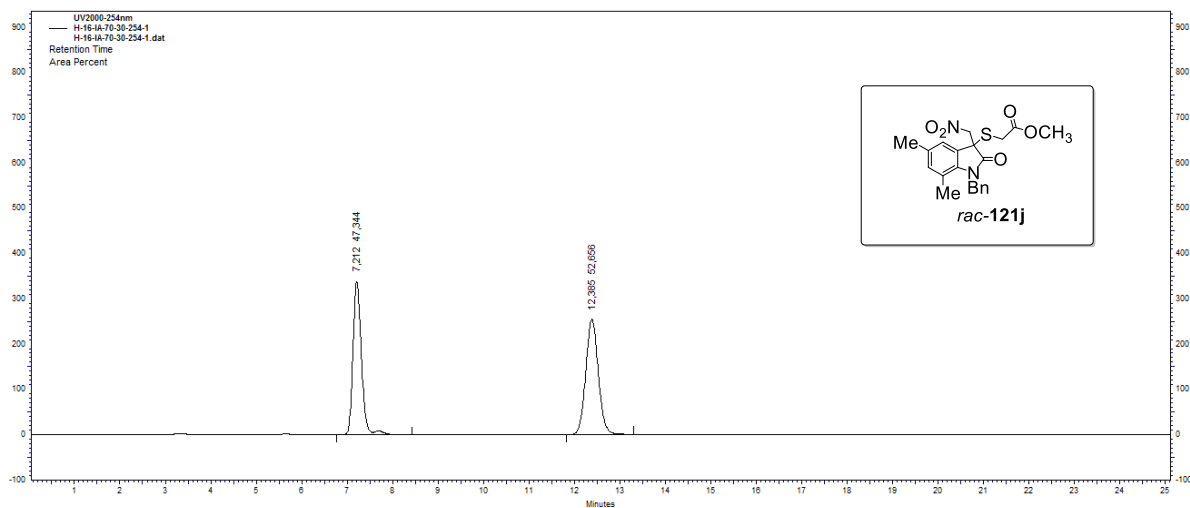


**Figure B. 19** HPLC chromatogram of *rac-121j*

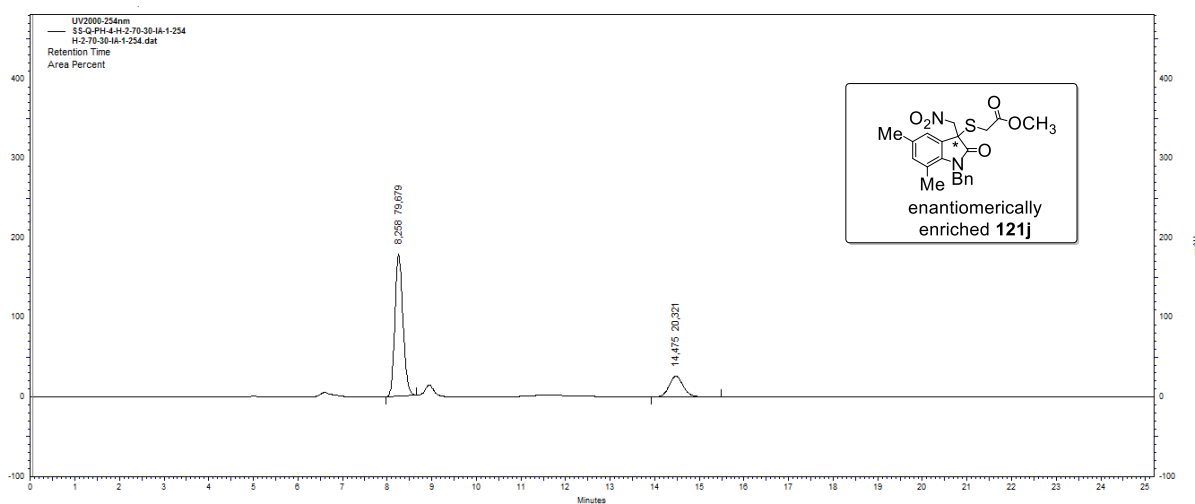


**Figure B. 20** HPLC chromatogram of enantiomerically enriched **121j**



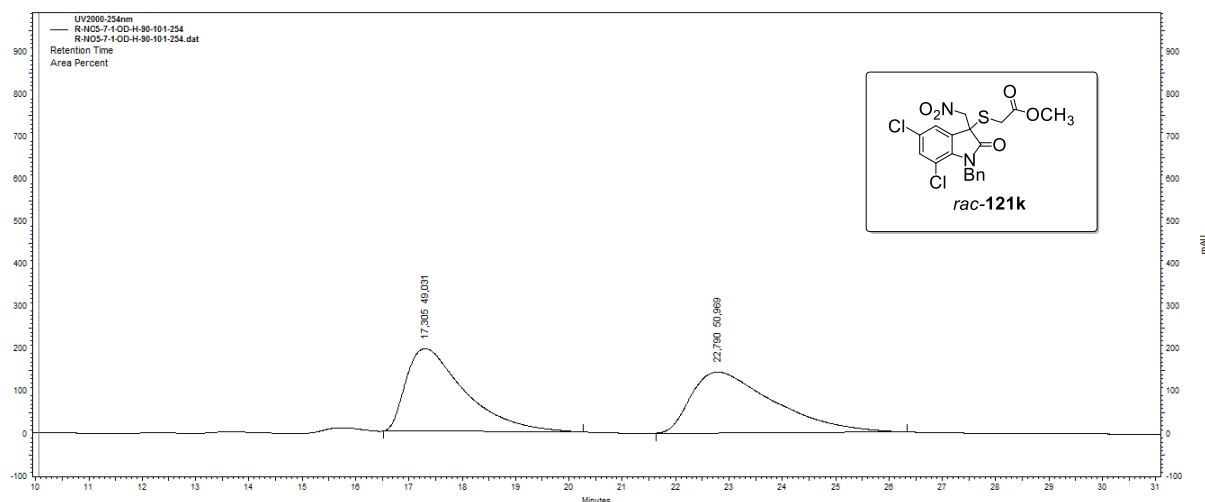


**Figure B. 21** HPLC chromatogram of *rac-121k*

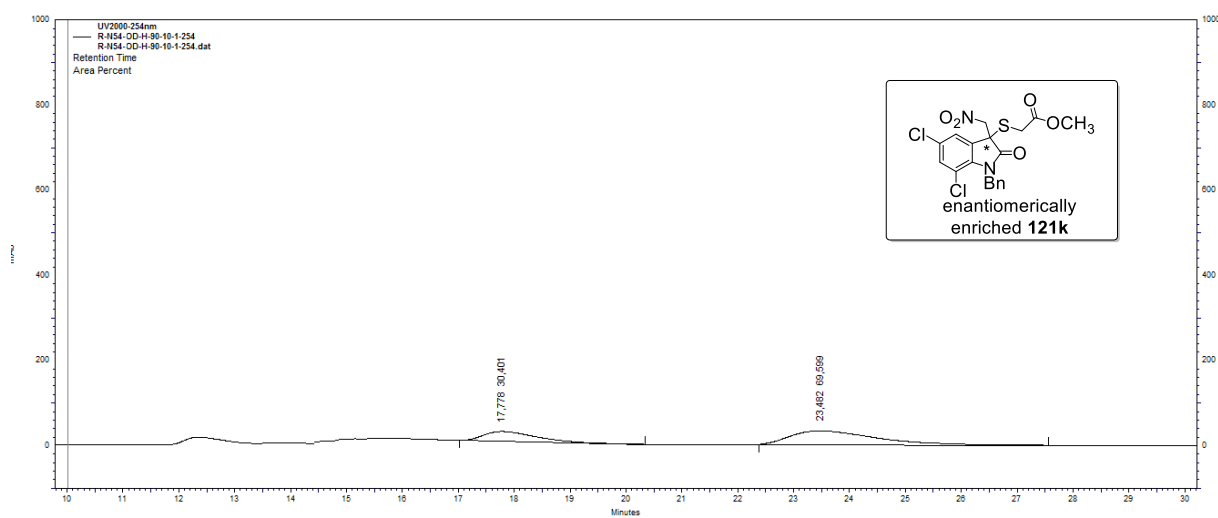


**Figure B. 22** HPLC chromatogram of enantiomerically enriched **121k**

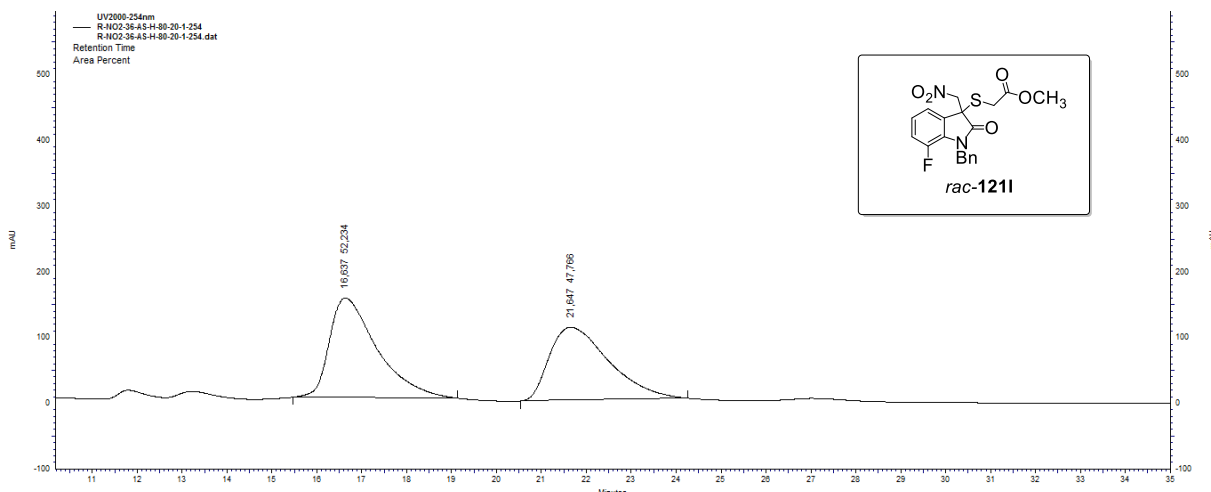


**Figure B. 23** HPLC chromatogram of *rac*-1211

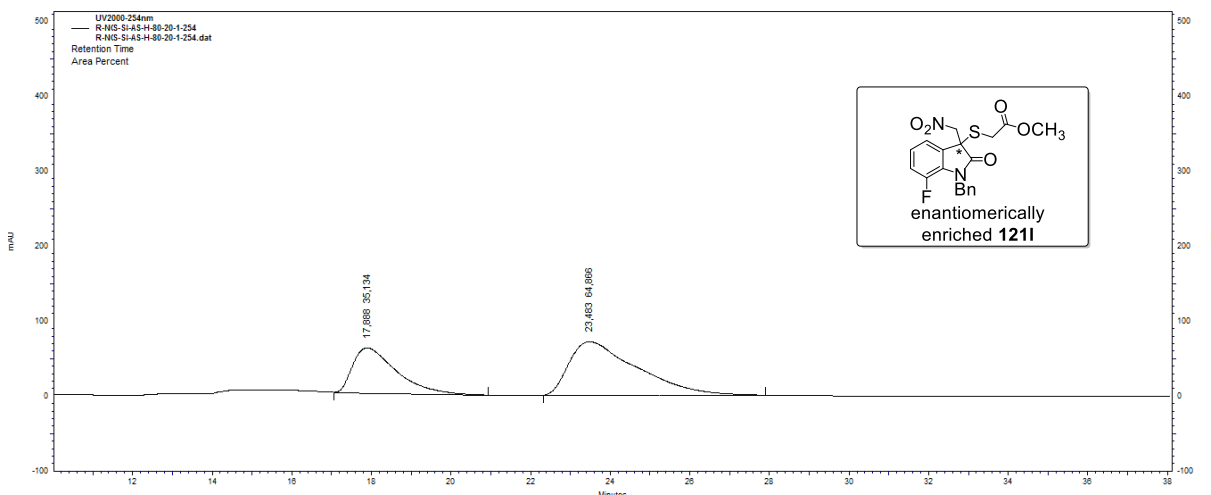


**Figure B. 24** HPLC chromatogram of enantiomerically enriched 1211

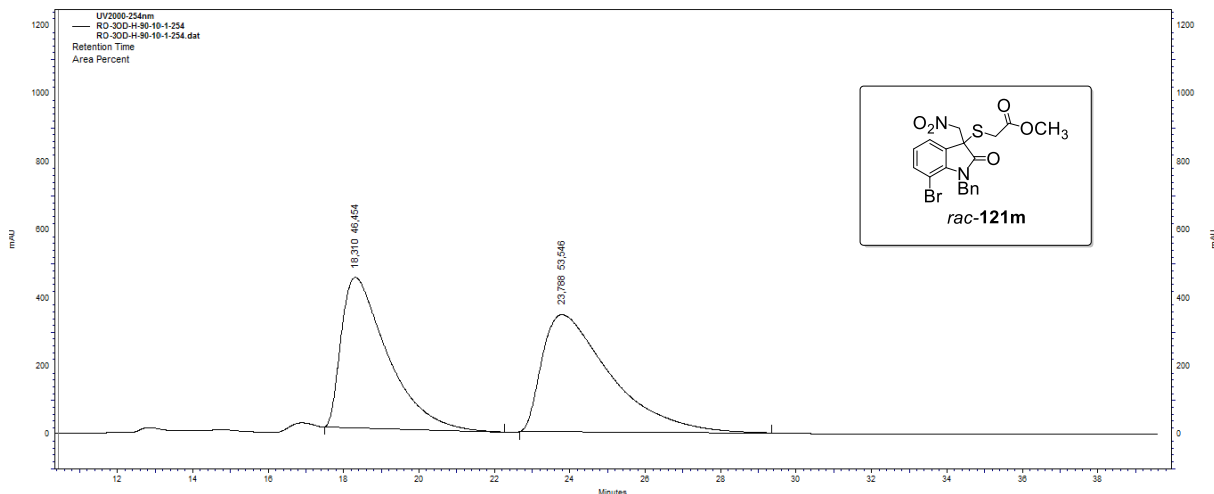


**Figure B. 25** HPLC chromatogram of *rac-121m*

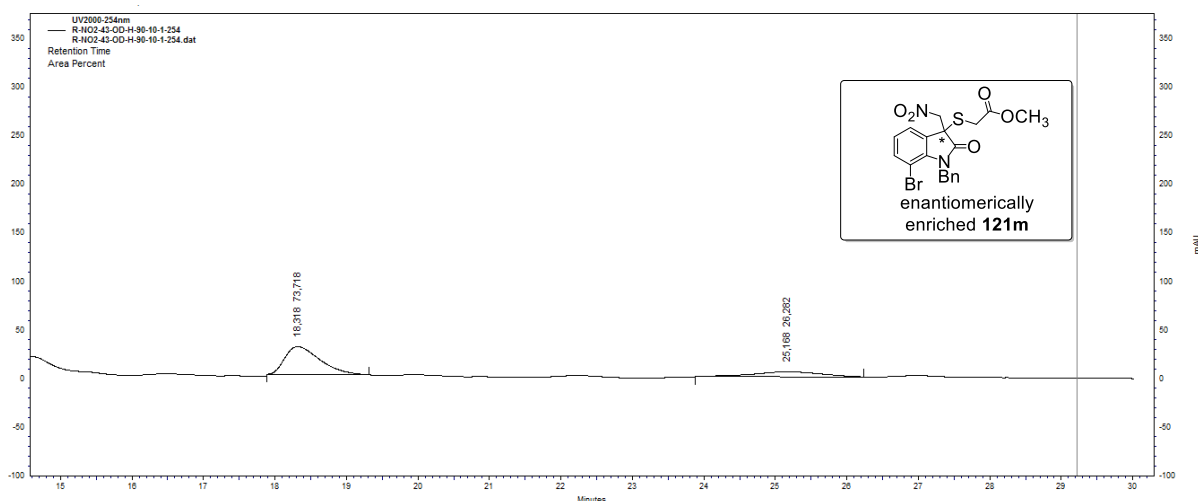


**Figure B. 26** HPLC chromatogram of enantiomerically enriched **121m**

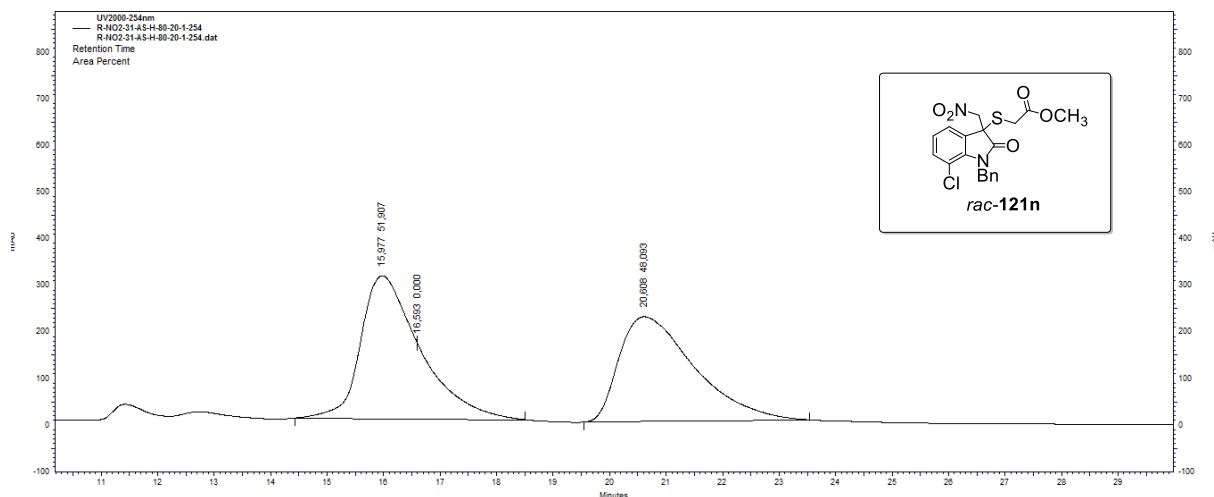


**Figure B. 27** HPLC chromatogram of *rac-121n*

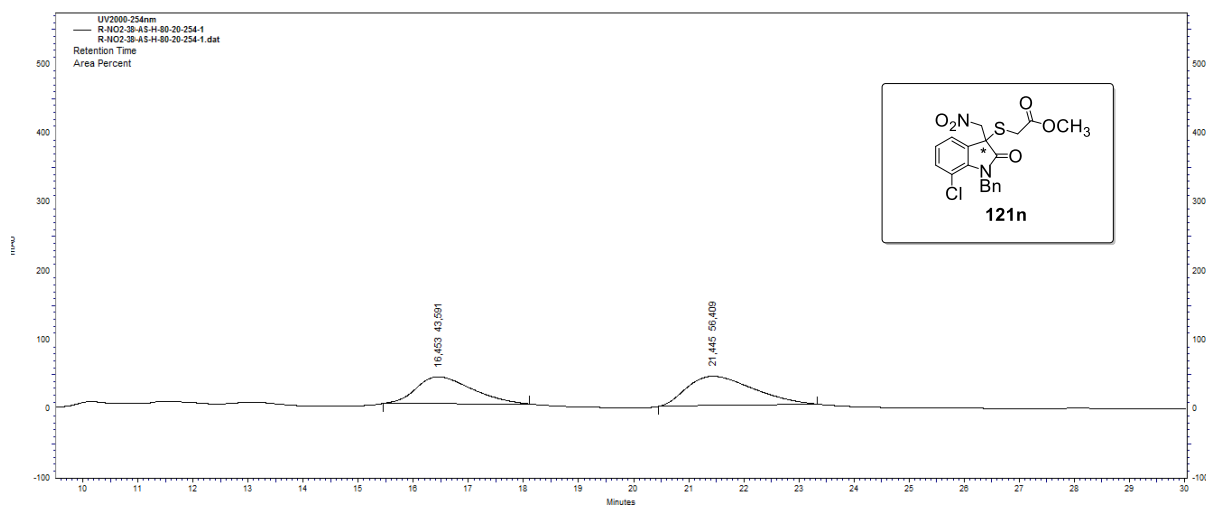


**Figure B. 28** HPLC chromatogram of enantiomerically enriched **121n**

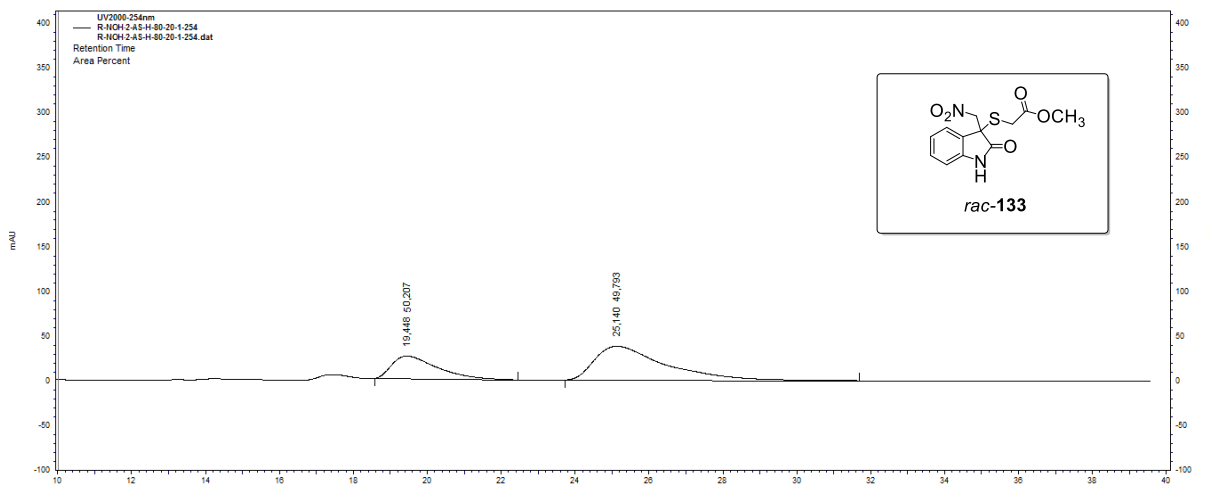


**Figure B. 29** HPLC chromatogram of *rac*-133

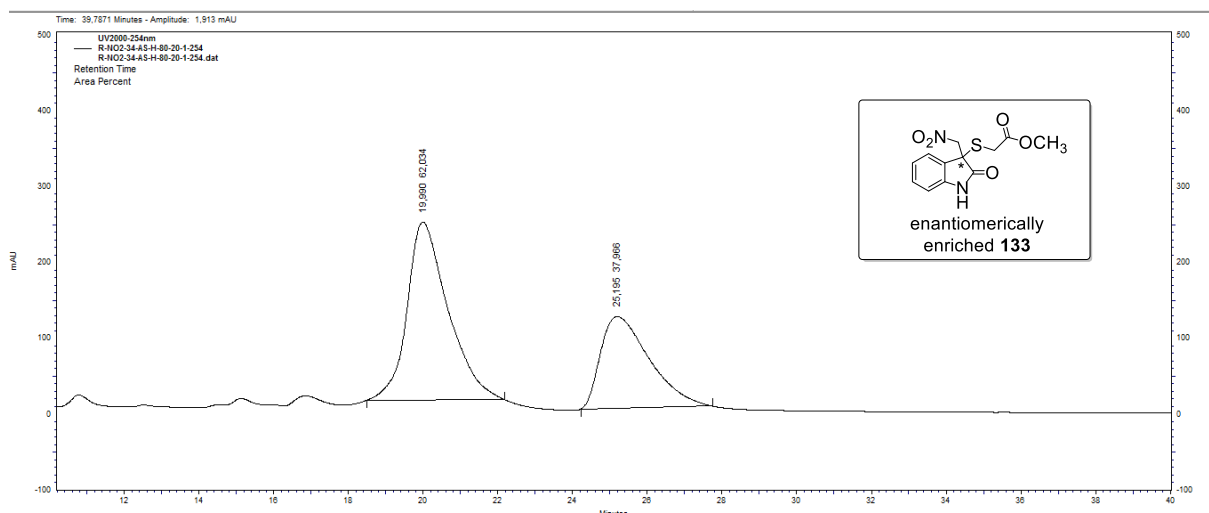


**Figure B. 30** HPLC chromatogram of enantiomerically enriched 133

